Alma Mater Studiorum – Università di Bologna

DOTTORATO DI RICERCA IN
Scienze Ambientali Tutela e Gestione delle Risorse Naturali

Ciclo XXII

Settore scientifico-disciplinare di afferenza: BIO/09

Experimental Studies on Electromagnetic Fields Effects on Biological Targets: Simulation and Dosimetry

Presentata da: ***Naimj Gambi***

Coordinatore Dottorato

Elena Fabbri

Relatore

Andrea Contin

Correlatori

Elena Fabbri

James Murphy

Esame finale anno 2010

Dedicated to my parents, Noemi and Roberto.

INDEX

Contents:

Chapter 1

INTRODUCTION

1.1 - AIM OF THE PRESENT STUDY

The main idea behind the present study is to investigate some effects of the electromagnetic fields (EMF) humans are exposed to on a daily basis, by an *in vitro* approach. Two different areas were investigated: one to assess possible detrimental effects of the daily use of GSM mobile phones, the other to identify possible positive effects of high frequency (HF) EMFs on human health, to be employed as a medical therapy in cancer treatments.

The first part of this study has been conducted at the Interdepartment Centre for Environmental Science Research (CIRSA), of the University of Bologna, campus of Ravenna, after joining the Environmental Physiology and Biochemistry (EPB) group of Prof Elena Fabbri. The second part of the research has been conducted at the Institute of Technology Sligo (IT Sligo), in Sligo, Ireland, after joining the Mitochondrial Biology and Radiation Research group (MiBRRG) of Dr James Murphy.

The RF research works were conducted primarily at a cellular level, *in vitro*. The research required also a range of subject material including computer modelling, physical tissue-specific simulation and experiments using biological samples.

For the GSM study, the expression of a stress-response protein and the activity of an enzyme involved in important cellular processes (such as neurotransmission) were evaluated in several cell lines after exposure to different high frequency (1.8 GHz) GSM signals. The present study also evaluated the bio-effects of several frequencies in the MHz range (144 and 434 MHz) and how cellular responses differed between tumour and non-tumour human cell lines. The same approach was adopted for the two areas under analysis: an initial phase of simulation of the exposure system employed through a mathematical model and a second phase of dosimetry through measurement on biological parameters after exposure of the biological targets.

1.2 - ELECTROMAGNETIC FIELDS

1.2.1 - STRUCTURE AND DESCRIPTION

The EMF is a physical field produced by electrically charged objects. It is one of the four fundamental forces of nature, describes the electromagnetic interaction and extends indefinitely throughout space.

The field propagates by electromagnetic radiation and can be viewed as the combination of an electric field and a magnetic field, though separate electric and magnetic fields exist. Electric fields exist whenever a positive or negative electrical stationary charge is present and exert forces on other charges within the field. The strength of the electric field is measured in volts per metre (V/m). Electric fields are strongest close to a charge or charged conductor, and their strength rapidly diminishes with distance from it.

Magnetic fields arise from the motion of electric charges (currents). In contrast to electric fields, a magnetic field is only produced once a device is switched on and current flows. The strength of the magnetic field is measured in amperes per meter (A/m), though in electromagnetic field research it can be defined by a related quantity, the flux density (measured in Tesla, T). Like electric fields, magnetic fields are strongest close to their origin and rapidly decrease at greater distances from the source. Also, higher electric currents produce stronger magnetic fields.

If only the electric field (E) is non-zero, and is constant in time, the field is said to be an electrostatic field. Similarly, if only the magnetic field (B) is non-zero and is constant in time, the field is said to be a magnetostatic field. However, if either the electric or magnetic field has a time-dependence, then both fields must be considered together as a coupled electromagnetic field using Maxwell's equations.

Electromagnetic waves were first postulated by James Clerk Maxwell and subsequently confirmed by Heinrich Hertz. Maxwell derived a wave form of the electric and magnetic equations, revealing the wave-like nature of electric and magnetic fields, and their symmetry.

The Maxwell's equations are:

I. Gauss' law for electricity $\oint \vec{E} \cdot d\vec{A} = \frac{q}{\varepsilon_0}$

II. Gauss' law for magnetism $\oint \vec{B} \cdot d\vec{A} = 0$

III. Faraday's law of induction $\oint \vec{E} \cdot \vec{ds} = -\frac{d\Phi_B}{dt}$

IV. Ampere's law $\oint \vec{B} \cdot \vec{ds} = \mu_0 i + \frac{1}{c^2}\frac{\partial}{\partial t}\int \vec{E} \cdot d\vec{A}$

where E = Electric field (V/m); ρ = charge density (C/m^3); i = electric current (A); B = Magnetic field (T); ε_0 = permittivity (F/m); J = current density (A/m^2); μ_0 = permeability (H/m); c = speed of light (m/s).

The behaviour of electric and magnetic fields, whether in cases of electrostatics, magnetostatics, or electrodynamics (electromagnetic fields), is governed in a vacuum by Maxwell's equations. Inside a linear material, Maxwell's equations change by switching the permeability and permittivity of free space with the permeability and permittivity of the linear material in question. Inside other materials which possess more complex responses to electromagnetic fields, these terms are often represented by complex numbers, or tensors.

One of the properties of the field is the reciprocal behaviour of electric and magnetic fields. According to Maxwell's equations, a time-varying electric field generates a magnetic field and vice versa. Therefore, as an oscillating electric field generates an oscillating magnetic field, the magnetic field in turn generates an oscillating electric field, and so on. These oscillating fields together form an electromagnetic wave.

Electromagnetic waves can be imagined as a self-propagating transverse oscillating wave of electric and magnetic fields (Fig. 1.1) and are typically described by these physical properties: frequency, f (Hz), wavelength, λ (m) and photon energy, E (J).

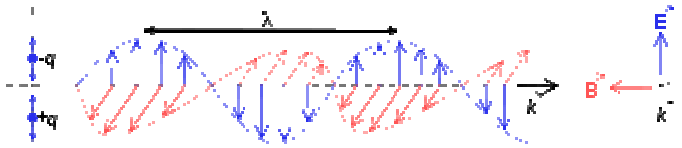

Fig. 1.1 – A plane linearly polarized wave propagating from right to left. The electric field is in a vertical plane, the magnetic field in a horizontal plane.

Frequencies range from $2.4 \cdot 10^{23}$ Hz (1 GeV gamma-rays) down to tiny fractions of Hertz (mHz) for magnetic pulsations, microhertz and nanohertz for astronomical scale waves. Photon energy is directly proportional to the wave frequency, while wavelength is inversely proportional to the wave frequency.

This relation is illustrated by the following equation:

$$\nu = c / \lambda$$

where c = 299,792,458 m/s (speed of light in vacuum).

Electromagnetic radiation (sometimes abbreviated EMR) is a ubiquitous phenomenon that takes the form of self-propagating waves in a vacuum or in matter. It consists of electric and magnetic field components which oscillate in phase perpendicular to each other and perpendicular to the direction of energy propagation. Electromagnetic radiation is classified into several types according to the frequency of its wave; these types include (in order of increasing frequency and decreasing wavelength): radiowaves, microwaves, terahertz radiation, infrared radiation, visible light, ultraviolet radiation, X-rays and gamma-rays. A small and somewhat variable window of frequencies is sensed by the eyes of various organisms; this is the visible spectrum, or light.

EM radiation exhibits both wave properties and particle properties at the same time.

1.2.2. - ELECTROMAGNETIC SPECTRUM

The electromagnetic spectrum is the range of all possible electromagnetic radiation frequencies (Fig. 1.2). The electromagnetic spectrum extends from below frequencies used for modern radio (at the long-wavelength end) through gamma radiation (at the short-wavelength end), covering wavelengths from thousands of kilometres down to a fraction the size of an atom. It is thought that the short wavelength limit is in the vicinity of the Planck length while the long wavelength limit is the size of the universe itself, although in principle the spectrum is infinite and continuous.

Generally, EM radiation is classified into several types according to the frequency of its wave; these types include (in order of increasing frequency and decreasing wavelength): radio waves, microwaves, terahertz radiation, infrared radiation, visible light, ultraviolet radiation, X-rays and gamma rays. The behaviour of EM radiation depends on its wavelength. When EM radiation interacts with single atoms and molecules, its behaviour also depends on the amount of energy per quantum (photon) it carries.

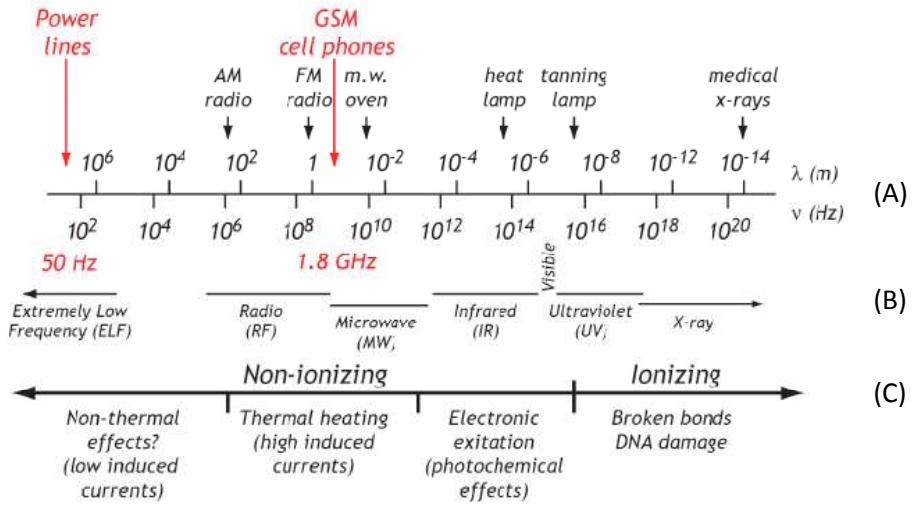

Fig. 1.2 – The electromagnetic spectrum. (A) illustrates the EM radiation classification based on wavelength (top) and frequency (bottom); (B) represent the EM radiation distinctive types (ELF, RF, MW, IR, UV, X-ray) and (C) summarizes the EM potential health effects for different radiation types.

ELF stands for Extremely Low Frequency and refers to the range 30 - 300 Hz. These frequencies were used by the US Navy and the Soviet Navy to communicate with submerged submarines. The frequency at which alternating current is transmitted from a power plant to the end user is 50 Hz in most part of world.

Radio frequency (RF) is a frequency or rate of oscillation within the range of about 30 kHz to 300 GHz. In particular, this band can be divided into: low frequency (LF), referring to the range of 30 kHz to 300 kHz, used in Europe, parts of Northern Africa and Asia for AM broadcasting; medium frequency (MF), referring to the range of 300 kHz to 3 MHz, used as the medium wave broadcasting band; high frequency (HF), referring to the range of 3 MHz to 30 GHz. Radiowaves generally are utilized by antennas of appropriate size, with wavelengths ranging from hundreds of metres to about one millimetre, which are used for transmission of data, via modulation. Television, mobile phones, wireless networking and amateur radio all use radiowaves. Radiowaves can be made to carry information by varying a combination of the amplitude, frequency and phase of the wave within a frequency band and the use of the radio spectrum is regulated by many governments through frequency allocation. When EM radiation impinges upon a conductor, it couples to the conductor, travels along it, and induces an electric current on the surface of that conductor by exciting the electrons of the conducting material. This effect (the skin effect) is used in antennas.

Microwaves (MW) are electromagnetic waves with frequency between 2 and 300 GHz. They are employed in wireless communication (e.g. the Bluetooth technology is based

on 2.4 GHz MW band), remote sensing (radar), spectroscopy and appliance. MW radiation can cause certain molecules to absorb energy and can determine a dielectric heating in water, fats and sugar contained in the food. This property is the one exploited around 2.4 GHz in microwave ovens.

Infrared (IR) radiation refers to a frequency range between 1 and 430 THz. Infrared imaging is extensively used for military and civilian purposes for night vision, thermal analysis, remote temperature sensing, weather forecasting, etc.

The visible spectrum is the portion of EM spectrum that can be detected by human eye and is in the range between 400 to 790 THz.

Ultraviolet (UV) is the EM radiation found in sunlight, ranging from 750 to 1500 THz in frequency.

Above 10^{16} Hz (X-rays and gamma-rays) the energy carried by the EM waves (which depends on the wave frequency, rather than on the field strength) becomes strong enough to break molecular bonds and is then called ionizing radiation. That means that the EM wave has enough quantum energy to eject an electron from an atom or molecule and therefore produce a positive ion (Fig. 1.3).

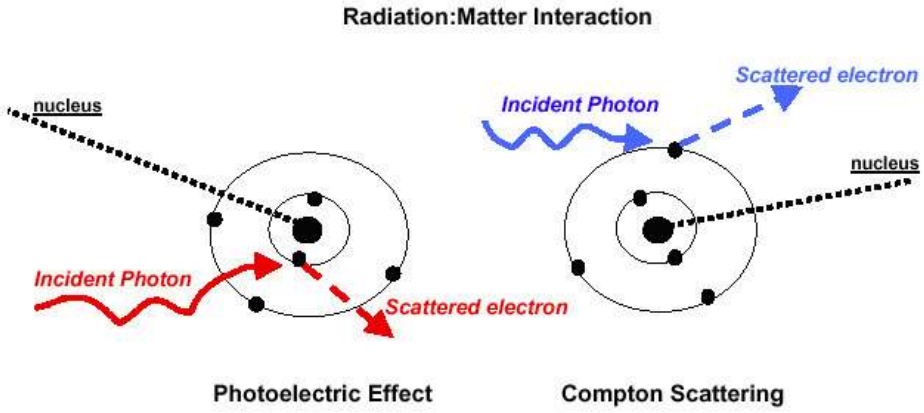

Fig. 1.3 – A scheme of the ionization reaction. An incident photon ejects an electron from an atom, ionizing it. Photoelectric effect (left) involves the interaction of the photon with the highly bound inner electrons, while Compton scattering effect (right) involves the interaction with outer electron that are bound more loosely.

This is a crucial distinction, since ionizing radiations can produce a number of physiological effects, such as those associated with risk of mutation or cancer, which non-ionizing radiations cannot directly produce at any intensity.

1.2.3 - ELECTROMAGNETIC FIELDS AND ENVIRONMENT

Electromagnetic radiation has been around since the birth of the universe; light is its most familiar form. Electric and magnetic fields are part of the spectrum of electromagnetic radiation which extends from static electric and magnetic fields, through radiofrequency and infrared radiation, to X-rays. Though such a natural electromagnetic background has always been present on earth, the anthropic activities increased the number of sources of electromagnetic fields, so that the electromagnetic natural level is hundreds of times higher since the latter 20^{th} Century. Mobile phones and wireless network make human lives easier, but the arising question is whether the waves from human-made EMFs are somehow damaging our health.

The general public is concerned about exposure to EMFs at home, at school and in public places, but a clear distinction must be made between low frequency (LF) and high frequency (HF) electromagnetic field, in terms of use, applications and effects.

The best known effects, based on more than 30 years of research, are those due to extremely low (ELF) EMFs, i.e. at supply frequency (50 Hz in UK, and 60 Hz in USA, with similar effects), arisen most markedly from high voltage power lines, substations and house wiring. EMFs from household appliances typically become insignificant beyond half a metre and exposure to them is generally short and can be controlled by the user. A main concern is about long- term exposure to externally imposed fields, particularly from power lines, and their potential effects in terms of increase in cancer or childhood leukaemia occurrence. Nonetheless, the UK National Radiological Protection Board Agency (NRPB-AG) concluded in 1994 that: "there is no persuasive biological evidence that ELF EMFs can influence any of the accepted stages in carcinogenesis", but stressed the need for urgent research. The NRPB stressed the inability of ELF fields to damage DNA directly, which is accepted, and considered cancer promotion (accelerating an existing cancer) but not indirect initiation of cancer.

Another main concern is about exposure to EMFs at other frequencies, i.e. radiofrequency. Research suggests relevant effects in cell signalling, cell regulation, immune suppression, melatonin synthesis and calcium uptake. NRPB-AG recognizes some positive findings but insufficient verification to be persuaded (http://www.europarl.europa.eu/). Moreover, few epidemiological studies associate the RF EMF exposure to an increase in cancer or childhood leukaemia occurrence. But these reports have not been conclusive in

indicating detrimental effects on human health (Rothman, 2000; Schuz et al., 2006). Published studies have also suggested associations of RF EMFs with depression, suicide and Alzheimer's disease. Minor ill effects, such as headaches and sleeplessness, are much more commonly reported at the anecdotal level. Continual buzzing in the ears, interfering with sleep and normal life, has also been reported. The studies conducted on these effects noted that all of these symptoms can also be easily attributed to stress and that they cannot be separated from nocebo effects (Röösli, 2008).

Nonetheless, it is now years since the number of mobile phones in Europe exceeded the number of people and phone network coverage is almost everywhere. Wi-Fi networks, phone masts, power lines, GPS receivers are considered some of the main causes of the growing amount of electromagnetic waves. Human beings are now almost constantly exposed to a “cocktail” of electromagnetic fields and the health risks are still to be fully characterized, despite the increasing number of research on the potential effects of this daily exposure.

The World Health Organization (WHO) stated that given the novelty of mobile telephony the public health consequences won’t be known until 2015, deadline for the submission of the data provided by Interphone project, a cooperative research among 13 countries, aimed at investigating the risk of cancer for the mobile phone users over 10 years of study.

At present there are no EU-wide laws governing the safety of mobile telephony, but a recommendation (http://www.europarl.europa.eu/). One of the EU Parliament report calls for action provides the precautionary principle, based on the International Commission on Non-Ionizing Radiation Protection (ICNIRP) and already used in other forms of public policy. It calls for the following steps: an EU limit of 3 volts per metre (already adopted by at least nine countries); antennas and phone masts set at a specific distance from schools and hospitals; maps of exposure to high-voltage power lines, radio frequencies and microwaves publicly available online.

Since it is well known that both ELF and HF EMFs are biologically active, even though the mechanism of action has not been completely explained (Hendee and Boteler, 1994; Maisch and Rapley, 1998), the current policy adopted by many EU countries is based on public information and precautionary principle, the latter enshrined in policy to limit harm when scientific knowledge is not conclusive (http://www.europarl.europa.eu/). On the

other hand, assessing the sanitary risks due to the electromagnetic field is extremely complicated and so far a high number of different theories have been published, dealing with this issue from different approaches. A multidisciplinary approach is to be preferred since it can take into consideration different aspects involved, such as biological, medical, epidemiological, physical and technological competence, as established in the last few years by the WHO and the ICNIRP.

1.2.4 - POSSIBLE BIOLOGICAL EFFECTS OF ELECTROMAGNETIC FIELDS

While it's clear that high-energy electromagnetic fields, such as X-rays, may introduce biological effects through ionizing damage, what is less certain is the extent to which low-energy non-ionizing EMFs may influence biological systems.

A main distinction between biological and health effects must be made. Biological effects are measurable responses to an external stimulus that are not necessarily harmful, because of the body mechanisms of reaction. Nonetheless biological effects that lead to irreversible changes or stress the organism for long periods of time may constitute a health hazard. An adverse health effect causes detectable impairment of the health of the exposed individual or of his or her offspring; a biological effect, on the other hand, may or may not result in an adverse health effect.

It is not disputed that electromagnetic fields above certain levels can trigger biological effects.

The human population conducts their daily lives in an ever increasing sea of electromagnetic waves, particularly in cities and public buildings. Man-made sources of electromagnetic fields that form a major part of industrialized life - electricity, microwaves and radiofrequency fields – are unable to break chemical bonds, but can penetrate a body according to their frequency and the properties of the medium passed through (Table 1.1). For the soft materials of a human body, roughly an aqueous medium, the wave penetration is nearly a tenth of its wavelength.

Table 1.1 – Wavelength and penetration depth of different kind of electromagnetic waves.

Frequency	Wavelength	Penetration
50 Hz	$6 \cdot 10^6$ m	$6 \cdot 10^5$ m
1 KHz	$3 \cdot 10^6$ m	$3 \cdot 10^4$ m
1 MHz	300 m	30 m
140 MHz	2.14 m	0.214 m
434 MHz	0.69 m	0.069 m
915 MHz	0.33 m	0.033 m
1 GHz	0.3 m	0.03 m
1.81 GHz	0.17 m	0.017 m

The amount of energy a body can absorb depends on the wavelength: electromagnetic waves that cannot penetrate deeply into a body can release a smaller amount of energy than those waves that can go deeper. This feature leads to the main distinction between low frequency electromagnetic waves (v<300 Hz) and high frequency electromagnetic waves (v>300 Hz).

The electric charges in a body are excited by the incoming electromagnetic field, thus the interactions with the human bodies are depending on the electromagnetic wave frequency. Low frequency waves have wavelengths higher than 1000 km; therefore a body perceive the electromagnetic field as if it was constant. Nonetheless they create electric currents inside the body, due to the oscillating magnetic field. Household appliance with a 100 μT magnetic field, which oscillate at a frequency of 50 Hz, can induce a current of $5 \cdot 10^{-6}$ A/m^2 inside human body. However high-voltage lines are characterized by 10 times smaller magnetic fields (10 μT), which induces lower electric currents: at a distance of 20-30 cm the induced current is in the range of 10^{-7} A/m^2. The limit above which acute effects can be detected is $2 \cdot 10^{-3}$ A/m^2.

Tiny electrical currents exist in the human body due to the chemical reactions that occur as part of the normal bodily functions, even in the absence of external electric fields. For example, nerves relay signals by transmitting electric impulses, many biochemical reactions from digestion to brain activities go along with the rearrangement of charged particles, and the heart is electrically active.

Low-frequency magnetic fields induce circulating currents within the human body and the strength of these currents depends on the intensity of the outside magnetic field. If

sufficiently large, these currents could cause stimulation of nerves and muscles or affect other biological processes.

High frequency electromagnetic fields (~2 GHz) can penetrate very shortly inside the bodies. Even for the waves emitted by mobile phones base stations the penetration inside the body is less than 10 cm, which is a very short distance compared to human body scale, and at the same time their oscillating frequency is so fast that the energy is transferred very quickly. Therefore such a short penetration doesn't allow the induction of electric currents inside the body, but the thermal effects due to the energy transfer can be in this case significant. A 600 W power, typical of a GSM base station antenna, can lead to a $5.4 \cdot 10^{-6}$ °C increase in body temperature when the distance between the antenna and the body is 30 cm.

GSM 900 handsets have 2 W peak and 0.25 W average of heating power. GSM 1800 handsets have half this power level. With a mobile phone with a maximum power of 1 W, the energy produced is 200 W/(m^2·sec), equal to one fourth of the energy produced by solar radiation. This energy could potentially lead to an over-heating of the parts that are in contact with the mobile phone (mainly ear, head and hand). A 0.1°C increase in the temperature of heads exposed for 15 minutes inside an adiabatic cage has been recorded. But in normal conditions, the physiological mechanisms for heat dispersion lower the temperature, by dispelling the heat through the blood stream. Thermal effects on humans are noticeably reduced and therefore considered negligible.

For many years the thermal effects have been the only acknowledged effects, but some research are recently showing also non-thermal effects, due to the interaction between the waves and the body's molecular structures. Nonetheless the consequences of non-thermal effects are still to be studied in depth.

Modelling the energy absorption by matter could be an interesting and extremely useful approach. The electric conductibility and the dielectric property of the crossed matter are two necessary parameters to gain a reliable measure of the specific absorption rate (SAR), considered a fundamental dosimetric quantity in this kind of studies. It is defined as the power absorbed per mass of tissue (W/kg) and it can be calculated from the electric field within the tissue as:

where σ is the sample electrical conductivity, |E| is the magnitude of the induced electric field and ρ is the sample density.

For humans it is almost impossible to calculate the exact SAR value, since the electrical conductivity in human body is not defined and the induced electric field is extremely hard to measure. Therefore it is usually averaged either over the whole body, or over a small sample volume (typically 1 g or 10 g of tissue). The value cited is then the maximum level measured in the body part studied over the stated volume or mass.

SAR is used to measure the rate at which RF energy is absorbed by a biological target when exposed to EMFs between 100 kHz and 10 GHz. It is commonly used to measure power absorbed from mobile phones and during magnetic resonance imaging (MRI) scans. The value will depend heavily on the geometry of the part of the body that is exposed to the RF energy and on the exact location and geometry of the RF source. Thus tests must be made with each specific source, such as a mobile phone model, and at the intended position of use. For example, when measuring the SAR due to a mobile phone the phone is placed at the head in a talk position. The SAR value measured is then the value measured at the location that has the highest absorption rate in the entire head, which for a mobile phone often is as close to the phone as possible.

Various governments have defined safety limits for exposure to RF energy produced by mobile devices that mainly exposes the head or a limb for the RF energy. In the United States the Federal Communication Commission (FCC) requires that phones sold have a SAR level at or below 1.6 watts per kilogram (W/kg) taken over a volume of 1 gram of tissue. In the European Union SAR limits have been set at 2 W/kg averaged over 10 g of tissue, as specified by the European Committee for Electrotechnical Standardization (CENELEC), following the International Electrotechnical Commission (IEC) standards (IEC 62209-1).

1.3 - APPLICATIONS OF NON-IONIZING ELECTROMAGNETIC FIELDS

Typical industrial application of non-ionizing electromagnetic field can be:

- Maritime transmission, video terminals (3 – 30 kHz)
- Maritime transmission, welding, fusion, temper, sterilization, AM radio transmission, telecommunication, radio navigation (100 kHz – 3 MHz)

- Heating, desiccation, gluing, welding, polymerization, dielectric substances sterilization, medical application, civic and international radio transmission, radio astronomy (3 – 30 MHz)
- FM radio transmission, TV-VHF emission, air traffic radar, mobile and portable transmitter, mobile telephony (30 – 300 MHz)
- Road traffic radar, meteorological radar, mobile telephony, telemetry, medical application, microwave ovens, alimentary industry process (300 MHz – 3 GHz)
- Altimeter, sea traffic radar, satellite communication, police radar (3 – 30 GHz)
- Radio astronomy, radio meteorology, microwave spectroscopy (30 – 300 GHz)

1.3.1 - GSM TRANSMISSION

The Global System for Mobile communications (GSM) is the most popular standard for mobile phones in the world. Its promoter, the GSM Association, estimates that 80% of the global mobile market uses this standard. GSM is used by over 3 billion people across more than 212 countries and territories. Its ubiquity makes international roaming very common between mobile phone operators, enabling subscribers to use their phones in many parts of the world. GSM differs from its predecessors in that both signalling and speech channels are digital, and thus is considered a second generation (2G) mobile phone system. This has also meant that data communication was easy to build into the system.

The ubiquity of the GSM standard has been an advantage to both consumers (who benefit from the ability to roam and switch carriers without switching phones) and also to network operators (who can choose equipment from any of the many vendors implementing GSM). GSM also pioneered a low-cost (to the network carrier) alternative to voice calls, the short message service (SMS, also called "text messaging"), which is now supported on other mobile standards as well. Another advantage is that the standard includes one worldwide emergency telephone number, 112. This makes it easier for international travellers to connect to emergency services without knowing the local emergency number.

Newer versions of the standard were backward-compatible with the original GSM phones. For example, Release '97 of the standard added packet data capabilities, by means

of General Packet Radio Service (GPRS). Release '99 introduced higher speed data transmission using Enhanced Data Rates for GSM Evolution (EDGE).

GSM is a cellular network, which means that mobile phones connect to it by searching for cells in the immediate vicinity. There are five different cell sizes in a GSM network—macro, micro, pico, femto and umbrella cells. The coverage area of each cell varies according to the implementation environment. Macro cells can be regarded as cells where the base station antenna is installed on a mast or a building above average roof top level. Micro cells are cells whose antenna height is under average roof top level; they are typically used in urban areas. Picocells are small cells whose coverage diameter is a few dozen metres; they are mainly used indoors. Femtocells are cells designed for use in residential or small business environments and connect to the service provider's network via a broadband internet connection. Umbrella cells are used to cover shadowed regions of smaller cells and fill in gaps in coverage between those cells.

Cell horizontal radius varies depending on antenna height, antenna gain and propagation conditions from a couple of hundred metres to several tens of kilometres. The longest distance the GSM specification supports in practical use is 35 kilometres. There are also several implementations of the concept of an extended cell, where the cell radius could be double or even more, depending on the antenna system, the type of terrain and the timing advance.

The structure of a GSM network (Fig. 1.4) is large and complicated in order to provide all of the services required. It is divided into a number of sections and these are each covered in separate articles:

- Base station subsystem (the base stations and their controllers)
- Network and switching subsystem (the part of the network most similar to a fixed network)
- GPRS core network (the optional part which allows packet based on internet connections)

All of the elements in the system combine to produce many GSM services such as voice calls and SMS.

One of the key features of GSM is the Subscriber Identity Module, commonly known as a SIM card. The SIM is a detachable smart card containing the user's subscription information and phone book. This allows the users to retain their information after switching handsets. Alternatively, the user can also change operators while retaining the

handset simply by changing the SIM. Some operators will block this by allowing the phone to use only a single SIM, or only a SIM issued by them.

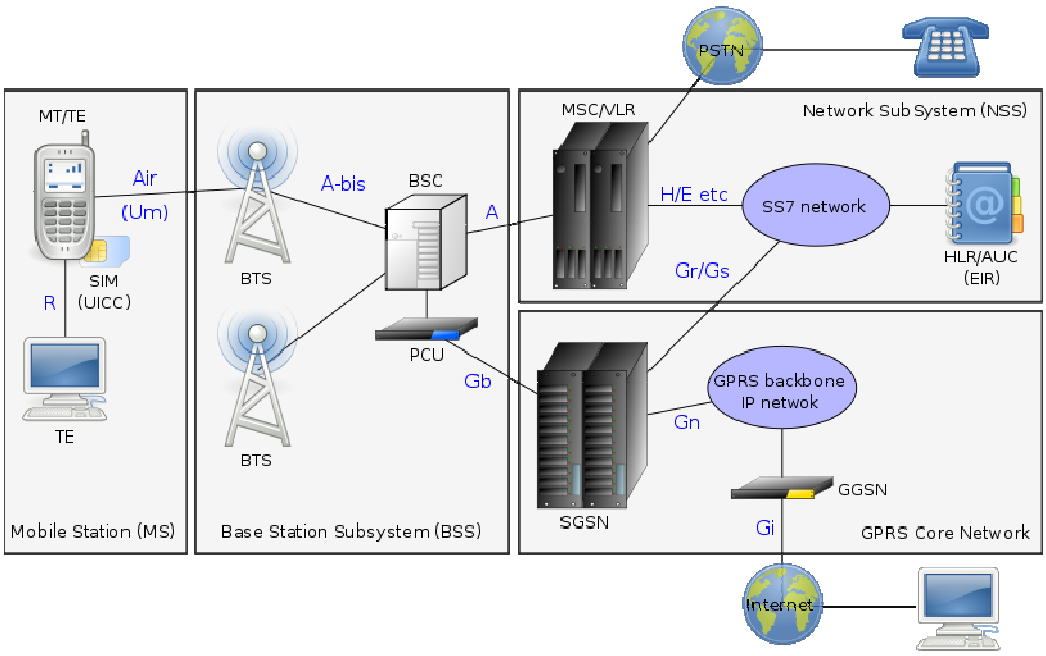

Fig. 1.4 – The structure of a GSM network: key elements subsystems (mobile station, base station, network and switching, and GPRS core network) are schematically represented.

GSM networks operate in a number of different frequency ranges (separated into GSM frequency ranges for 2G and UMTS frequency bands for 3G). Most 2G GSM networks operate in the 900 MHz or 1800 MHz bands. Some countries in the Americas (including Canada and the United States) use the 850 MHz and 1900 MHz bands because the 900 and 1800 MHz frequency bands were already allocated. Most 3G networks in Europe operate in the 2100 MHz frequency band, though 3G is not based on the GSM technology. The rarer 400 and 450 MHz frequency bands are assigned in some countries where these frequencies were previously used for first-generation systems.

The transmission power in the handset is limited to a maximum of 2 W in GSM 850/900 and 1 W in GSM 1800/1900.

Table 1.2 – The features of the two main GSM frequency ranges.

	Base station transmit	**Handset transmit**	**Peak handset power**
GSM 900	935-960 MHz	890-915 MHz	2 W
GSM 1800 (PCN)	1805-1880 MHz	1710-1785 MHz	1 W

GSM uses a combination of frequency division multiple access (FDMA) and time division multiple access (TDMA). This means that within each band there are a hundred or so available carrier frequencies on 200k Hz spacing (the FDMA bit), and each carrier is broken up into time slots so as to support 8 separate conversations (the TDMA bit). Correspondingly, the handset transmission is pulsed with a duty cycle of 1:8; and the average power is one eighth of the peak power. Once a call is in progress, the phones are designed to reduce the radiofrequency (RF) output power to the minimum required for reliable communication - under optimum conditions, the power can be set as low as 20 mW (one hundredth of full power). Battery consumption and radiation output of the handset is further reduced by using 'discontinuous transmission' (DTX); the phone transmits much less data during pauses in the conversation.

The basic handset transmission consists of carrier bursts of 0.577 ms duration, repeating every 4.615 ms, giving a repetition rate of 216.7 Hz. This means that for one eighth of a so-called frame is being used for transmitting the signal by a mobile. One timeframe has duration of 4.616 ms and each time frame is divided into eight 577 μs slots. The mobile emission can occur only during one of this 577 μs slot. The energy transferred to the biological target is therefore all gathered in one slot, in which it will be 8 times higher than the average. The modulation used in GSM is Gaussian minimum-shift keying (GMSK), a kind of continuous-phase frequency shift keying. In GMSK, the signal to be modulated onto the carrier is first smoothed with a Gaussian low-pass filter prior to being fed to a frequency modulator, which greatly reduces the interference to neighbouring channels (adjacent channel interference). Owing to the coding and control protocols, every 26^{th} pulse is omitted during a conversation, leading to a component in the output modulation at 8.33 Hz.

The general consensus of the scientific community and the relevant radiation - protection bodies is that there is no significant evidence of a health risk from mobile phones. Nevertheless, some people still claim to suffer headaches and other symptoms which they blame on their phone. Long term effects, of course, can only be observed after a long time. The official line is basically that they are safe, but some caution wouldn't go amiss. The emitted RF energy will be much reduced by using the phone in a good signal area (e.g. line of sight to the base-station), whereas use in a poor signal area like inside a lift or a tunnel will result in the phone using a much higher power.

People should consider the following points: with a 2 W transmitter power the RF field strength, within a couple of centimetres of the aerial, is quite high (around 400 V/m). For comparison, most electronic equipment is usually only guaranteed to operate normally in fields up to 3 V/m. Use of a phone within a few metres of electronic equipment can cause interference, and possible malfunction.

The pulsed structure of the output has, rightly or wrongly, also been a source of concern for human well-being, mainly because the component at 8 Hz is close to brainwave frequencies.

Besides the magnetic component of the RF field, a mobile phone would be expected to emit a weak, low frequency magnetic field. This will be generated by the power wiring inside the phone as the 2 W transmitter (around 1 A from the 2 V battery) is switched on and off. Although the strength of this field is much less than the Earth's constant magnetic field, recent studies have indicated that even very weak switched magnetic fields are capable of affecting neurons in the brain, and of aborting epileptic fits.

What is for sure is that RF energy to which the public are exposed from base stations is typically less than one thousandth of the strength of that from holding a handset to the ear. Technically higher power television transmitters have been operated on similar frequencies (to GSM 900) for many years (albeit with different modulation structure), and yet have not caused such an outcry.

1.3.2 - MEDICAL DEVICES

Studies on the biological effects of high frequency electromagnetic fields have resulted in significant developments in medical application for electromagnetic fields, after the development of high-strength superconducting magnets. Antennas and electromagnetic devices are an integral part of medical applications ranging from imaging to hyperthermia treatment and communications for tissue-implanted devices.

The medical use of high frequency EMFs is well established and is currently employed by physiotherapists to accelerate recovery from strains (Van Nguyena and Marks, 2002) and is also used in oncology for breast tumour ablation through hyperthermia (Wu et al., 2006: Van Wieringen et al., 2009) and as an adjunction in radiotherapy (Franckena et al., 2009).

The use of heat in cancer treatment dates back to the ancients with the application of red-hot irons by Ramajama (2000 B.C.), Hippocrates (400 B.C.) and Galen (200 A.D.). In more recent times, Westermark (1898) placed hot water circulating cisterns into advanced carcinomas of the uterus and found palliative shedding of some tumours. Coley (1927) introduced "toxin" therapy for cancer, but stated that responses were associated with temperatures of 39-40° for several days duration, suggesting that the febrile reaction might have been the tumoricidal agent. Simultaneously Keating-Hart and Doyen (1910) introduced electro-coagulation of tumours, which is still in use today. Warren (1933) was one of the first to apply infrared and high frequency current heating of tumours and found objective remissions of some cancers. With the subsequent development and popularity of X-irradiation therapy, hyperthermia research was all but abandoned until modern times when the selective thermo-sensitivity of tumour cells was more fully appreciated (Storm, 1981).

Numerous recent studies have shown the usefulness of controlled local hyperthermia as an adjunct in tumour therapy. Application of microwave or ultrahigh frequency (UHF) energy can be used to produce the required heating.

An increased interest in applications of electromagnetic techniques in medical diagnosis and therapy has been observed since 70's. In therapy, there are indications that local and/or whole body hyperthermia provides successful modality in treatment of some malignant tumours. Microwave energy is one of the effective ways of inducing rapid hyperthermia, but difficulties are experienced in heating deep laying tissues and heating a relatively large volume of tissue.

In general, the desired characteristics of a microwave radiator include: an effective deposition of the energy in a defined tissue volume (e.g. in the muscle without overheating the skin), good impedance matching, minimum leakage of microwave energy into the outside of the treated area and lightweight, rugged and easy to handle design (Bahl et al., 1980).

At temperatures between 41-45°C, cancer cells are more sensitive to heat than their normal cell counterparts. *In vitro* and *in vivo* tumour models have shown irreversible damage and complete regression of various tumours at 42-45˚C, while normal cells were killed at least one degree higher temperature of more than double the duration of heating. That's because less-well oxygenated cells seem to be most vulnerable to thermal injury (Storm, 1981). Hyperthermia causes alteration in both DNA and RNA synthesis, as well as

depression of multiple cellular enzymatic systems required for cell metabolism and division. Its major model of action may be to increase cell and lysosome membrane permeability, causing selective internal destruction of the cancer cell.

The organs and organ systems affected by microwave/radio frequency (MW/RF) exposure are reported to be susceptible, in terms of functional disturbance and/or structural alterations. Some reactions to MW/RF exposure may lead to measurable biological effects which remain within the range of normal (physiological) compensation which can be used for therapeutic purposes. Some reactions on the other hand, may lead to effects which may be potential or actual health hazards.

Most of the biological data are explained by thermal energy conversion, almost exclusively as enthalpy energy (heating) phenomena. This conclusion, however, does not provide a predictive model of the biological consequences of non-uniform absorption of energy in animals and humans that can result in unique biological effects. Furthermore, induced temperature gradients in deep body organs may act as a functional stimulus to alter normal function both in the heated organ and in other organs of the system. It should also be pointed out that temperature rises from diverse aetiologies may induce chromosomal alterations, mutagenesis, virus activation, and inactivation, as well as behavioural and immunological reactions. The non-uniform pattern of microwave absorption, with differing rates of temperature rise at absorption sites, results in a pattern of heating which cannot be replicated with radiant, convected, or conducted heat (Michaelson, 1980).

An improvement to microwave application has been gained about 10 years ago through the development of a needle-like medical device, which ablate dysfunctional tissue by RF application. This is called radio frequency ablation (RFA) and is a medical procedure where tumour or other dysfunctional tissue is ablated using microwave energy to treat a medical disorder. Once the diagnosis of tumour is confirmed, a needle-like RFA probe is placed inside the tumour. The radiofrequency waves passing through the probe increase the temperature within tumour tissue that results in destruction of the tumour. Generally RFA is used to treat patients with small tumours that started within the organ (primary tumours) or that spread to the organ (metastasis). RFA has shown promise as a technique for treating solid tumours in the ideal size of 5-7 cm (Gao et al., 2008) which cannot be removed surgically (Bauditz et al., 2008).

Another device proposed for treating cancer is the Kanzius RF Machine, a radiowave generator that warms nanoparticles attached to or absorbed within cancer cells. The warming kills the cancer cells with little or no damage to nearby cells. Unique physical characteristics (a protein, a receptor, etc.) of specific cancer cell lines are identified, a "targeting molecule" is chemically attached to a gold nanoparticle or carbon nanotube, and the combination is injected into the bloodstream of the patient. The targeting molecule eventually delivers the nanoparticle to the cancer cell (Cardinal et al., 2008).

1.3.3 - RADIOWAVE CANCER THERAPY

Few therapeutical approaches to date have been reported to demonstrate divergent properties in tumour and normal tissue as may be observed from radiowave exposure (Lazebnik et al., 2007). Lazebnik et al. (2007) have shown breast tumour tissue and normal tissue to have different properties when exposed to radiowaves in the 100 MHz – 20 GHz range, with cancerous tissue showing an approximative 10 fold higher dielectric constant and 50-100 fold greater effective conductivity than normal tissue in the 100-500 MHz range. Several different applicators are now commercially available for treating various tumour locations, such as the BSD2000 (BSD Medical Hyperthermia Systems, USA) and a RF-phased array heat applicators. Deep-seated tumours that are located more than 3 cm under the skin surface can be treated by deep regional hyperthermia provided by focused EM energy radiated at about 100-140 MHz delivering up to 50 W per dipole (Li et al., 2008).

External heating devices appropriate for deep hyperthermia in the intact breast include ultrasound phased arrays (Hynynen et al., 2001) and radio-frequency (RF) electromagnetic phased arrays (Gromoll et al., 2000). Ultrasound is a local modality for heating small targets in the breast (up to about 2 cm diameter (Malinen et al., 2004)), whereas heat generated by RF electromagnetic devices is delivered regionally across a much larger area. RF phased arrays have been developed previously for deep hyperthermia in the pelvis (Wust et al., 1991) and in the extremities. These arrays apply RF frequencies in the 60–140 MHz range for increased penetration while delivering heat to deep targets. A microwave phased array system has also been constructed for thermal therapy in the breast (Fenn et al., 1999).

To exploit the greater penetration depths afforded by RF applicators, a four channel RF phased array applicator has been developed for hyperthermia cancer treatments in the

intact breast. This phased array operates at 140 MHz, which increases the penetration depth substantially over that achieved by microwaves. This RF phased array has been characterized with measurements of the electric field, and these measurements are consistent with the fields predicted by finite-element simulations. Additional finite element and bio-heat transfer modelling results suggest that this array is capable of delivering therapeutic heat in an idealized model of the breast. These measurement and simulation results show that this RF phased array system can focus the electric field within a water tank and in simulated tumour targets in the breast (Wu et al., 2006).

Most clinicians view RF as merely a vehicle by which direct and focused heating may be achieved. A more recent developed technique that involves non-thermal EMF effects is electroporation and is employed in the treatment of radiotherapy and chemotherapy resistant tumours and usually combined to other cancer therapies (Hofman et al., 1999). Radiowave therapy is not a microwave treatment, even though it is based on non-ionising, radiofrequency radiation, while radiotherapy uses X-rays or y-rays (ionizing radiation). A new approach to cancer cure is based on the use of both of them altogether: patients are exposed to radiofrequency electromagnetic waves, acting as a sensitizing agent prior to low-dose, external-beam radiotherapy.

In particular, the metabolism of cancer cells seems to be affected at the specific frequency of 434 MHz, which is supposed to have a non-thermal effect on the physiology of cancer cells (Holt, 1977).

The amount of RF energy that is absorbed by human body tissue and the rate at which the energy decreases with the depth of penetration depends on both the type of tissue that the energy passes through and on the frequency of the incident radiation. At radio frequencies below 4 MHz the body is essentially transparent to the energy. As the frequency is increased, more energy is absorbed by the human body. Radiowaves at the specific frequency of 434 MHz have a non-thermal effect on the physiology of cancer cells, namely increased cell division or some changes in the electrochemistry of cells evidenced by resonance effects (Holt and Nelson, 1985; Holt, 1988; Trotter at al., 1996; Holt 1997; Kirson et al., 2004).

Differences have been observed in the power spectrum of the radiowave waveform emitted by cancer patients' bodies during radiowave treatment (Fig. 1.5), compared to the spectrum emanating from people without cancer (Joines et al., 1980). The power spectrum,

or spectral density, describes the power contribution to a signal at various frequencies. This can be measured by a spectrum analyzer.

The changes in radiowave reflection pattern and absorbed power caused by a cancer ceases within one to two minutes of death. This effect is thought to be due to the interaction of 434 MHz and charged radicals present in cancer cells (Holt, 1977). This postulation was supported with the observation that when a tumour decreased in size during the course of a treatment the power spectrum would gradually return to the "normal" unimodal shape. This difference can be attributed to an electrical resonance effect in cancer cells when they are stimulated by RF energy, specifically at 434 MHz. This resonance effect could be attributed to some change in the electrical conductivity of malignant cells, although this was not elucidated.

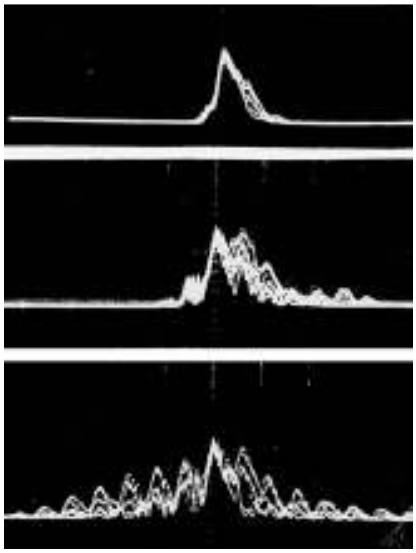

Fig. 1.5 – Changes in the power spectrum of the radiowave waveform emitted by patients' bodies during radiowave treatments. Top: patient without cancer, middle and bottom: patients with cancer. From Holt, 1977.

The proportion of cancer cells killed by using H-wave polarised 434 MHz electromagnetic radiation applied fifteen minutes before low doses (0.5 to 0.8 Grays) of X-radiation (140, 220, 330 KV, 4 MeV and Co^{60} sources) is between three and over one hundred times better than X-radiation alone. This increased sensitivity to X-radiation varies with the cancer's site, with the physical features of host and cancer, with the cancer growth rate, with the 434 MHz dose delivered and absorbed, with the normothermic X-radiation sensitivity and other as yet unknown factors (Holt and Nelson, 1985; Trotter et al., 1996; Van der Zee et al., 2000).

Few cancer therapeutic approaches to date have been reported to demonstrate such divergent properties in tumour and normal tissue as may be observed when tissues are exposed to high-frequency radiowaves (Lazebnik et al, 2006). The observation of such contrasting properties provides great impetus to develop and exploit the full therapeutic potential of radiowave exposure and more specifically to investigate this relatively novel approach to cancer therapy.

The precise sub-cellular effects of exposure to high energy RF have yet to be elucidated limiting our ability to exploit its therapeutic potential to the full. This part of the study is a preliminary research from initial *in vitro* exposures to confirm if tumour prostate cells are more RF sensitive than non-tumour prostate cells. The long term rationale is addressed, in a methodical manner, how to maximize the targeting of only tumour cells, without damaging non-tumour cells, and will examine the efficacy of RF as a stand-alone approach to cancer therapy.

1.4 - EXPERIMENTAL EXPOSURE SYSTEMS

1.4.1 - 1.8 GHz GSM EXPOSURE SYSTEM

Following the specifications outlined by Schönborn et al. (2000), this setup consists of two 128.5 × 65 × 424 mm^3 brass single-mode waveguide resonators operating at a carrier frequency of 1800 MHz, and placed inside a commercial incubator (fig. 1.6).

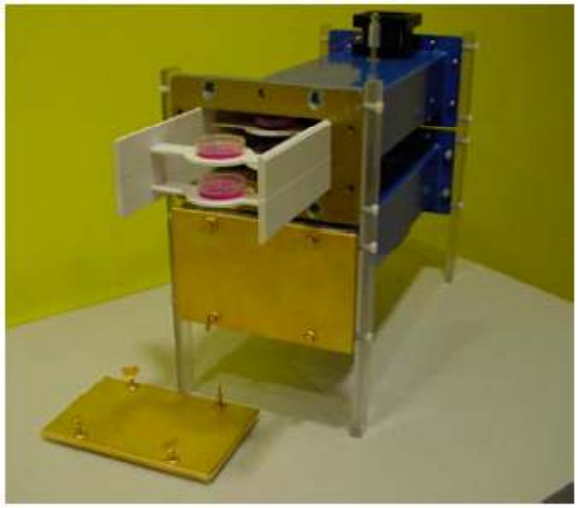

Fig. 1.6 – The 1.8 GHz GSM exposure system.

The waveguides (cross section: 129.6 mm, 64.8 mm) and coupler were optimized to achieve a resonance with minimal field disturbance inside the waveguide cavity. This was achieved by adjusting the length for a resonator mode at 1800 MHz.

A flat loop coupler (Fig. 1.7) on one end of the waveguide and an end-short plate on the other end were gold plated to ensure good RF contacts.

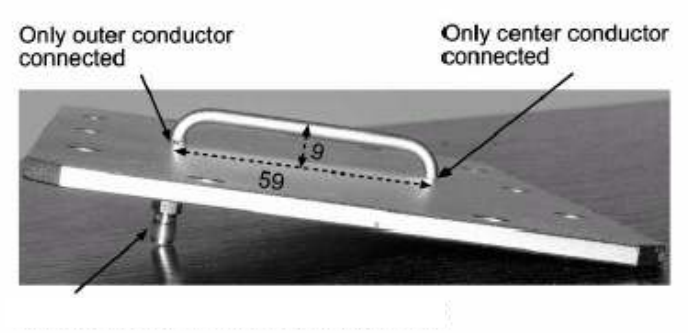

Fig. 1.7 – The short-end plate with bent semi-rigid cable.

This resonant waveguide enables the exposure of cells at a carrier frequency, which approximates exposure from mobile communication systems like DCS (uplink: 1710–1785 MHz; downlink: 1805–1880 MHz), PCS (uplink: 1850–1910 MHz; downlink: 1930–1990 MHz), and universal mobile telecommunication system (UMTS, uplink: 1920–1980 MHz; downlink: 2110–2170 MHz).

The exact resonance frequency is determined prior to exposure by a frequency sweep for maximum field strength at the monopole field sensor. Time cycles of 0.546 ns allow a frequency of 1.8 GHz magnitude. After the signal is generated, an oscillating electric field is produced along the antenna and an oscillating magnetic field circulates around the antenna (Fig. 1.8). Only the waves which hit the walls of the waveguide at the right angle can survive, because the E-field must be zero at the walls.

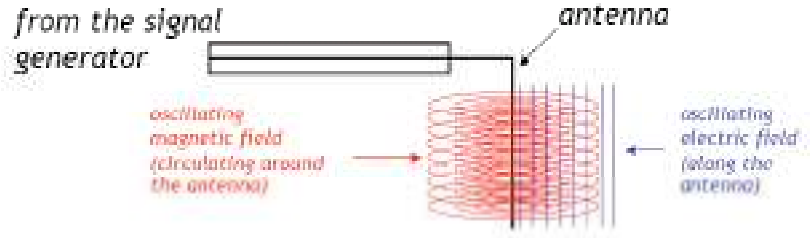

Fig 1.8 – A scheme of how the electromagnetic field is generated inside the waveguides of the exposure system.

For the RF signal source the following requirement were specified: the carrier frequency is 1800 MHz and the modulation is GSM like. At these conditions a 1.8 GHz electromagnetic field will induce a 2 W/kg of SAR on the cell monolayer. This value is the safety limit for local exposure to telecommunication established by the International Commission on Non-Ionizing Radiation Protection (ICNIRP) and it's calculated over 10 g of biological matter for the extremities.

Each resonator is equipped with a plastic holder hosting six 35 mm Petri dishes (effective inner diameter 33 mm) arranged in two stacks (Fig. 1.9).

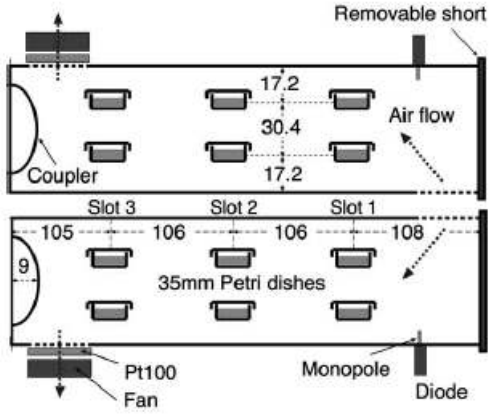

Fig. 1.9 – Side view of geometry and functional parts of the exposure system. The configuration for the cell monolayer is shown (all dimensions in millimetres).

The waveguide behaves as a resonant cavity, in which the interferences among waves create a stable field configuration. There are fixed points (nodes) in which the electric field is maximum and magnetic field is null (Fig. 1.10). This electromagnetic field can therefore be considered static.

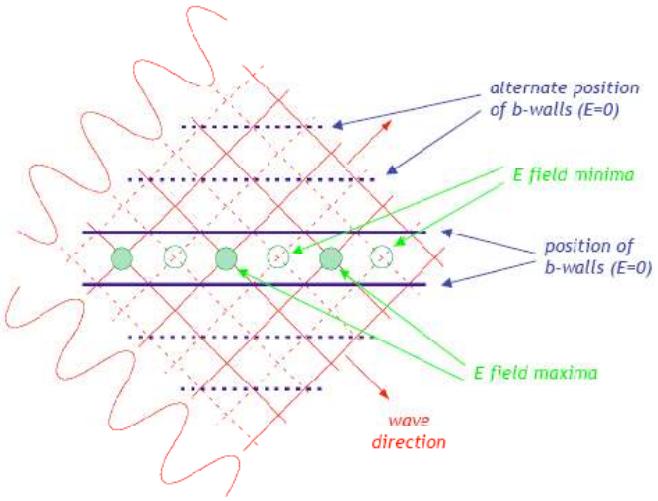

Fig. 1.10 – The configuration of the electric field generated by the antenna.

The waveguide cavities were optimized for cell monolayer exposure (Schuderer et al., 2004). The dishes are placed in the H-field maxima of the standing wave inside the waveguide (Fig. 1.11) and therefore their position inside the exposure system is fixed and unchangeable.

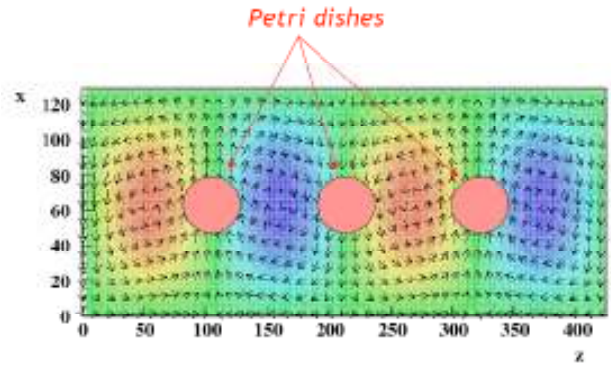

Fig. 1.11 – The theoretical distribution of the E-field (colours) and the H-field (arrows) inside the waveguide and the geometrical collocation of the petri dishes.

The function of the wave propagating inside the waveguide is:

$E = E_0 \cos(\omega t - kr)$

where k is the wave number k = ($n_a \cdot \pi/a$; $n_b \cdot \pi/b$; $n_l \cdot \pi/b$) and r is the position vector in relation to the antenna. The possible frequencies of this electromagnetic field are:

$$v = \frac{\omega}{2\pi} = \frac{kc}{2\pi} = \frac{c}{2\pi}\sqrt{\frac{n_a^2}{a^2} + \frac{n_b^2}{b^2} + \frac{n_l^2}{l^2}}$$

since the electric field is parallel to b direction, n_b is 0.

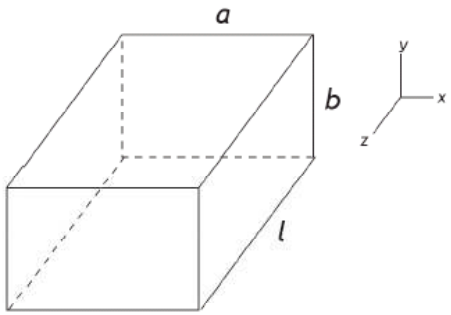

a=129.6 mm
b=64.8 mm
l=425 mm

Note: the resonant frequency is slightly reduced when the Petri dishes are inserted, due to the high conductivity of the medium.

na	nb	nl	frequency (GHz)
1	0	1	1,209
2	0	1	2,340
3	0	1	3,488
1	0	2	1,355
2	0	2	2,418
3	0	2	3,541
1	0	3	1,568
2	0	3	2,544
3	0	3	3,628
1	0	4	1,824
2	0	4	2,710
3	0	4	3,746
1	0	5	2,109
2	0	5	2,909
3	0	5	3,892
1	0	6	2,412
2	0	6	3,135
3	0	6	4,064

Fig 1.12 – The resonant frequencies possibly achieved according to the geometrical features of the waveguide employed.

All the resonant frequencies can be then calculated: among them there is the one used for GSM mobile phone transmissions (Fig. 1.12).

An electromagnetic field probe is placed inside each waveguide, in order to find the desired frequency able to create the right resonance.

When the exposure system is started up, the antenna emits a series of signals, very close to the theoretic frequency of 1.824 GHz, which are measured by the electromagnetic field probe, in order to detect the desired one. This frequency is influenced by the presence of conductor materials, which can reduce the resonant frequency to 1.818 GHz.

The carrier frequency, modulation, periodically repeated on- and off-time of exposure and the SAR level are controlled by a computer. In particular, the waveform and the exposure/sham condition are assigned to the two waveguides by the computer controlled signal unit. All exposure conditions and monitor data are encrypted in a file, which is decoded only after data analysis in order to ensure blind conditions for the experiment.

The described concept is used for GSM modulation in the following way (Fig.1.13). The GSM burst, defined according to ETSI-GSM recommendation, is stored at the function generator and is applied to the AM modulation input of the RF generator. The frame structures of the basic crest factor and DTX crest factor modes are stored on the radio frame generator. Switches between both frame structures are software controlled and carried out by the data logger. Software regulation of the output power of the RF generator according to statistical functions is used to simulate the environmental events of a GSM phone conversation like channel fading, handovers, etc.

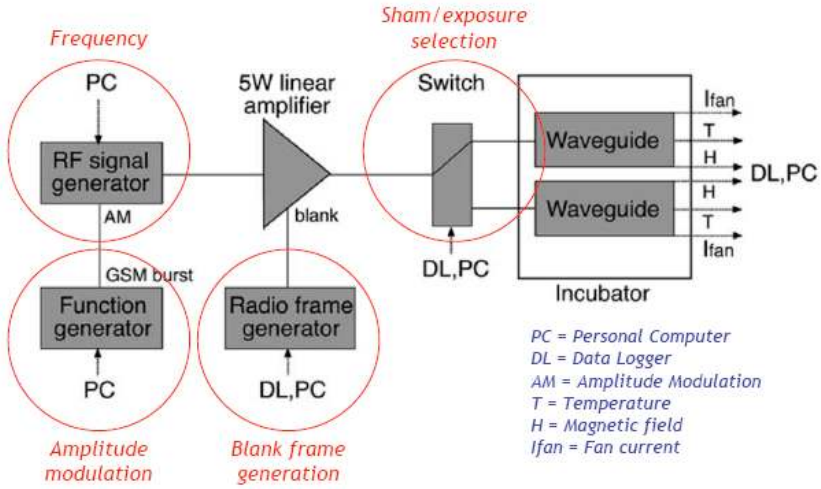

Fig 1.13 – The scheme of the experimental setup.

A flexible signal unit is present to enable complex modulation (Fig. 1.14) such as:

1) continuous wave;

2) pulse or sinusoidal modulation at any frequency and repetition rate: a 217 Hz amplitude modulation is usually applied to mimic the TMDA which GSM signal is based on. The pulse modulation is furthermore equal to a multiple amplitude modulation (23.4% of 217 Hz; 21.6% of 434 Hz and 18.9% of 651 Hz). This creates a wave summation that produces square waves.

3) GSM signals simulating:

i) the basic GSM mode (basic) active during talking into the phone: a further 8.34 Hz pulse modulation is added (217 Hz/26). As in a mobile emission, one out of every 26 frame is left signal-free for technical reasons.

ii) the DTX mode active while listening: the wave is modulated at 217 Hz, but the signal is emitted only for short periods. As in a mobile reception, the few emitted signal are in order to keep the phone in touch with the base station.

iii) conversation covering temporal changes between basic and DTX: this condition alternates 50 seconds of Basic mode with 97 seconds of DTX mode, in order to simulate a real conversation on the phone.

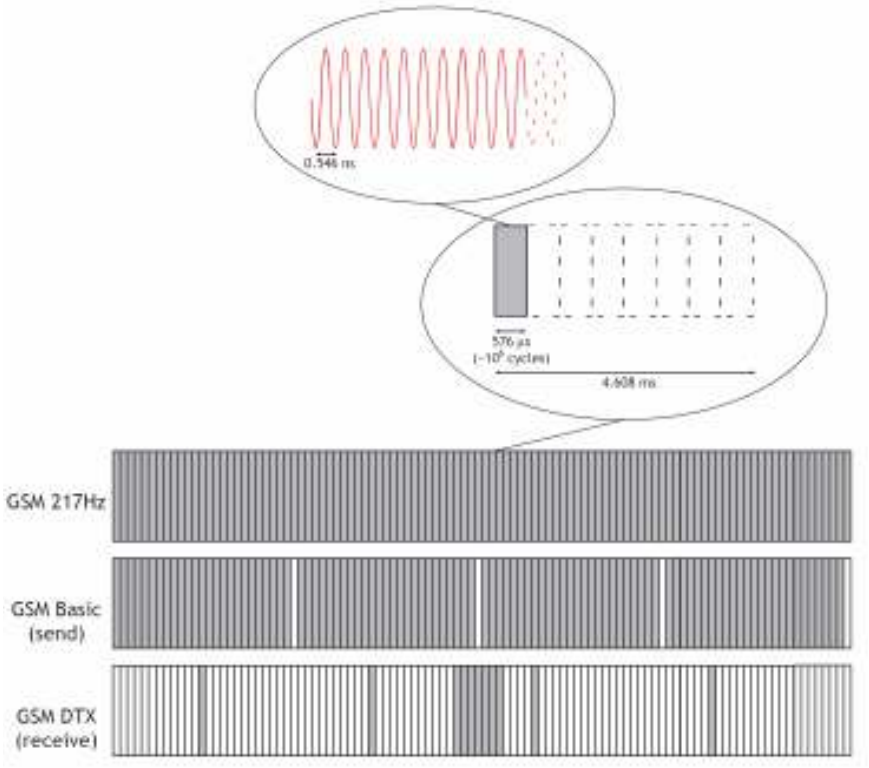

Fig. 1.14 – A scheme of the GSM signal modulation.

To guarantee sufficient air circulation, the waveguides are equipped with Papst 612 DC ventilators (St. Georgen, Germany), which take in air through two slots near the end of the waveguide. The driving currents of the ventilators are continuously monitored in order to control their performance. The air temperatures in the waveguides are monitored with probes fixed outside the waveguides, in the air flow produced by the fans.

Temperature is a very important parameter for *in vitro* investigation of cells, because of the possible effects that result in a temperature difference between exposed and sham exposed. The forced airflow exchange system allows excellent temperature control with no differences between exposed and unexposed waveguides.

Nonetheless the energy carried by the electromagnetic wave can increase the medium temperature following the equation:

$$\frac{dT_{medium}}{dt} = -\frac{T_{medium} - T_{incubator}}{\tau} + \frac{SAR_{medium}}{c_w}$$

where τ is convection time (180 s) and c_w is water specific heat.

If the cell medium is exposed to the electromagnetic fields, the temperature will increase due to the absorption in the medium. A temperature change in the cell medium is determined by heat convection with a time constant τ and the heat source introduced by the electromagnetic field. The absorption in the cell medium across this step gradient is much faster, than the heat transfer to the surrounding environment. It is therefore appropriate to use a temperature T_{medium} and a medium averaged specific absorption rate SAR_{medium} to describe the temperature changes.

1.4.2 - 144-434 MHz RADIOWAVE THERAPY EXPOSURE SYSTEM

Monolayer cultured cells were exposed to RF at 144 MHz and 434 MHz at different input power levels, by means of a TEM cell, a device which generates transverse electromagnetic mode propagating electromagnetic fields. It is a state of art testing cell, according to the Standard IEC 61000-4-20, developed by WaveControl (Spain) to test specific products or subsystems for electromagnetic emissions and/or immunity to comply with the European electromagnetic compatibility (EMC) directive and other National and International regulations.

This exposure system is made of the following components: transceiver, amplifier, meter, TEM cell, and grounding sink (fig. 1.15).

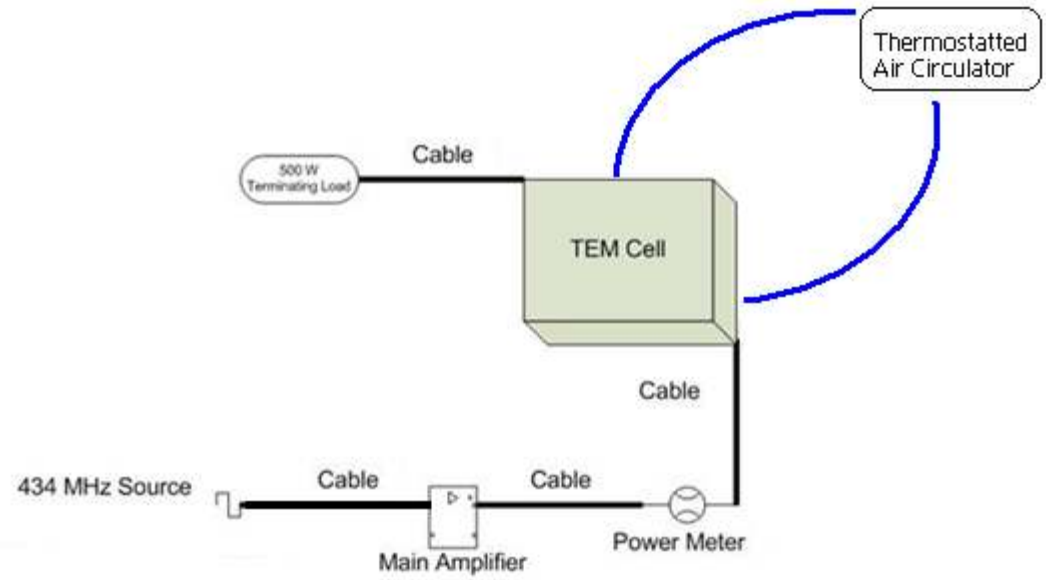

Fig. 1.15 - The scheme of the 144-434 MHz experimental setup.

The transceiver employed is the FT-7800E (Yaesu, UK), a high quality Dual Band FM transceiver providing 50 W of power output on the 140 MHz band and 40 W of power output on the 430 MHz band. The frequency range for the transmission is 144-146 MHz and 430-440 MHz. The high power output of the transceiver is produced by its amplifier, with a direct flow heat sink and thermostatically-controlled cooling fan maintaining a safe temperature for the transceiver's circuitry. This is designed for use with antennas presenting an impedance of near 50 Ohms at all operating frequencies.

The amplifier (70 cm, Discovery Linear Amp, UK) is a desk top linear RF amplifier with a nominal output of 1000 W, covering the range 430-440 MHz and forced air cooled to give the operator the ability to work at full output power for as long as required. The amplified has been empowered to obtain a higher emission power: the improvement has been effected by optimizing the position of some components inside the RF box, in order to produce 500 W out for 40 W in and 600 W out for 60 W in (Table 1.3). It is therefore achieving its specified 10 dB gain.

The power delivered to the TEM cell was measured using a Thruline Model 43a Power Meter (Bird, USA) in order to characterize every exposure regime tested in this study.

Table 1.3 – The power levels of the exposure regimes employed.

TRANSCEIVER		METER
POWER	FREQUENCY	POWER
High	144 MHz	55 W
Low	434 MHz	70 W
Midi2	434 MHz	100 W
Midi1	434 MHz	190 W
High	434 MHz	380 W

The WaveCell (Fig. 1.16) is the device, provided by WaveControl, which generates transverse electromagnetic (TEM) mode propagating electromagnetic fields, from 30 MHz up to 2700 MHz for radiated immunity and radiated emission, independently from the radiator/antenna. Its external dimensions are 180 x 80 x 83 cm (length x width x height) and the inner usable test volume is 35 x 35 x 25 cm (length x width x height).

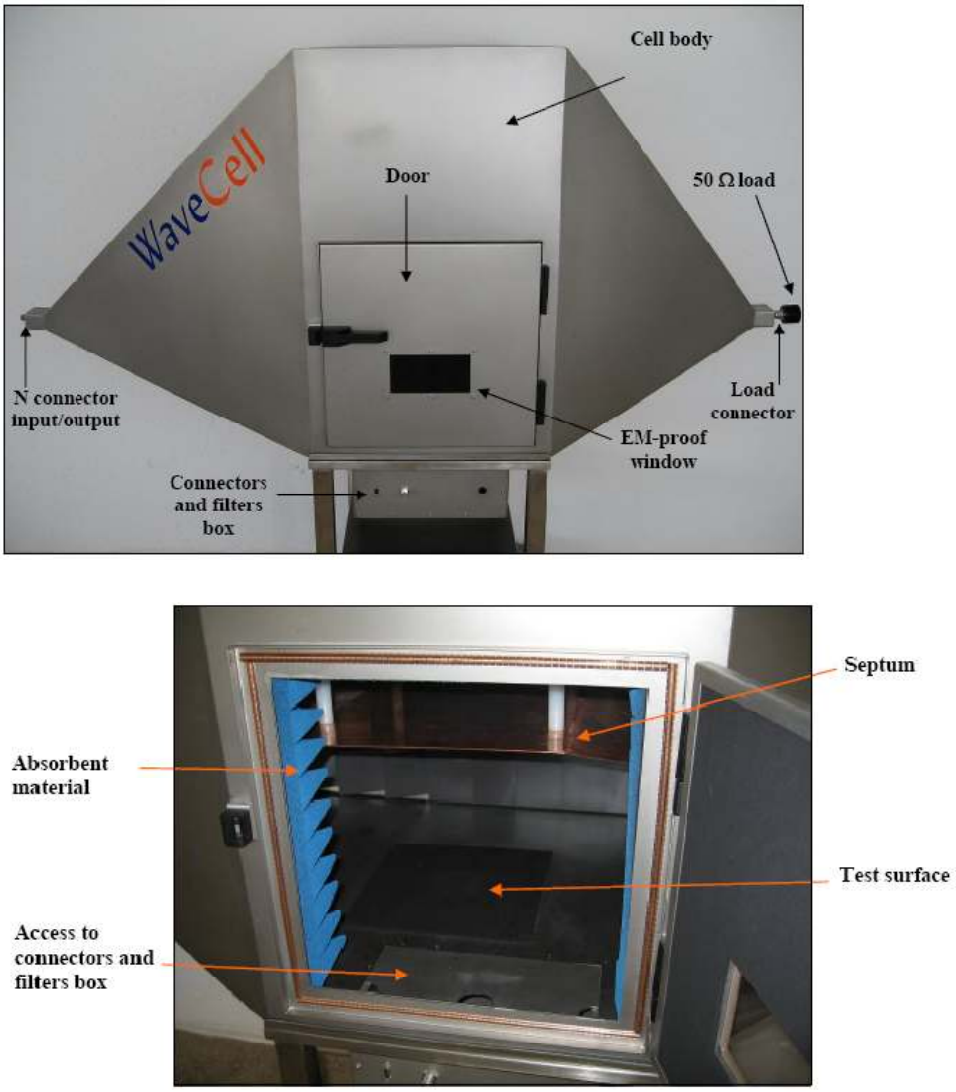

Fig. 1.16 – The TEM cell employed in this study: external view (top) and internal view (bottom).

The transceiver is connected to the amplifier, which is connected to the TEM cell by an N-power input connector (standard IEC type). The TEM cell is eventually terminated by a connection to a Termoline coaxial resistor heat sink (Bird, USA).

Inside the TEM cell a metallic septum generates the electromagnetic field and receives the emissions radiated by the equipment under test, thanks to its features as a conductor. A wave guide allows optical fibre cables to pass through it, at the same time preventing the passage of electromagnetic waves in the cell's working frequencies.

The useful test volume is in the centre of the cell under the septum 5 cm above the cell bottom (Fig. 1.17). Therefore a conductive material (polystyrene) support is placed in that specific position to locate and raise the equipment under test, also to avoid any unwanted contact of the equipment to ground.

Fig. 1.17 – The useful test volume inside the TEM cell.

Petri dishes, flasks, 6-well and 96-well plates can be placed on this support and cells are exposed to the same electromagnetic field conditions (Fig. 1.18).

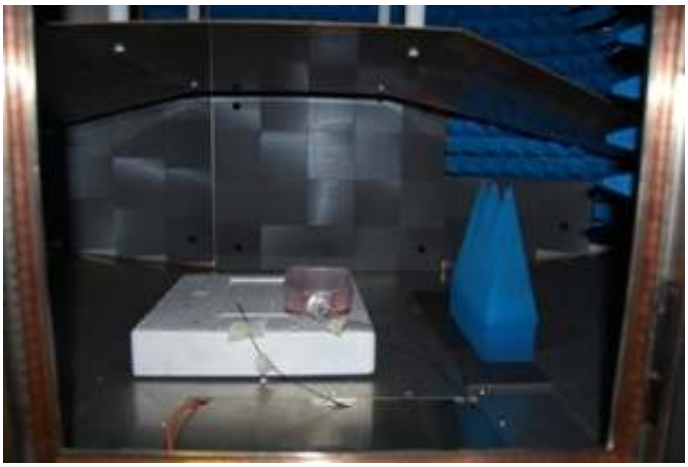

Fig. 1.18 – The exposure setup inside the TEM cell.

As for the wave propagation inside the TEM cell, any electromagnetic field can be described as a superposition of well-known wave types called field modes. The following vector sums represent this.

$$\underline{E} = \underline{E}_{TEM} + \underline{E}_{TE_{10}} + \underline{E}_{TM_{10}} + \dots$$

$$\underline{H} = \underline{H}_{TEM} + \underline{H}_{TE_{10}} + \underline{H}_{TM_{10}} + \dots$$

where E represents the total electric field, and H represents the total magnetic field. There is no component of the x- and y-fields in the longitudinal direction, that is, the direction of wave propagation. There are only transverse components of the x- and y-fields. The TEM wave does not have to have a longitudinal component.

$|E_{TEM}|$ and $|H_{TEM}|$ is given by the field wave impedance:

$$\Gamma_{TEM} = \frac{|\underline{E}_{TEM}|}{|\underline{H}_{TEM}|} = \sqrt{\frac{\mu_0}{\varepsilon_0}} = 120\pi \ \Omega$$

for propagation in air. The propagation velocity of the TEM mode is given by the material constant likewise:

$$c_{TEM} = \frac{1}{\sqrt{\mu_0 \cdot \varepsilon_0}} = c_0 .$$

and this is the speed of light.

The WaveCell is designed according to the new IEC 61000-4-20 EMC standard – "Testing and measurement techniques - Emission and immunity testing in transverse electromagnetic TEM waveguides". It has the status of a basic EMC publication in accordance with IEC guide 107, and it relates to emission and immunity test methods for electrical and electronic equipment using various types of transverse electromagnetic (TEM) waveguides. The calibration procedure for field immunity tests according to IEC 61000 is schematized in Figure 1.19.

The IEC 61000-4-20 defines the field uniformity properties inside the test volume and describes a procedure called “total radiated power method”. This procedure is used to correlate the measured values to equivalent open area test site (OATS) values. This method is based on a three voltage measurement made in a TEM Cell from which the total radiated power of the EUT may be calculated. The total radiated power is then used to simulate the maximum EUT field over a ground plane based on a model of parallel dipoles (source and receive dipole) transmitting the same total power.

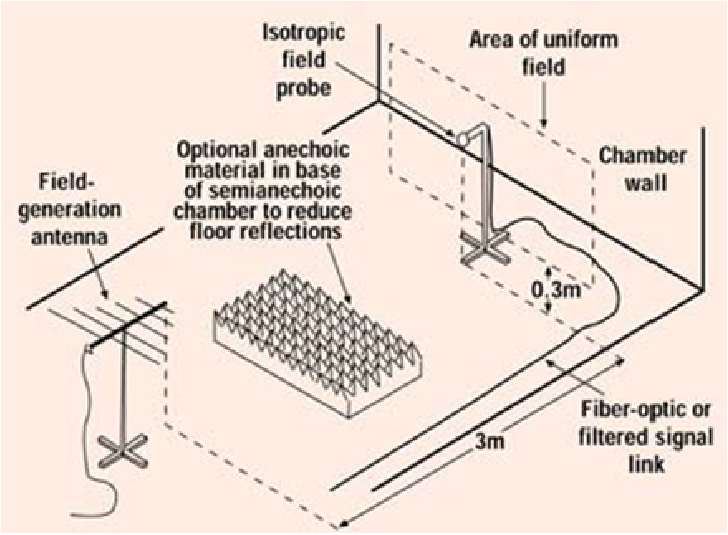

Fig. 1.19 – A field calibration inside the TEM cell according to IEC 61000.

The TEM verifications are very important because allow the simulation of the far field propagation characteristic.

For field monitoring in radiated immunity measurements and field homogeneity measurements, an RF-transparent EF Cube (WaveControl, Spain) broadband electromagnetic field probe is used. EF Cube is a broadband electromagnetic field probe that allows field measurement with minimum disturbance of the electromagnetic environment due to its small size and fibre optic connection. The EF Cube probe is isotropic, comprising 3 orthogonal sensors, so that it will give an accurate value for the electromagnetic field regardless of polarization and its direction. The probe measures and gives the value of the field on 3 axes and makes a vectorial sum to obtain the total field. It is powered by a rechargeable battery and is connected to a PC using a fibre optic connection and a small fibre-USB converter. The frequency range is 30 - 3000 MHz and the field measurement range is 1 - 150 V/m with a sensitivity of 1 V/m.

The probe can be used with or without frequency correction: in the first case it's possible to indicate the frequency at which the measurements are taken, so the software eliminates the uncertainty introduced by the probe frequency response. In the second case the EFCube works as a broadband probe with no frequency correction, with the uncertainty indicated in the specifications.

The temperature inside the TEM cell is kept constant by means of a thermal device (Fig. 1.20): the TEM cell is placed inside an insulating chamber, built on purpose, where an

Air-Therm ATX air-circulator (World Precision Instrument, USA) provides a precise temperature controlled air heating.

Fig. 1.20 – The chamber built around the TEM cell, and the thermal devices adopted to maintain the temperature constant at 37˚C.

The temperature is monitored by I652 fibre optic RF-neutral temperature probes (Luxtron Fluoroptic, USA), which are placed inside the TEM cell and located in culture medium (to measure the cells temperature) and in close vicinity, though non adjacent, to the culture (to monitor the air temperature). These sensors are electrically quiet and shielded for very high impedance recording.

1.5 - BIOLOGICAL TARGETS

The exposure systems previously described were employed to expose some biological targets (cultured cells) to different radio frequency electromagnetic fields, in order to evaluate cellular responses post exposure.

To investigate the potential effect of high frequency (1.8 GHz) GSM EMFs, two biological targets were chosen: human trophoblast and rat PC-12 cell lines.

To evaluate the bio-effects of HF (144-434 MHz) radiowave therapy EMFs, human non-tumour derived prostate cells (PNT1A) and tumour derived prostate cells were employed, as well as human trophoblasts.

1.5.1 - HUMAN TROPHOBLAST CELL LINE

Trophoblasts are formed by undifferentiated cells (cytotrophoblasts) that proliferate and differentiate either to syncytiotrophoblasts or to extravillous trophoblasts (EVTs) (Chakraborty et al., 2002).

EVT cells migrate towards the endometrium and occasionally the myometrium. Here EVTs play an important role in the remodelling of the uterine vasculature to guarantee adequate exchanges between mother and foetus (Graham et al., 1993; Chakraborty et al., 2002). The proliferation, migration and invasiveness of EVTs are finely regulated by several stimuli, including hormones, prostaglandins, cytokines and hypoxia, and alteration of such integrated processes may also lead to early pregnancy failure.

Trophoblast cells preserve all markers of parental EVT, and thus represent a good model for the *in vitro* study of molecular mechanisms at the basis of placentation.

Several aspects of malignant and trophoblastic invasion are similar, if not identical; these features together with their high sensitivity to external stimuli make trophoblasts an attractive model for investigating possible detrimental effects of high-frequency EMFs on cell physiology, particularly on reproductive tissues.

No studies have addressed the possible effects of high frequency EMFs on trophoblast cells, and in general conflicting evidence is available regarding the interaction between high frequency EMFs and reproductive tissues. It has been reported that high-intensity microwave exposure increased embryo lethality at the early stages of mouse gestation (Nawrot et al., 1985) and induced micronucleus formation in the erythrocytes of offspring in rats (Ferreira et al., 2006). A large increase in HSP70 protein levels was reported *in vitro* in human amnion cells (Kwee et al., 2001). However, there is no epidemiological evidence indicating that occupational or daily life exposures to microwaves harm the reproductive process (Robert, 1999). Nakamura et al. (2003) did not observe microwave effects on rat utero-placental circulation or placental endocrine and immune functions. Similarly, Finnie et al. (2009) did not see any stress response using HSPs as an immunohistochemical marker during whole of gestation exposure of fetal mouse brains to mobile phone radiofrequency fields.

1.5.2 - RAT PC-12 CELL LINE

Cell lines that are capable of continuous replication and that display differentiated properties have long been recognized as useful model systems for several studies. Chromaffin cells and neurons are related cell types for which such models are highly desirable. Since mature neurons are non-dividing, a maximally useful neuronal model should be modulable between a state in which it can replicate and a state in which it is non-dividing as well as neuronally differentiated. In addition, neurons not only display many specialized and characteristic properties, such as electrical excitability and neurite outgrowth, but they also exist as a number of distinct phenotypic classes. One system that fulfils the above requisites in many respects is the PC-12 line of pheocromocytoma cells. This line promises to be highly useful for studying both chromaffin cells and neurons (Greene and Tischler, 1982).

Among the most striking properties of the PC-12 line is its capacity to respond to nerve growth factors (NGF), proteins that profoundly influence the growth and development of sympathetic and certain sensory neurons. The overall effect of NGF on PC-12 cells is to convert them from the population of replicating chromaffin-like cells to a population of non-replicating sympathetic-neuron-like cells (Greene and Tischler, 1982).
In the absence of NGF and in the presence of serum, they maintain their proliferation properties (D'Ambrosi et al., 2004). In growth medium, the PC-12 cells have a round or polygonal shape and tend to grow in small clumps. The apparent doubling time of the PC-12 cells is long – about 92 hr (Greene and Tischler, 1976). PC-12 cells propagated *in vivo* or in culture without NGF are readily classifiable as pheocromocytomas by current morphological and chemical criteria. PC-12 cells are comparable to other pheocromocytomas in that they synthesize, store, and secrete large quantities of cathecolamines. Other reported biochemical markers in PC-12 cells that are of unknown prevalence in human pheocromocytomas are choline acetyltransferase, acetylcholinesterase, and gamma-aminobutyric acid. None of these markers has been reported in normal chromaffine cells. In culture medium containing horse serum but not NGF, PC-12 cells synthesize, store, and release acetylcholine (Greene, 1978).

In summary, the PC-12 cell line appears to be a useful model system for the study of numerous endpoints in neurobiology and neurochemistry. These may include the mechanisms of action of NGF and its role in development and differentiation of neural stem

cells; initiation and regulation of neurite outgrowth; and metabolism, storage, uptake and release of catecholamines. PC-12 cells may also be useful for studies related to treatment of certain classes of tumours (Greene and Tischler, 1976). PC-12 cells also prove useful in the study of various aspects of acetylcholine metabolism as well as the regulation and specification of neurotransmitter properties in developing neurones (Greene and Rein, 1977a; 1997b).

Although the PC-12 cellular model can only partially mimic the whole body complexity of an intact organism, it allows a more direct investigation of the several overlapping pathways propagating a biological process (D'Ambrosi et al., 2004). Nonetheless, to fully interpretate the effects of the EM radiation, every biological level should be investigated. Potential damages occurred at molecular levels might be more sharply registered by selecting highly purified materials (i.e., enzymes, hormones, or receptors) as biological targets. (Barteri et al., 2005). Cell models allow experimental control under defined culture conditions and a deep understanding of cellular mechanisms of reaction to external EMF (D'Ambrosi et al., 2004). And eventually, *in vivo* studies can highlight the ability of the organism to compensate for induced changes by homeostatic mechanism (Galvin et al., 1981).

1.5.3 - HUMAN PROSTATE NON-TUMOUR (PNT1A) AND TUMOUR (PC-3) CELL LINES

Prostate cancer is the most common form of male cancer in the Western world (Dijkman and Debruyne, 1996). It is thought that most elderly men have foci of prostate cancer but most of these tumours are latent and only a few patients will develop life-threatening disease. Individual patients can have multiple tumour foci, of which only one or a few will actually progress to a metastatic stage (Lang et al., 2000).

Cell lines derived from tumours and tissues have been historically instrumental for understanding of biology at the molecular level and are used in experimental research. There are general environmental differences between cells growing *in vitro* and in heterogeneous tissue *in vivo*. The general differences in gene expression include an up-regulation of genes involved in proliferation and metabolism. Although cell lines differ from normal and tumour tissues, the low availability of tissue samples make cell lines the best model for future molecular cell biology research (Pawlowski et al, 2009).

PNT1As are human post pubertal prostate normal cells, immortalised with SV40. They were established by immortalisation of normal adult prostatic epithelial cells by transfection with a plasmid containing SV40 genome with a defective replication origin. The primary culture was obtained from the prostate of a 35 year old male at post mortem. The cells contain the SV40 genome and express large T protein. They present the phenotype of differentiated luminal prostatic cells with the expression of cytokeratin 8 and 18 (markers for luminal glandular epithelia) and vimentin. Cytokeratin14, a marker of epithelial basal cells, is not expressed. PNT1A cells are non-tumourigenic in nude mice.

PC-3s are human Caucasian prostate adenocarcinoma. They were established from a grade 4 prostatic adenocarcinoma from a 62 year old male Caucasian. PC-3 cell lines were originally derived from advanced androgen independent bone metastasis|metastasized prostate cancer. The cells grow in agar and produce tumours in nude mice. They exhibit low acid phosphatase and testosterone-5-alpha reductase activity and express prostate specific antigen. PC-3 and DU145 human prostate cancer cell lines are the "classical" cell lines of prostatic cancer. PC-3 cells have high metastatic potential compared to DU145 cells which have a moderate metastatic potential.

In 1924 the German physiologist and medical doctor Otto Heinrich Warburg advanced the hypothesis that tumour cells have a fundamentally different metabolism to normal cells, in that they rely to a large extent on the less-energy productive process of anaerobic respiration (fermentation) even when there is sufficient oxygen present for the cells to use rather than utilizing the more efficient process of aerobic respiration (Warburg, 1956). In other words, cancer cells tend to behave as partial anaerobes while normal cells function as obligate aerobes.

The theories of Dr Warburg have in recent times gained more attention in view of findings linking the impairment of mitochondria with a breakdown in normal cell apoptotic processes and tumour growth (Bonnet et al., 2007). The implication of mitochondrial dysfunction in tumour growth is shown in a review by Ristow (2006) which observes that the hallmarks of cancer growth, increased glycolysis and lactate production in tumours, have raised attention recently due to novel observations suggesting a wide spectrum of oxidative phosphorylation deficits and decreased availability of ATP associated with malignancies and tumour cell expansion. The most recent findings suggest that forcing cancer cells into

mitochondrial metabolism efficiently suppresses cancer growth, and that impaired mitochondrial respiration may even have a role in metastatic processes.

1.6 - BIOLOGICAL ANALYSES

To assess the possible detrimental effects of the daily use of GSM mobile phones, two main biological parameters have been investigated, both regarding the interaction between RF EMF and the cellular proteins: the expression of a stress-related protein (heat shock protein 70) and the activity of one of the main cellular enzymes (acetylcholinesterase).

The second part of the present study was aimed at evaluating RF EMF exposure at 144 MHz and 434 MHz using 5 W and 50 W input powers (SAR ranging from 0.5 to 1.6 W/kg) and their effect on principal cellular processes as proliferation, DNA content, and protein content, as well a potential DNA damage, in several human cell lines.

1.6.1 - HEAT SHOCK PROTEINS

Since the first studies on the heat shock response (Ritossa 1962), much work has been done to understand the role of heat shock proteins (HSPs), whose synthesis is dramatically enhanced by high temperatures. Crucial information is now available about the proteins themselves, the coding genes, and the control of the response to heat (Scharf et al 1998; Feder and Hofmann 1999). A number of HSP inducers other than heat have also been recognized, including hypoxia, heavy metals, oxygen radicals, radiation, osmotic changes, etc, and different HSPs have been identified and grouped according to their molecular weight (De Maio 1999). HSPs appear to be ubiquitous in animals and plants and are critical for heat, oxidative, and high-light stress resistance. It is now clear that not all HSPs are stress-inducible, and constitutive isoforms, referred to as molecular chaperones, appear to be essential for protein folding or trafficking and regulated proteolysis in unstressed cells. The expression of the HSP-coding genes is under the control of specific transcription factors, and there is evidence that such regulation differs among organisms, depending greatly upon their life history and adaptation capacity.

HSPs are an evolutionarily highly conserved class of polypeptides expressed in almost all organisms in response to endogenous and exogenous stressors (Scharf et al

1998). HSPs are classified into several families based on their size: HSP105/HSP110, HSP90, HSP70, HSP60, HSP40 and HSP28. Of these families, HSP70 is the most conserved amongst species and is involved in the cellular stress response. In general, however, they are believed to provide protection to the cell by interacting with hydrophobic domains of polypeptides unfolded by stress stimuli and to promote protein renaturation or definitive elimination (De Maio 1999). Exposure of cells to a mild thermal stress protects them from further exposure to stronger, otherwise lethal, insults other than heat. These findings have prompted new attempts at manipulation of the HSP response in medicine, as well as in biology.

In the current study, the expression of the HSP70 protein was evaluated in cells of the trophoblast cell line after exposure to GSM 1817 MHz sinusoidal waves.

1.6.2 - ACETYLCHOLINESTERASE

In vivo, acetylcholinesterase (AChE) is an extrinsic membrane-bound enzyme responsible for rapid hydrolysis of the neurotransmitter acetylcholine (ACh), liberating choline and acetate within 1 msec of its release at the cholinergic synapses.

ChE activity has been studied in vertebrates (e.g. Kousba et al., 2003; Sanchez-Hernandez and Moreno-Sanchez, 2002; Yi et al., 2006) and invertebrates (e.g. Diamantino, 2003; Caselli et al., 2006; Gambi et al., 2007), although less characterized in the latter organisms.

A neurotransmitter role for acetylcholine has been known since the discoveries of Dale (1914). The occurrence of ACh-like activity in human placental extracts was then demonstrated by bioassay methods. It is now established that human term placenta contains about 112 nmol ACh/g wet tissue, which is about 7 fold higher than that of the brain tissue (Sastry, 1997). The action of ACh as a chemical transmitter is terminated due to the hydrolysis by AChE. There are several ways in which the function of ACh in the placenta may be terminated: (1) hydrolysis of ACh by placental cholinesterases, (2) release of ACh into maternal and foetal circulations, diffusion and hydrolysis by maternal and foetal circulations, and (3) reuptake of released ACh by the placental trophoblasts. The degradation products of ACh, choline and acetate, may be reutilized in the ACh synthetic pathway of the placenta. The results from Hahn et al., (1993) suggested also that placental AChE can no longer be considered as derived from maternal blood, but it's primarily located within human placental tissue.

In utero exposure to poisons and drugs is frequently associated with spontaneous absorption and placental malfunction. The major proteins interacting with these compounds are acetylcholinesterase and butyrylcholinesterase (BChE), which attenuate the effects of such xenobiotics by their hydrolysis or sequestration (Sternfeld et al., 1997). The major mechanism for eliminating pharmacologically active substances is enzymatic biotransformation in the serum and organs, such as the liver. Cocaine, for instance, is extensively metabolized by BChE to ecgonine methyl ester, and this biotransformation pathway accounts for the major enzymatically mediated elimination of cocaine in human beings. If a pregnant woman is compromised in her ability to eliminate cocaine, the foetus may have an increased risk for cocaine-related adverse outcomes. The placenta may act as a metabolic interface between mother and child and may protect the foetus from maternal cocaine use, thanks to its ability to metabolize cocaine by AChE and BChE (Simone et al., 1994).

Finally, it was demonstrated by Souza et al. (2005) that AChE plays a major role also against pre- and perinatal exposure to pesticides, which is deleterious on foetal and natal development.

AChE is a glycoprotein that exists in hydrophobic and hydrophilic forms. The hydrophilic species work within the cell to break down excess concentrations of intracellular acetylcholine. The hydrophobic (lipid-linked) varieties are primary agents of ACh inactivation, working at the synaptic cleft or the neuromuscular junction to break ACh and to ensure rapid inactivation of ACh. Although the individual chemical qualities vary widely between the various forms of AChE, the mechanism of catalysis for all the species remains similar (Vukova et al., 2005).

PC-12 cells have been shown to synthesize three different molecular forms of AChE, and secrete AChE by both a constitutive and a highly regulated pathway. This secretion involves specific sorting of the different molecular forms of AChE (Schweitzer, 1993). In PC-12s only one AChE molecular form is secreted constitutively, and this secretion is carried out independently of extracellular Ca^{2+}. In contrast, cellular membrane depolarization causes an increase in the rate of secretion of the other two forms of AChE; this increase in secretion absolutely requires extracellular Ca^{2+} (Schweitzer, 1993).

AChE activity can be modulated by the membrane hydrophobic environment of the enzyme and depends on membrane fluidity and surface charge. AChE activity is a good tool

for measuring the structural transformation of the membrane under the action of various factors, such as modulated microwave (MW) fields (Kujawa et al., 2003).

It has been postulated that microwave irradiation might cause protein denaturation; indeed, there are reports suggesting that non-thermal exposure to microwaves affects protein structural rearrangements. Some authors are of the opinion that the targets of MW effects are cell proteins (Vukova et al., 2005).

Enzymatic activity was also shown as a sensitive indicator of changes caused by irradiation. (Krokosz and Szweda-Lewandowska, 2005). Modulated MW exposure has been reported to influence enzyme complexes. As it seems, the field interactions at the microscopic level are related to the dielectric properties of bio-macromolecules and enzyme complexes, cell membranes, or ion channels. Thus, there are effects of MW irradiation on membrane-related enzymes and neurotransmitters (Vukova et al., 2005).

This neurochemical endpoint was investigated in the present study to determine whether the enzyme activity might be affected by exposure to modulated RF fields. The activity of AChE was chosen as a biological marker because of its presence in the cell membrane and its physiologically important role in many different biological processes (Dutta et al., 1992).

1.6.3 - CELLULAR PROCESSES

CELL PROLIFERATION

Cell endpoints refer to the outcomes from the *in vitro* studies. These are measurements of the proportion of cells that survive or are killed by the treatment as well as the proportion that stop growing or slow down dividing. Hence, the studies shall measure these endpoints: cell death (the rate at which cells die either due to apoptosis or necrosis), cell survival and cell proliferation (the number of cells that are dividing in a culture).

An xCELLigence real-time cell analyzer (Roche, UK) system was applied in the current study to provide real-time proliferation testing through a sensitive monitoring of cellular impedance. This technique utilizes a series of microwells, whose bottoms are 80% covered with microelectrodes to provide an advance in sensitivity in cell sensing compared to previous techniques. The real time cell analyzer measures cell viability by monitoring cell proliferation and morphology using a dimensionless unit called the cell index (CI) which is based on the impedance changes caused by cells interacting with the microelectrodes. The

results obtained using xCELLigence have been shown to be comparable to more traditional cytotoxicity assays such as the MTT, neutral red uptake (NRU), lactose dehydrogenase, and acid phosphatase tests (Boyd et al., 2008).

In this study the data generated on the xCELLigence were correlated with those from the survival and the colorimetric (i.e. PicoGreen and Bradford) assays.

Cell survival was determined also by cell counting using a Z2 Coulter Counter (Beckman Coulter, California USA), which provide the number of cells in the cell suspension through a very accurate electrical sensing zone method. Any possible effect of RF EMF on cell proliferation can be therefore confirmed by a cell count test, by means of simply counting the survived cells 1 and 7 days after the exposure.

CELLULAR DNA CONTENT

The possibility of effects of exposure to RF radiation on genetic material (DNA) is very important. Damage to the DNA of somatic cells can lead to the development of cancer or cell death. Changes in the DNA of germ cells can lead to mutations that can be transmitted to subsequent generations (Vijalayaxmi and Obe, 2004). RF-radiation exposures have been reported to result in alterations in DNA fragment patterns in brain and testes cells of mice (Sarkar et al., 1994), single- and double-strand breaks in the DNA of brain cells in rats (Lai and Singh, 1995; Lai and Singh, 1997), and dicentric chromosomes, acentric fragments and micronuclei in human blood lymphocytes (Garaj-Vrhovac et al., 1992; Tice et al., 2002).

Among 53 reports on genotoxicity investigation after RF radiation, published during 1990–2003, 58% of the conclusions did not identify increased cytogenetic damage after RF-radiation exposure, 23% of those studies indicated a genotoxic potential of RF-radiation exposure, while in the 19% the observations were inconclusive (Vijalayaxmi and Obe, 2004). The absence of an increase in genotoxicity in mammalian somatic cells exposed to RF radiation, reported in the great majority of investigations, agrees with the large volume of published epidemiological and experimental findings that do not support the concept that *in vivo* and *in vitro* exposure to RF radiation is carcinogenic (Heynick et al., 2003).

Despite the majority of the studies did not show any affect at non thermal level, the potential effect of RF on DNA not only stimulated scientific interest but also received considerable public attention and raised public concern to a higher level. (Vijalayaxmi and

Obe, 2004). Therefore DNA analysis is still considered one of the main cellular endpoints to be investigated in RF studies.

Also, in the last decade, few reports demonstrated that the quantification of free-circulating DNA in plasma/serum samples might be a promising biomarker in a number of pathologies (Chorostowska-Wynimko and Szpechcinski, 2007). The occurrence of free DNA circulating in the blood of patients with cancer is one of the most intensively studied issues, due to a permanently high morbidity and mortality of the disease worldwide (Szpechcinski et al., 2008). A diagnostic cancer test based on a quantitative test of DNA has been recently recommended because of its potential application as a non-invasive, rapid, sensitive and cost-effective tool for molecular diagnosis, monitoring response to therapy, and prognosis of clinical outcome in cancer (Szpechcinski et al., 2008).

Thus, DNA quantification using PicoGreen fluorescent dye (Molecular Probes, USA) that selectively binds double-stranded DNA, has been chosen in the present study as an advantageous technique in terms of cost and time effectiveness and procedure simplicity.

Among other commercially available fluorochromes, PicoGreen assay demonstrates exceptionally high detection limit up to 25 pg/ml and perfect linearity up to 1000 ng/ml, making the test appropriate for human DNA analysis (Szpechcinski et al., 2008). Also, some DNA content determined by PicoGreen proved to be several fold higher than the plasma DNA amount measured by real time PCR. Such difference may be accounted for by the fact that the first method can detect nearly all DNA fragments, whereas the latter measures only amplifiable DNA (Szpechcinski et al., 2008). The amount of total DNA inside the cells was compared to the total protein content, in order to find any possible correlation between these two parameters, which would help to understand the mechanism of action of RF EMF on cell lines.

CELLULAR PROTEIN CONTENT

Many authors are of the opinion that RF exposure causes a great effect on proteins: denaturation (De Pomerai et al., 2000), over-expression (Kwee et al., 2001; Leszczynski et al., 2002; Sanchez et al., 2006), increase in synthesis (Dimberg, 1995; Kwee et al., 2001) structural alterations (Galvin et al., 1981; Lixia et al., 2006), enzyme activity changes (Barteri et al., 2005; De Pedro et al., 2005), etc. Measuring the total cellular protein content can

provide a measurement of changes in cellular physiology, and can easily underline the different response in tumour and non-tumour cells.

Total protein quantification can be performed by Bradford assay, a method based on the binding of dye to the proteins which results in a dye–protein complex with increased molar absorbance. This method is considered easy to perform, practical and more sensitive than other methods (Okutucu et al., 2007).

The comparison among these endpoints aims to establish if different RF exposure regimes exert different effects on tumour or non-tumour prostate cells. Any possible detrimental effect on PC-3s which is not exerted on PNT1As could be applied for more in-depth studies, aimed to find any potential application of RF in the MHz range in future cancer therapy design.

Both these endpoints (cellular DNA content and cellular protein content) provide for an initial interpretation of cellular events. It is recognized that for more in depth analysis other endpoints have to be investigated, nonetheless they can provide a rough idea of how radiowave treatments can influence differently tumour and non-tumour cells.

1.6.4 - NUCLEAR DNA DAMAGE

The molecular DNA damage was assessed in tumour and non-tumour cell lines after 1.8 GHz, 144 MHz and 434 MHz exposure regimes by evaluating the gene expression of two proteins involved in single and double strand break repair: PARP1 and Cernunnos-XLF.

DNA double strand breaks are considered as the most harmful DNA lesions and are repaired by either homologous recombination or non-homologous end joining (NHEJ). The major NHEJ pathway relies on a set of core proteins (Fig. 1.21).

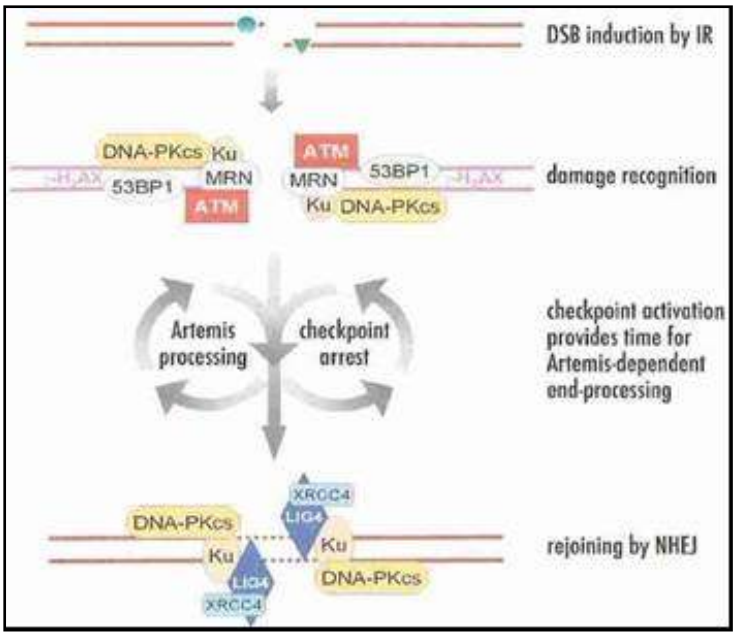

Fig. 1.21 – A scheme of the NHEJ pathway.

The two DNA ends of the double strand break (DSB) are recognized and bound by the ring-shaped heterodimer Ku70/Ku80 that recruits the DNA-dependent protein kinase catalytic subunit (DNA-PKcs). The assembled DNA-PK holoenzyme then exhibits serinethreonine protein kinase and DNA endbridging activities. The kinase activity regulates DNA end access to processing enzymes like the DNA-PKcs-associated Artemis nuclease. Finally, the XRCC4/DNA ligase IV complex is responsible for the ligation step. Another core NHEJ factor is Cernunnos-XLF, a factor with a predicted structural similarity to XRCC4 that has been identified as an XRCC4-interacting protein. Cernunnos-XLF is the homologue of the yeast Nej1p protein in *Saccharomyces cerevisiae* and belongs to a larger family of functionally conserved proteins that are required for NHEJ (Ahnesorg et al., 2006; Buck et al., 2006; Callebaut et al., 2006; Drouet et al., 2006; Wu et al., 2007).

Poly(ADP-ribose) polymerase-1 (PARP1) is a nuclear enzyme activated by binding to DNA breaks, which causes PARP1 auto-modification. PARP1 activation is required for regulating various cellular processes, including DNA repair and cell death induction (Rancourt and Satoh, 2009).

PARP1 is one of the best known proteins with DNA-damage scanning activity. This nuclear enzyme, also known as the ‘Cinderella of the genome’, is an unfailing housekeeper that signals DNA rupture and participates in base-excision repair.

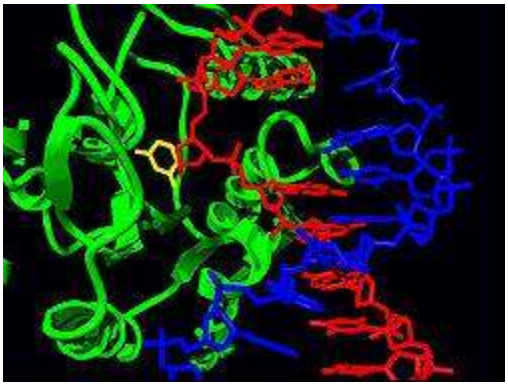

Fig 1.22 – The structure of the base-excision repair enzyme uracil-DNA glycosylase.

When only one of the two strands of a double helix has a defect, the other strand can be used as a template to guide the correction of the damaged strand. In order to repair damage to one of the two paired molecules of DNA, there exist a number of excision repair mechanisms that remove the damaged nucleotide and replace it with an undamaged nucleotide complementary to that found in the undamaged DNA strand:

1. Base excision repair (BER), which repairs damage to a single nucleotide caused by oxidation, alkylation, hydrolysis, or de-amination. The base is removed with glycosylase and ultimately replaced by repair synthesis with DNA ligase (Fig. 1.22).
2. Nucleotide excision repair (NER), which repairs damage affecting longer strands of 2–30 bases. This process recognizes bulky, helix-distorting changes such as thymine dimers as well as single-strand breaks (repaired with endonuclease enzymes).
3. Mismatch repair (MMR), which corrects errors of DNA replication and recombination that result in mispaired (but normal, that is non- damaged) nucleotides following DNA replication.

Upon binding to DNA strand breaks, PARP1 metabolizes NAD^+ into branched polymers of ADP-ribose that are transferred to a set of nuclear proteins including DNA polymerase I and II, Ca^{2+}-Mg^{2+}-endonuclease, histones, several chromatin-binding proteins and PARP1 itself. Poly ADP-ribosylation has been proposed to function in genome repair by modifying architectural proteins proximal to DNA breaks, thus facilitating the opening of the condensed structure of chromatin required for the recruitment of the repairing complex.

PARP1 is also one of the best known caspase substrates and its cleavage is universally adopted as an apoptotic hallmark and is an important modulator of the death

program triggered by p53, suggesting additional mechanisms through which the enzyme operates in cell death (Chiarugi, 2002).

Chapter 2

MATERIALS AND METHODS

2.1 - CELL CULTURES

2.1.1 - HUMAN TROPHOBLASTS

Trophoblast cells (HTR-8/SVneo) (Fig. 2.1) were kindly provided by Prof Carla Biondi of Department of Biology and Evolution, Section of General Physiology, University of Ferrara. They were grown in RPMI 1640 medium supplemented with 10% foetal bovine serum (FBS), 2mM l-glutamine, and 2% penicillin/streptomycin, all from Gibco (Italy). Cells were maintained at 37˚C in a normal atmosphere containing 5% CO_2. For the experiments, cells were seeded at a density of 1×10^6 cells in 35 mm-diameter Petri dishes.

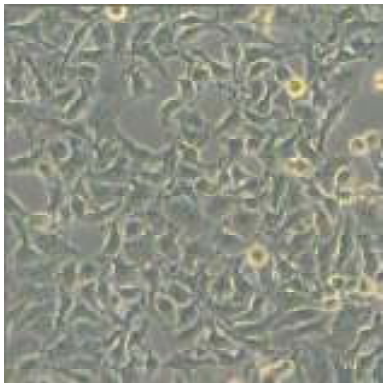

Fig 2.1 – Human trophoblast cells (40x magnification).

2.1.2 - RAT PC-12s

PC12 cells (Fig. 2.2) were kindly provided by Prof Laura Calzà of BioPharmaNet-DIMORFIPA, University of Bologna, Bologna, Italy. They were grown in a medium consisting of: 84% DMEM (Dulbecco's Modified Eagle Medium (1x), liquid High Glucose), 10% heat-inactivated horse serum, 5% heat-inactivated foetal calf serum, 1% Penicillin-Streptomycin (10000 units/ml penicillin and 10 mg/ml streptomycin in 0.9% sodium chloride, Sigma). DMEM medium, horse and foetal calf sera were from GIBCO (Italy).

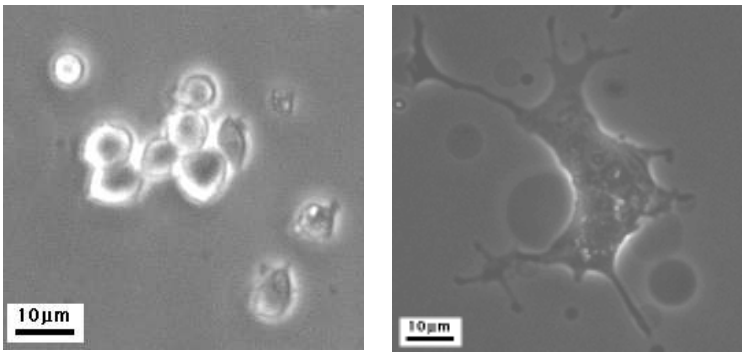

Fig 2.2 – Rat PC-12 cells: undifferentiated (left) and differentiated (right).

Prior to an experiment, the cells were removed from the dishes with the aid of Trypsin-EDTA (0.25% Trypsin with EDTA 4Na) 1x (Invitrogen) and counted with a haemocytometer (Greene and Tischler, 1976). Approximately 2.5 x 10^5 cells in 2 ml of culture medium were plated 2-3 days before each experiment into tissue culture dishes.
After 24–48 h cell seeding, medium was removed from Petri dishes and semi-confluent cell monolayer was incubated in serum-free medium and then exposed to the treatments.

2.1.3 - HUMAN PROSTATE CELLS (PNT1As AND PC-3s)

Human PNT1A and PC-3 cell lines (Fig. 2.4) were purchased from ECACC (UK). Cells were cultured in RPMI 1640 medium added with 10% foetal bovine serum in an incubator at 37°C with 5% CO_2. Cells used for experiments were at the exponential growth phase. Prior to RF exposure, cells were spanned down, resuspended and seeded.

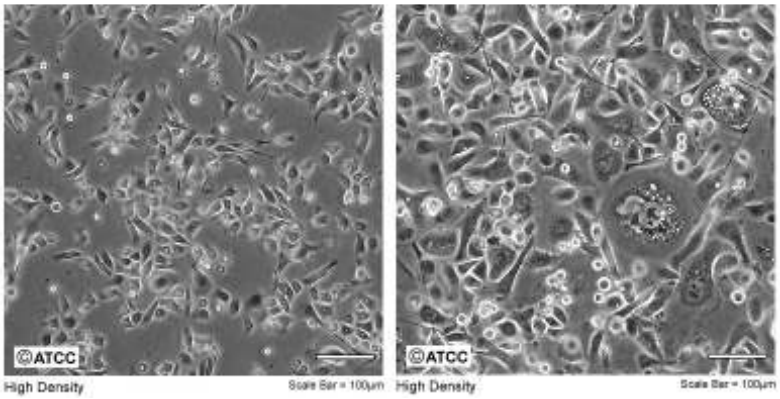

Fig 2.3 – Human non-tumour prostate cells (PNT1As, left) and tumour prostate cells (PC-3s, right).

For the experiments 2 x 10^4 PNT1A cells/well and 1 x 10^4 PC-3 cells/well were seeded on the 96-well plates, 7 ml of PC-3 and PNT1A cell suspension at 5 and 10 x 10^5 cell/ml respectively were placed inside T25-flasks, 1 x 10^5 PNT1A cells/well and 5 x 10^4 PC-3 cell/well were seeded on the 6-well plates. The cells were seeded 24 hours prior to the exposure, being allowed to settle down and attach to the bottom to form a monolayer before exposure.

Cell culture plastic-wares were purchased from Sarstedt (Germany), reagents for cell culture from Sigma-Aldrich (UK).

2.2 - EXPERIMENTAL EXPOSURE SYSTEMS

2.2.1 - 1.8 GHz GSM EXPOSURE SYSTEM

The 1.8 GHz exposure system has been developed and built by the Foundation for Research and Information Technologies in Society (IT'IS Foundation, Switzerland). Its main features are described in the introduction.

Briefly, the apparatus CIRSA is equipped with is composed of two separate metal waveguides behaving as perfect electric conductors, enabling blind exposures. Before every exposure, the PC connected to the apparatus randomly chooses which waveguide will be irradiated. The other one, the sham waveguide, remains switched off and is the control chamber. There is an antenna inside each waveguide where the circulating electric current produces an electric field and therefore a linked magnetic field. The intensity of the electric current determines the carrier frequency of the electromagnetic wave. The waveguide behaves like a resonant cavity, in which the interferences among the waves produce a stable field configuration. Therefore the field can be defined as static.

All experiments were performed at a carrier frequency of 1.8 GHz with intermittent exposure (5 min field on, 10 min field off). This kind of intermittency was chosen because it can be considered more in line with the real use of mobile phones than a constant exposure. Cells were subjected to continuous wave (CW, carrier frequency only) and to the following GSM signals:

• GSM-217 Hz (speaking only): signals were amplitude modulated by rectangular pulses with a repetition frequency of 217 Hz and a duty cycle of 1:8, following the Time Division Multiple Access (TDMA) GSM scheme (Pedersen, 1997). Every 26^{th} frame is idle, adding an 8 Hz modulation component to the signal.

• GSM-Talk (34% of speaking and 66% of hearing): GSM-Talk generates temporal changes between GSM-217 Hz and GSM-DTX and simulates a conversation with average periods of speaking and of hearing. The DTX mode (discontinuous transmission) is active during periods of non-speaking into the phone. The transmission is reduced to 12 active frames per 104 frames. The frame structure of the DTX signal results in 2, 8, and 217 Hz modulation components. Experiments for each modulation scheme were carried out with four different exposure periods (1, 4, 16, and 24 h). For each condition, at least three independent

experiments were performed. Within each experiment, six Petri dishes were sham-exposed and six were HF-EMF-exposed as stated previously.

A temperature of 37˚C was kept during the exposure in the two waveguides, thanks to two ventilators, and was continuously monitored with Pt100 probes. Direct temperature measurements were also performed using a temperature probe inserted in the medium (T1V3, SPEAG).

2.2.2 - 144-434 MHz RADIOWAVE THERAPY EXPOSURE SYSTEM

Human prostate cells (PNT1As and PC-3s) were exposed under strictly controlled conditions. The cell cultures were exposed by means of a RF exposure system made of a FT-7800E Transceiver (Yaesu, UK), a WaveCell transverse electromagnetic (TEM) cell (WaveControl, Spain), a custom adapted Discovery Linear Amplifier (Linear Amp, UK) and a dummy load. The cell cultures were exposed in the TEM cell to a 144 and 434 MHz field at 5 and 50 W, resulting in a SAR value ranging from 0.5 (for the 144 MHz 5 W exposure regime) to 2.6 W/kg (for the 434 MHz 50 W exposure regime) in the cell culture layer.

During the exposures the E-field was monitored by an EF cube broadband electromagnetic field probe (WaveControl, Spain), that enables field measurement with minimum disturbance of the electromagnetic environment due to its small size and fibre optic connection. Electric field measurements ranged from 5 to 155 V/m, according to the different exposure conditions.

The exposure time of 60 min was chosen, following the results of the first set of experiments, assessing 10, 30, 60 minutes of exposure. For double exposures, cells were exposed to RF 4 hours after the end of the first exposure.

The temperature was set at 37˚C for the start of each exposure using an Airtherm ATX air circulation system (World Precision Instrument, UK). Two highly accurate I652 temperature probes (Luxtron Fluoroptic Thermometer, USA) were fixed inside the TEM cell: one inserted into a flask, to monitor the medium temperature, the other placed on the bottom of the TEM cell, to monitor the air temperature.

2.2.3 - NUMERICAL DOSIMETRY

A complete numerical dosimetry was calculated for each exposure systems. The electromagnetic field distribution in the TEM cell and the SAR distribution inside the Petri

dishes were calculated by the use of the finite difference time domain (FDTD) method, by means of the Comsol Multiphysic (version 3.2) finite element system.

Exposure setups modelling was made in co-operation with Bologna Physics Department, thanks to Dr Pietro Mesirca and with the Antenna & High Frequency Research Centre, thanks to Dr Padraig McEvoy and Dr Giuseppe Ruvio.

The software is based on multiphysics modules, allowing a model and a solution to each problem through a different physical approach (acoustics, diffusion, electromagnetic, fluid mechanics, heat transfer, structural mechanics and so on). A sequential analysis was performed and the problem was firstly solved investigating the electromagnetic waves harmonic propagation. These results were then used as independent variables in a second analysis aimed at assessing the heat transfer by conduction.

Therefore, two kinds of measurement were carried out: electric field distribution and temperature increase inside the culture medium, on the layer were cell grow. These measurements allowed a reliable evaluation of the SAR and the temperature changes for each exposure regime applied.

2.3 - BIOLOGICAL ANALYSES

After 24–48 hours cell seeding, medium was removed from culture dishes or flasks and semi-confluent cell monolayer was incubated in serum-free medium and then exposed to the treatments. Samples for cell count were taken 1 and 7 days after each exposure, samples for PicoGreen and Bradford assays were taken 4 hours and 24 hours after, while the cell index was real time recorded by the RT-CES system (xCELLigence, Roche) from 24 hours before to 24 hours after each exposure.

To avoid the variability inherent to the assay used, all tests were performed for three independent experiments. Means values and standard deviation were calculated, and statistical significance of the differences between exposed samples and controls was evaluated by t-test and ANOVA. When it was not possible to perform the t-test, because of the small number of replicates, Mann-Whitney Rank Sum Test has been run. All pairwise multiple comparison has been performed by Tukey test.

2.3.1 - HSP70 PROTEIN EXPRESSION

After the experimental treatment, cells were washed with ice-cold Phosphate-Buffered Saline solution (PBS), detached by scraping, and transferred to 1.5 ml conical tubes. After a 10 min centrifugation at 800 xg at 4˚C, the pellet was resuspended in ice-cold 10 mM Na-phosphate buffer, pH 7.4, containing 1% Nonidet-P40, 0.5% Na deoxycholate, 0.1% SDS, 1 g/ml pepstatin A, E-64, bestatin, leupeptin and aprotinin, and 25 g/ml PMSF. After 30 min on ice, samples were centrifuged at 9000 xg at 4˚C for 20 min. The supernatant was diluted 1.5 times with Laemmli buffer, boiled for 5 min, and kept at -20˚C until analysis. Sample protein content was assessed according to Lowry et al. (1951) using bovine serum albumin as standard.

Protean III apparatus (28 mA, 2 h at 4˚C), and the resolved proteins were transferred onto a nitrocellulose membrane (300 mA, 1 h at 4˚C). Blots were then probed with rat anti-human HSC70 (1:2000), mouse anti-human HSP70 (1:2000) or mouse anti-human β-tubulin (1:200) monoclonal antibodies for 1 h, and, after washing, rabbit anti-rat IgG polyclonal antibody (1:6000) and rabbit anti-mouse IgG polyclonal antibody (1:6000) conjugated with horseradish peroxidase for 1 h. Immunoblots were developed using enhanced chemiluminescence (ECL) reagent and were analyzed with the ImageMaster system (Amersham-Pharmacia, Italy); quantification of band intensities was performed using TotalLab software version 1.0. Tubulin expression was used to assess equal loading of samples. Given the inherent variation between film development, data were normalized to reference samples that were included in each experiment.

2.3.2 - ACETYLCHOLINESTERASE ACTIVITY AND KINETICS

For the estimation of intracellular AChE, the medium was removed and the cells were washed with PBS 1x (Gibco, Italy) and lysed using ice-cold phosphate buffer containing 1% Nonidet P-40 (Sigma, Italy). The homogenate was centrifuged for 10 min at 3000 xg at 4°C and the resulting supernatant was used for the intracellular enzyme determination (Curtin et al., 2006). The remaining pellet was resuspended with H_2O, in order to obtain membrane AChE.

The general scheme of enzymatic reaction can be summarized as follows:

$$\mathrm{Enz + AcCh} \underset{k_2}{\overset{k_1}{\rightleftharpoons}} \mathrm{(EnzAcCh)} \xrightarrow{k_3} \mathrm{EnzAc + Ch}$$

$$\mathrm{EnzAc + H_2O} \xrightarrow{k_4} \mathrm{Enz + AcOH}$$

where: Enz is the enzyme, AcCh is the substrate (acetylcholine), and Ch and AcOH are the products (choline and acetic acid, respectively). The reaction rate of the acetylcholine hydrolysis is:

$$v = \frac{\mathrm{d[Ch]}}{\mathrm{d}t} = \frac{k_3[\mathrm{Enz}]_0[\mathrm{AcCh}]_0}{[\mathrm{AcCh}]_0 + K_\mathrm{M}} = \frac{V_\mathrm{M}[\mathrm{AcCh}]_0}{[\mathrm{AcCh}]_0 + K_\mathrm{M}}$$

and the steady-state rate constants are derived from the equations:

$$V_\mathrm{M} = k_3[\mathrm{Enz}]_0; \quad K_\mathrm{M} = \frac{k_4(k_2 + k_3)}{k_1(k_3 + k_4)}; \quad k_\mathrm{cat} = \frac{k_3 k_4}{(k_3 + k_4)}$$

The enzyme reaction rate was determined using acetylthiocholine as substrate. The concentration of the reaction product (thiocholine) was measured according to the modified Ellman's method, based on the following reactions:

$$\mathrm{Acethylthiocholine} \xrightarrow{\mathrm{AChE}} \mathrm{Thiocoline + Acetate}$$

$$\mathrm{Thiocoline + DTNB} \xrightarrow{\mathrm{fast}} \mathrm{5\text{-}thio\text{-}2\text{-}nitro\text{-}benzoic\ anion\ (yellow)}$$

The concentration of the yellow anion of 5-thio-2-nitrobenzoic anion (ε=13600 M^{-1} cm^{-1} at λ=412 nm) allows assessment of hydrolase's activity. Kinetics measurements were carried out to verify the catalytic properties of the enzyme after different exposure times using the native sample as a standard.

Extracts were analyzed for total AChE activity by the method of Ellman et al. (1961), using acetylthiocholine (ASCh) as substrate, in a reaction mixture containing 0.05 mg enzyme, 50 µl of 0.33 mM dithionitrobenzene (DTNB), and 10 mM tris-HCl sodium phosphate buffer (pH 7.2) in a final volume of 1200 µl. 50 µl of 0.5 ASC was added to let the reaction start. The substrate was used at 12 to 16 concentrations ranging from 0.001 mM to 20 mM in order to evaluate the AChE kinetics parameters under the different conditions tested.

The absorbance change at 405 nm was monitored with a Multi Sample DU800 Beckman spectrophotometer. Reading was repeated for 5 to 25 min at 1 min intervals to verify that the reaction occurred linearly. The blank reaction was measured without substrate, to evaluate the reaction of thiols with DTNB. All trials were performed in

triplicates and data are expressed as nmol·min^{-1}·mg of protein^{-1} (Rieger et al, 1980; Schweitzer, 1993; Heo et al, 2002).

Kinetics preliminary experiments indicated that data follow the same trend as Michaelis-Menten kinetics. For this reason the Michaelis–Menten equation was used to estimate kinetics parameters Km and Vmax. All the data fitted well to this plot, following the model:

t=Vmax-X/(Km+x)

with a correlation coefficient R^2>0.95 for all the tests performed.

The Michaelis constant (Km) and the equilibrium constant were calculated using the Michaelis-Menten equations, followed by Lineweaver-Burk transformation. Parameters of the equation, Vmax and Km were expressed with their standard errors.

2.3.3 - CELL PROLIFERATION RATE

The xCELLigence is a real-time cell electronic sensing system (RT-CES) from Roche (UK), composed of three parts: an electronic sensor analyzer, a device station, and a 96-well e-plate, consistent with dimensions of standard flat-bottom 96-well culture plate. The well bottom has incorporated circle-on-line sensor electrode arrays (circle diameter 90 mm, line with 30 mm, and line-to-line spacing 110 mm). The gold microelectrodes cover about 80% of the area of the bottom. The device station, which is connected with e-plates, is placed in the incubator and connected to the electronic sensor analyzer through electrical cables. Cell index (CI) is the parameter used to represent cell status based on the electrical impedance measurements, which is calculated by frequency-dependent impedance according to the formula:

$$CI = \max_{i=1\ldots N}\left(\frac{R_{cell}(f_i)}{R_b(f_i)} - 1\right)$$

where $R_b(f_i)$ and $R_{cell}(f_i)$ are the frequency-dependent electrode resistances without or with cells present, respectively, at different frequencies (n is the number of frequency points at which the impedance is measured, i.e., n ¼ 3 for 10, 25, and 50 kHz). Each frequency is applied for ~ 100 ms to each well. CI is a relative value to indicate how many or how cells attach to the electrodes. Under the control of the RT-CES software, experiment data are measured automatically by the sensor analyzer.

Cell calibration on the xCELLigence was performed to determine the optimal cell seeding number for each cell line. Cells were seeded, as described above, in a 96-well e-plate. Following RF exposure of cells seeded in an e-plate, cell proliferation rate was analyzed continuously in real time for 24 hours using this instrument. The CI was recorded four times per hour for the duration of the experiment. The relative rate of cell proliferation was then determined for each data set at 4 hour intervals using the xCELLigence software and data are presented as a fraction of the rate in sham exposed samples at the relevant 4 hourly interval.

2.3.4 - CELL SURVIVAL ASSAY

Cell proliferation was also determined by cell counting using a Z2 Coulter Counter (Beckman Coulter, USA). Cells were counted 1 and 7 days after the end of the exposure, and compared to their respective controls. For each analysis, three replicate dishes were used, and at least three independent experiments were performed. 0.5 ml of cell suspension was added to a coulter vial, containing 19.5 ml of Isoton solution.

Cell number in the cell suspension was then calculated by means of the following formula:

Density (cell/ml) = (number of cells x 2) x 20 / 0.5

Cell numbers are presented as a percentage of sham-exposed cell populations. Data are presented as the mean +/- standard deviation of 3 or more separate experiments.

2.3.5 - RELATIVE QUANTIFICATION OF CELLULAR DNA

Following seeding and exposure of cells, as described above, total DNA per well was determined 24 hours post exposure or sham exposure using PicoGreen dsDNA kit (Molecular Probes, USA), according to the manufacturer's instructions, in a Fluostar Optima Microplate Reader (BMG, USA) employing an emission wavelength of 520 nm and excitation of 480 nm. Briefly, PicoGreen dye was diluted 1:200 with 1x Tris/EDTA (TE) buffer. Each reaction contained 50 µl of a dye solution and a sample of DNA / DNA standard made up to 50 µl in TE buffer in a 96 well plate (Sarstedt, Germany) (Szpechcinski et al., 2008). Data was then normalized against changes in cell number and are expressed as a fraction of sham-exposed cell populations. Data are presented as the mean +/- standard deviation of 3 or more separate experiments.

2.3.6 - QUANTIFICATION OF TOTAL PROTEIN

Following seeding and exposure of cells, as described above, total protein per well was determined 24 hours post exposure / sham exposure using a Bradford Assay kit (Sigma, UK) with some minor modifications of the procedure described by Bradford (1976). Briefly, 190 µl of Bradford assay solution and 10 µl of either sample, H_2O (blank) or Bovine Serum Albumin standard was maintained in a 96 well plate (Sarstedt, Germany) for 5 minutes. The absorbance was then read at 595 nm in a Fluostar Optima Microplate Reader (BMG, USA). Data was then normalized against changes in cell number and are presented as a fraction of sham-exposed cell populations. Data are presented as the mean +/- standard deviation of 3 or more separate experiments.

2.3.7 - NUCLEAR DNA DAMAGE MARKER ANALYSIS

Total RNA was extracted from control and treated cells using the RNeasy Mini kit (Qiagen, UK) according to the manufacturer's protocol. RNA concentration and quality were verified by UV spectroscopy and electrophoresis using a 1.2% agarose gel under denaturing conditions. First-strand cDNA for each sample was synthesized from 1 g of total RNA using the Transcriptor First Strand cDNA Synthesis Kit (Roche, UK). A combination of anchored-oligo (dT) primers and random hexomer primers has been used, in order to increase the sensitivity of the retro-transcription (RT) reaction. Reactions were performed in a total volume of 20 µl, according to the manufacturer's protocol. The thermal program consisted of 10 min at 25˚C, 30 min at 55˚C and 5 min at 85˚C. As a normalization control for each RT-PCR experiment, housekeeping primers, specific for the 18S rRNA, were used in PCR reactions with each gene target. Primer pairs used for each gene product are described in Table 2.1.

RT-PCR reactions were performed in a total volume of 30 µl containing 6 µl milliQ water, 10 µl REDTaq Ready Mix (Sigma, UK), 2 µl Forward and Reverse primers (1 mM final concentration each) and 2 µl template cDNA (from 1 µg total RNA).

The thermal program was performed on the C1000 Thermal Cycler (BioRad, UK) and consisted of an initial denaturation (94˚C, 3 min), followed by 30 cycles (for PARP1 and XLF primers) and 35 cycles (for 18S primers) of denaturation (94˚C, 40 s), annealing (62˚C, 2 min), extension (72˚C, 30 s), and a final extension step (72˚C, 1 min).

To ensure that quantification was performed at the midpoint of the linear phase of amplification, for each gene, preliminary RT-PCRs were carried out using both different annealing temperature of each cDNA sample and different PCR cycle numbers. Equal aliquots of each PCR sample were separated on a 1.2% wide-range agarose gel using TAE buffer (1x) and stained with 0.1 µl/ml gel red (Sigma, UK). A D3812 molecular marker (Sigma, UK) has also been used.

Agarose gel band intensities were analyzed and quantified with the Versadoc 5000 Imaging Systems (Bio-Rad, UK).

Table 2.1 – The primers sequences.

	XLF
LEFT PRIMER	aagaaccagtcacataaagttctgc
RIGHT PRIMER	tatttttagtagagacagggtttcacc
	PARP1
LEFT PRIMER	agtacattgtctatgatattgctcagg
RIGHT PRIMER	gagaagttagagaaaacctttaacacg
	18s
LEFT PRIMER	cttagagggacaagtcgcg
RIGHT PRIMER	ggacatctaagggcatcaca

Traditionally PCR is performed in a tube and the products are analyzed by gel electrophoresis. Real time PCR (Q-PCR) permits the analysis of the products while the reaction is actually in progress. This is achieved by using fluorescent dyes which react with the amplified product.

DNA fragments, containing the genes that code for PARP1 and Cernunnos-XLF proteins were amplified in the LightCycler Carousel-based System (Roche Applied Science, UK) following the manufacturer's instruction. The PCR amplification was performed in a 20 µl volume, using the LightCycler FastStart DNA Master plus SYBR Green I kit (Roche), 5 µl cDNA and 5 mM mixed primers solution. The initial denaturing step at 95˚C for 10 minutes was followed by 35 cycles of 95˚C for 10 sec, 65˚C for 5 sec and 72˚C for 12 sec. The melting curve analysis was performed at 65˚C according to the protocol supplied.

Chapter 3

RESULTS

3.1 - SIMULATION

3.1.1 - MATHEMATICAL MODEL OF THE 1.8 GHz GSM EXPOSURE SYSTEM

Dosimetric investigations for the characterization of the RF setup used in this project included the analysis of the performed finite difference time domain (FDTD) simulation and their validation with direct measurements. The FDTD method can simulate complex models by binding stability criteria to a time integration scheme. The waveguide resonator, including medium with meniscus, petri dishes and dish holder were simulated and evaluated.

Geometry

The very first step was to design the geometry of the model, by using a graphic interface (CAD tools) to respect the real proportions of the apparatus. The waveguide was drawn, the antenna was added at one of the shortcut ends, the petri dishes, containing the culture medium, were then located in the H-field maxima (Fig. 3.1).

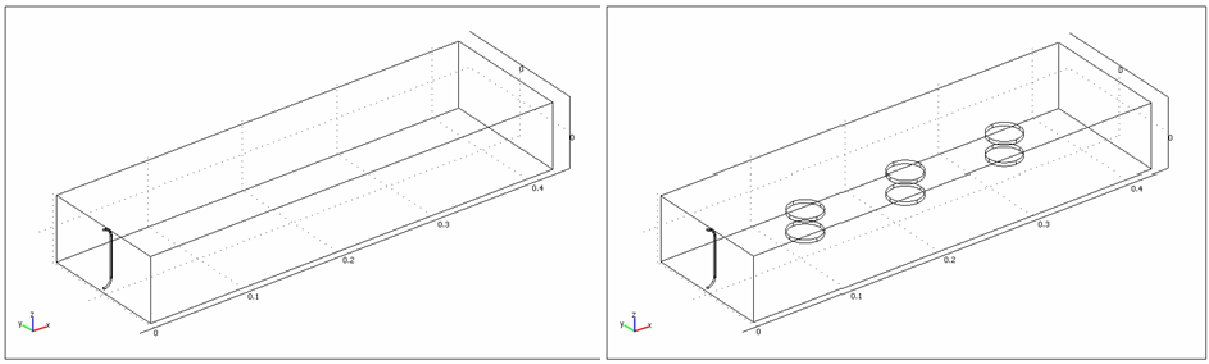

Fig 3.1 – The geometry of the model: the waveguide and the antenna only (left) and with the medium layer inside the petri dishes (right) in the fixed positions of the experimental system.

The plastic of the petri dishes and of their holder can be considered completely transparent to electromagnetic fields, and therefore they are not drawn in the model. The 3 ml medium volume (5 mm height medium + measured meniscus volume) has been chosen to guarantee a high inductive coupling.

EM Subdomain Settings

Specific parameter settings were assigned to the geometry components, in order to give the model its peculiar characteristics. The physics quantities that identify the real apparatus were defined and the parameters were set at the boundary, domain and subdomain conditions. Other values were calculated: to get the electric field that leads to a SAR of 2 W/kg in the cells exposed, a circulating surface current of $9 \cdot 10^6$ A/m is required.

EM Module Parameters

The relative static permittivity (ε_r) of a material under given conditions is a measure of the extent to which it concentrates electrostatic lines of flux. It is the ratio of the amount of stored electrical energy when a potential is applied, relative to the permittivity of a vacuum. The relative static permittivity is the same as the relative permittivity evaluated for a frequency of zero.

It is defined as

$$\varepsilon_r = \frac{\varepsilon}{\varepsilon_0}$$

where ε is the static permittivity of the material, and ε_0 is the electric constant (ε_0=8.8541878176 $\cdot$ 10^{-12} F/m). The higher the relative permittivity, the more insulating a material will be, therefore it will be strongly opposed to the current.

Electrical conductivity (σ) or specific conductance is a measure of a material's ability to conduct an electric current. When an electrical potential difference is applied to a conductor, the movable charges flow and give rise to an electric current. The conductivity σ is defined as the ratio of the current density to the electric field strength:

$$\sigma = \frac{J}{E}$$

and is the reciprocal (inverse) of electrical resistivity, ρ.

Relative permeability (μ_r) is the ratio of the permeability of a specific medium to the permeability of free space given by the magnetic constant ($\mu_0 = 4\pi \cdot 10^{-7}$ H/m):

where ε_0 is the electric constant and c is the speed of light:

In electromagnetism, permeability is the degree of magnetization of a material that responds linearly to an applied magnetic field. A good magnetic core material must have high permeability. Materials with a variable μ value are considered ferromagnetic and present a magnetization much larger than other materials. Ferromagnetic materials can present spontaneous magnetization, and this gives rise to the hysteresis loops. Materials with a constant μ are considered non-ferromagnetic and can be divided into diamagnetic and paramagnetic. Diamagnetism is the property of an object which causes it to create a magnetic field in opposition to an externally applied magnetic field, thus causing a repulsive effect. Specifically, an external magnetic field alters the orbital velocity of electrons around their nuclei, thus changing the magnetic dipole moment in the direction opposing the external field. Diamagnets are materials with a magnetic permeability less than μ_0 (a relative permeability less than 1). Consequently, diamagnetism is a form of magnetism that is only exhibited by a substance in the presence of an externally applied magnetic field. It is generally a quite weak effect in most materials, although superconductors exhibit a strong effect. Paramagnetism is a form of magnetism which occurs only in the presence of an externally applied magnetic field. Paramagnetic materials are attracted to magnetic fields and have a relative magnetic permeability greater than one (or, equivalently, a positive magnetic susceptibility). The magnetic moment induced by the applied field is linear in the field strength and rather weak. It typically requires a sensitive analytical balance to detect the effect. Unlike ferromagnets, paramagnets do not retain any magnetization in the absence of an externally applied magnetic field, because thermal motion causes the spins to become randomly oriented without it. Thus the total magnetization will drop to zero when the applied field is removed. Even in the presence of the field there is only a small induced magnetization because only a small fraction of the spins will be oriented by the field. This fraction is proportional to the field strength and this explains the linear dependency. The attraction experienced by ferromagnets is non-linear and much stronger. The dielectric parameters of the waveguide, antenna and medium are listed below.

Table 3.1 – The electromagnetic parameters used in the model.

		WAVEGUIDE	ANTENNA	MEDIUM
	library material	gold	copper	RPMI
relative permittivity	ε_r	1.00054	1	75.8
electrical conductivity	σ (S/m)	0	5.998e7	2.3
relative permeability	μ_r	1	1	
	boundary conditions	PEC	surface current	continuity
	Js (A/m)		$9.6 \cdot 10^6$	

As an initial condition, the electric field is considered null in every direction. The boundary conditions are that the waveguide can be considered a Perfect Electric Conductor (PEC), the surface electric current circulating on the copper antenna is $9.6 \cdot 10^6$ A/m and the culture medium has a continuity feature.

Mesh

COMSOL Multiphysics is a program based on finite element analysis, so it returns a discrete answer, not a continuous one. The spatial distribution of this discrete answer is called mesh, which can also be seen as the subdivision of a complex geometry into simple shape units. Triangular or square units are used to divide a bi-dimensional structure, so that the mesh is characterized by sides and vertex. Tetrahedrons, hexahedrons and prisms are the mesh subunit for tridimensional structures and in this case the mesh is characterized by faces, sides and vertex.

The mesh is an approximation of the original geometry, and the number of mesh elements will affect the degree of freedom of the model and the accuracy of the results. Choosing different meshes allows different solutions: the finer the mesh, the more precise the results, but the slower the calculations.

For this model a fine mesh with 22141 elements has been used, which implies 30718 degrees of freedom to solve the problem.

Solver

This finite element analysis is based on systems of equations that can be solved by Gauss' law or Kramer's rule. Two approaches can be used: a direct solver that can solve these equations by progressive eliminations of unknowns, or an iteration process, that uses

preconditioning matrix, mainly diagonal matrix, to gain matrix products. The best solution will be chosen among these matrix products, depending on the residuals analysis.

For the mathematical model of the 1.8 GHz exposure system a stationary linear harmonic propagation analysis was employed. A SPOOLES direct solver, based on a symmetric matrix, was chosen.

Electromagnetic Analysis

After inserting the parameters into the model, the first test was the electromagnetic field analysis.

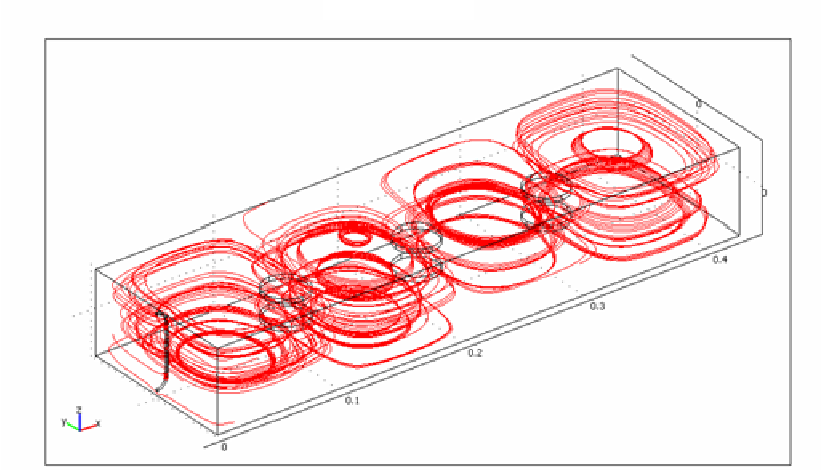

Fig 3.2 – The magnetic lines of force distribution as calculated by the model.

The magnetic lines of force distribution was visualized inside the waveguide (Fig. 3.2) and it appears exactly as expected. This is confirmed by the petri dishes: they have a fixed position that is supposed to be coincident to the H-field maxima. And this is precisely what can be seen in the model graphical distribution: the petri dishes are located in the zones where the most magnetic lines of force distribution converge, in other words in the zones of highest magnetic field intensity.

The same was done for the normalized electric field distribution inside the waveguide volume (Fig. 3.3). It appears exactly as expected and once again the petri dishes are located in the zones where the electric field is the lowest. These first results show that the model fits the requirement of the experimental setups.

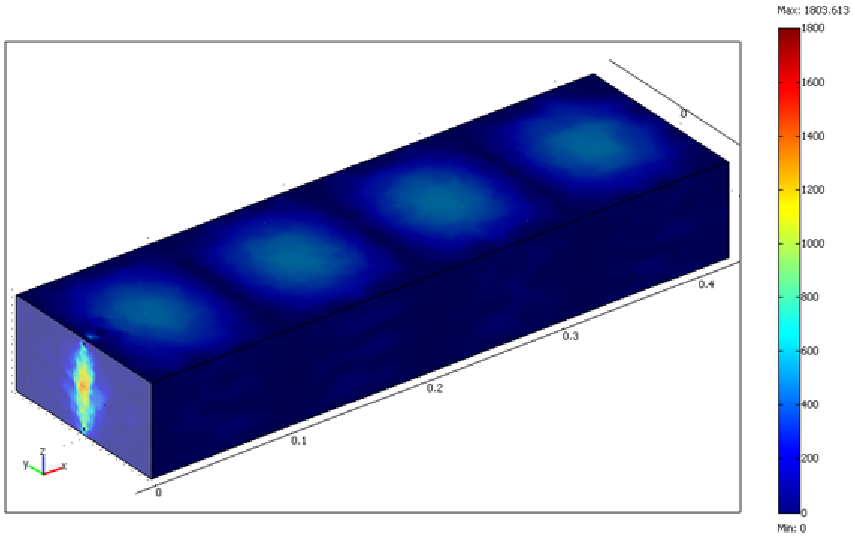

Fig 3.3 – The normal electric field distribution inside the waveguide as calculated by the model.

Then the electric field distribution inside the culture medium was evaluated (Fig. 3.4), particularly on the bottom of each petri dish, where the cells are in adhesion.

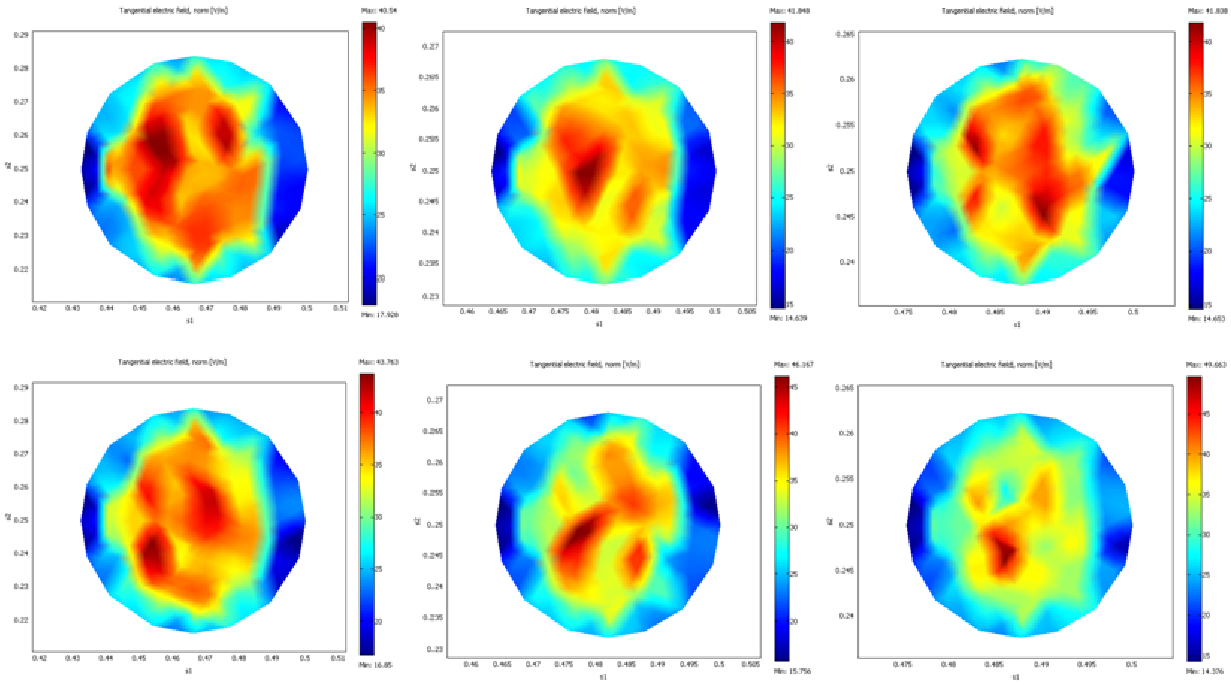

Fig 3.4 – The electric field distribution at the bottom of each petri dish as calculated by the model.

The Electric field values were calculated by the model across each dish. Then the E-field averages and the SAR values were calculated (Table 3.2).

Table 3.2 – The electric field and SAR values inside each petri dish as calculated by the model.

Electric Field (V/m)							
	Petri1	Petri2	Petri3	Petri4	Petri5	Petri6	Average
Average	30.03	28.05	28.85	30.64	29.56	29.76	29.49 ± 2.53
Std Err	2.34	2.36	2.45	2.67	2.69	2.68	
Un-homogeneity (%)	11.67	20.98	16.37	14.9	17.89	17.34	16.52
Un-homogeneity (%) among petri							3.09

It's important to underline that the un-homogeneity of the E-field distribution inside each petri is less than 20%, which is the limit for this kind of exposure system. The un-homogeneity among the dishes is about 3.09%, which is a good value. This datum is very important because it verifies that the exposure conditions inside each petri dish are exactly the same.

Finally, the SAR due to this electric field was estimated: on the irradiated cells SAR is 2.00 W/kg on average, which is the expected value for the RF exposure regimes supplied by this exposure system.

Thermal Module

The following step was the analysis of the interactions between the electromagnetic fields and the cells: in particular the temperature changes due to the heat transferred by the electromagnetic energy were assessed.

A physical parameter connecting the electromagnetic module to the thermal module was to be found. A dependent variable provided by the electromagnetic module analysis was used as an independent variable inside the thermal module, in order to perform a thermal analysis predictive of the actual RF heat transfer. The chosen variable is the Resistance Heating (Qext = Qav_emwh), which represents the heat produced by the electromagnetic field.

Thermal Parameters

Thermal properties of the cell culture medium were provided as new parameters to the model (Table 3.3).

Thermal conductivity (k) is the property of a material that indicates its ability to conduct heat. It appears primarily in Fourier's Law for heat conduction. In other words, it is

defined as the quantity of heat, ΔQ, transmitted during time Δt through a thickness x, in a direction normal to a surface of area A, due to a temperature difference ΔT, under steady state conditions and when the heat transfer is dependent only on the temperature gradient. Alternatively, it can be thought of as a flux of heat (energy per unit area per unit time) divided by a temperature gradient (temperature difference per unit length)

The density of a material (ρ) is defined as its mass per unit volume

$$\rho = \frac{m}{V}$$

that is measured kilograms per cubic metre (kg/m³).

Heat capacity (C_P) is the capacity of a body to store heat. It is typically measured in units of J/°C or J/˚K (which are equivalent). If the body consists of a heterogeneous material with sufficiently known physical properties, the heat capacity can be calculated as the product of the mass m of the body (or some other measure of the amount of material, such as number of moles of molecules which are present) and the specific heat capacity c, (an intensive property) for the material.

The heat transfer coefficient (h), in thermodynamics and in mechanical and chemical engineering, is used in calculating the heat transfer, typically by convection or phase change between a fluid and a solid. There are numerous methods for calculating the heat transfer coefficient in different heat transfer modes, different fluids, flow regimes, and under different thermo-hydraulic conditions. Often it can be estimated by dividing the thermal conductivity of the convection fluid by a length scale. The heat transfer coefficient is often calculated from the Nusselt number (a dimensionless number). The heat transfer coefficient has SI units in watts per metre squared-Kelvin (W/(m^2˚K)).

$$h = \frac{k}{l} = \frac{0.12W(^\circ K \cdot m)^{-1}}{0.0008m} = 150W(^\circ K \cdot m^2)^{-1}$$

The waveguide structure and the antenna can be considered negligible for the thermal analysis therefore no parameter value was established for them.

The initial temperature was set at 37˚C (310˚K), according to the constant temperature provided by the incubator.

Table 3.3 – The thermal parameters used in the model.

		CULTURE MEDIUM
thermal conductivity	k (isotropic) (W/(m·°K))	0.6
density	ρ (kg/m^3)	1000
heat capacity	C_P (J/(kg·°K))	4.2
heat source	Q	Qav_emw2
initial temperature	T (t_0) (°K)	310
heat transfer coefficient	h (W/(°K·m^2))	171.4 W/(°K·m^2)
external temperature	Tinf (°K)	310

Thermal Analysis

The solver eventually provided the data of the temperature changes inside the cell culture medium layer (Fig. 3.5 and 3.6), showing remarkably that the difference among the six petri dishes is very small.

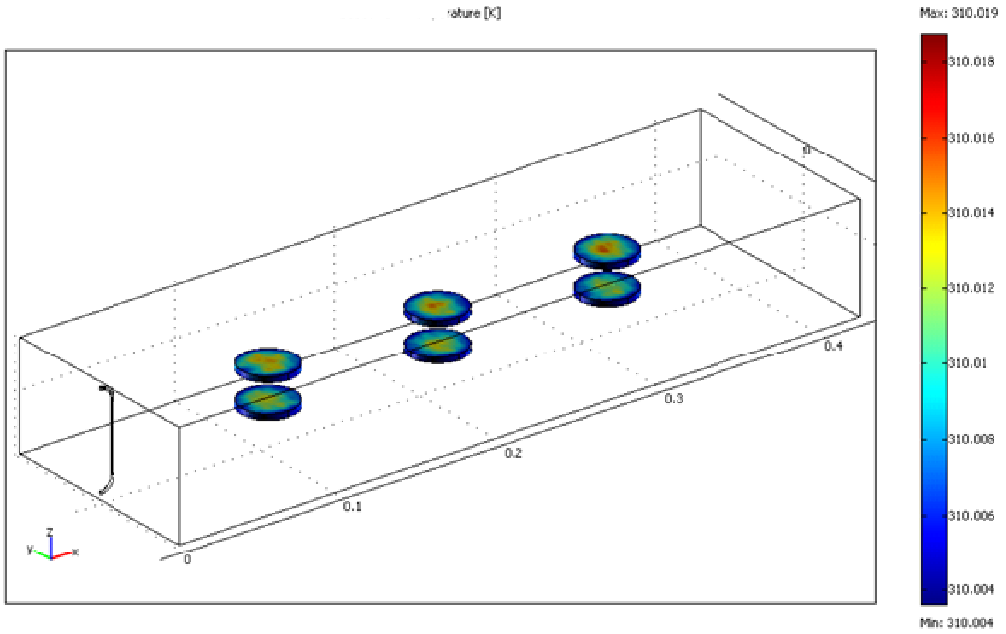

Fig 3.5 – The temperature increase due to the applied electromagnetic field inside the medium layer, as calculated by the model.

The thermal analysis was performed at the bottom of each petri dish. Then the temperature increase averages were calculated (Table 3.4).

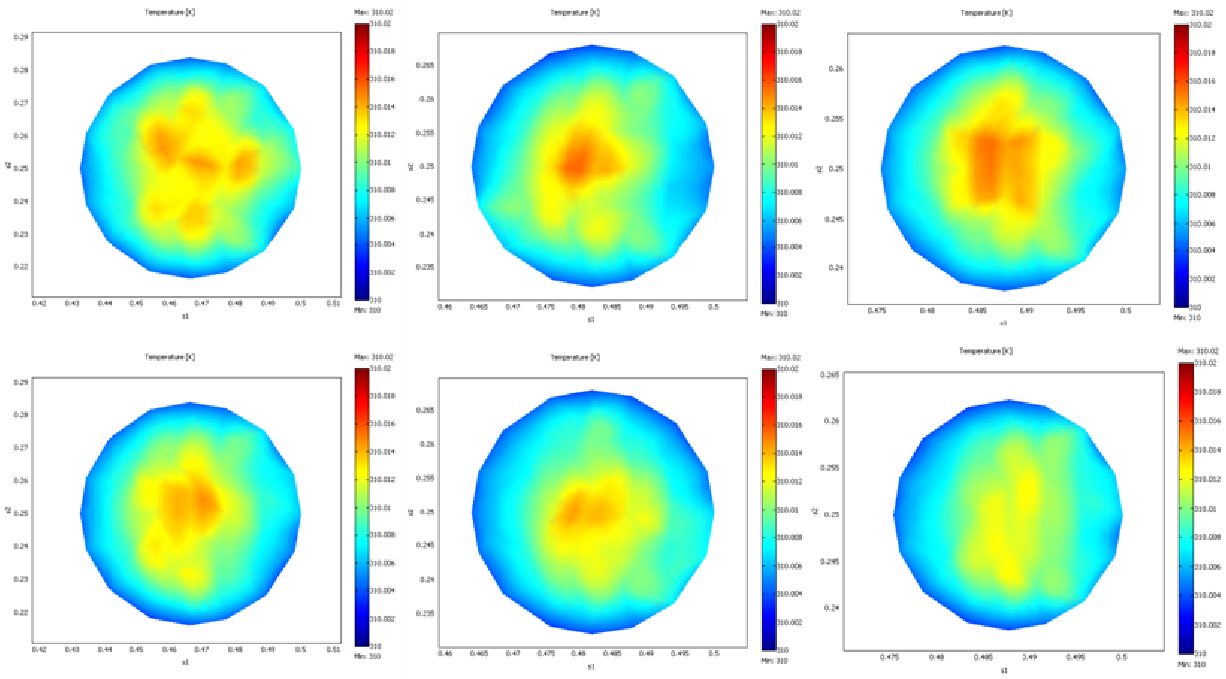

Fig 3.6 – The temperature increase due to the applied electromagnetic field at the bottom of each petri dish, as calculated by the model.

Table 3.4 – The temperature values inside each petri dishes as calculated by the model.

Temperature (˚K)							
	Petri1	Petri2	Petri3	Petri4	Petri5	Petri6	Average
Average	310.0093	310.0084	310.0089	310.0087	310.0082	310.0082	310.0086 ± 0.0011
Std Err	0.0011	0.0011	0.0012	0.0011	0.0011	0.0010	
Un-homog (%)	0.0012	0.0021	0.0017	0.0014	0.0016	0.0012	0.0015

These results show that the temperature change due to the presence of electromagnetic fields is very small: since the temperature rise is 0.0086 °K on average, it can be considered absolutely negligible.

The un-homogeneity inside each petri is extremely low and temperature is uniformly distributed without localized “hot spots”. This result is very important because inside each petri dish every single cell should be exposed at the same conditions as the others.

Also, the un-homogeneity among different dishes is very small, so it can be inferred that each petri is exposed at the same condition as the others. Therefore that the cells exposed to this RF exposure system should not suffer any thermal effect and that any effect potentially measurable is probably due to the presence of an external electromagnetic field rather than to a hyperthermia effect.

3.1.2 - MATHEMATICAL MODEL OF THE 144-434 MHz RADIOWAVE THERAPY EXPOSURE SYSTEM

A similar approach was adopted for the RF exposure system MiBRRG group is equipped with. A mathematical model of the TEM cell was also realized.

Geometry

The very first step was to design the geometry of the TEM cell, by using a graphic interface (Fig. 3.7).

In order to simplify the model only the volume of the TEM cell below the septum and the volume where the culture medium layer is placed (5 mm height) were drawn.

The plastic of the flasks, the petri dishes and the 96-well plates used for exposing the cells, as well as the polystyrene support can be considered completely transparent to electromagnetic fields, and therefore they were not drawn in the model.

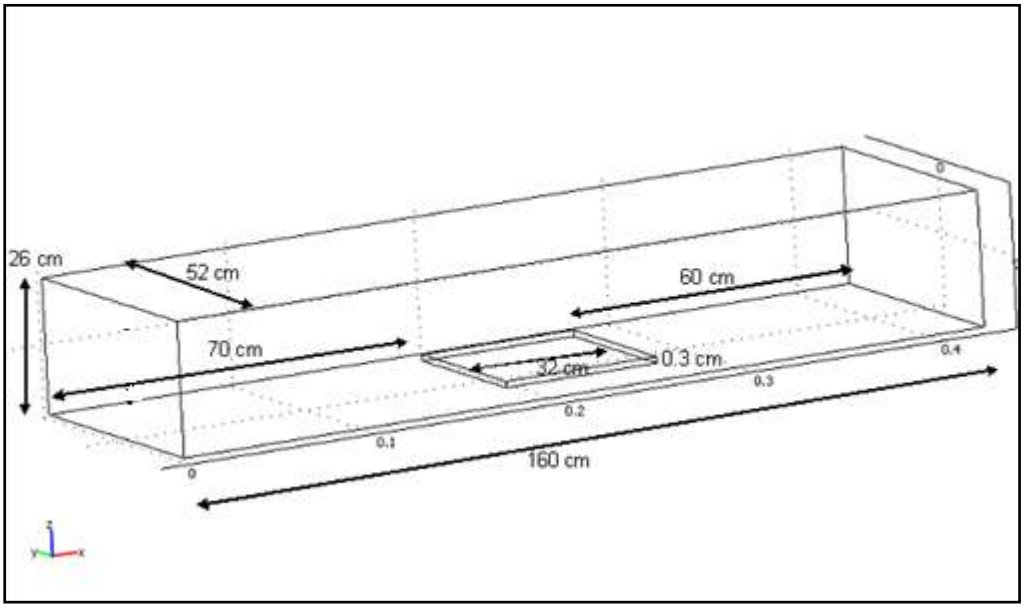

Fig 3.7 – The geometry of the model (TEM cell and medium layer in their real dimension).

EM Subdomain Settings

Specific parameter settings were assigned to the geometry components, in order to give the model its peculiar characteristics. The physics quantities that identify the real apparatus were defined and the parameters were set at the boundary, domain and

subdomain conditions. Other values were calculated to get the frequency and input power required.

EM Module Parameters

The dielectric parameters of the medium are the same used for the 1.8 GHz exposure system (see table 3.1).

Mesh and Solver

The selected mesh was a fine one, which generated 9040 elements in the model, so that the solver will work on a problem with 12542 degree of freedom. The solver was once again stationary linear and based on a SPOOLES method, and it made a harmonic propagation analysis based on a symmetric matrix.

Electromagnetic Analysis

The electromagnetic analysis was performed inside the volume of the culture medium (Fig. 3.8).

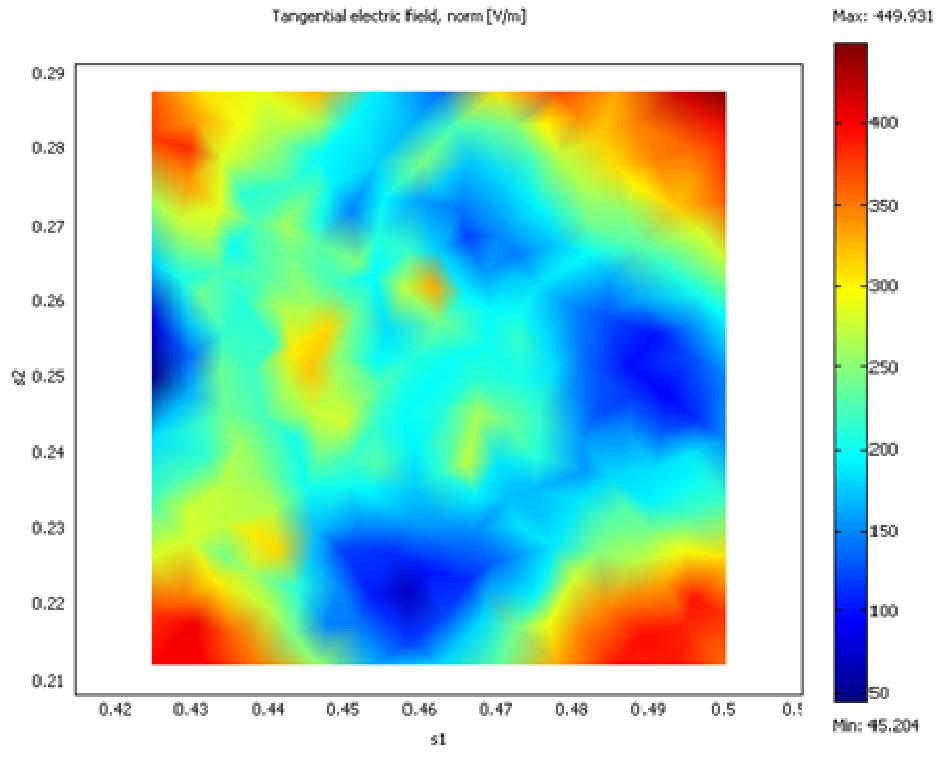

Fig 3.8 – The electric field distribution at the bottom of the medium layer as calculated by the model.

The normalized electric field distribution was calculated on the bottom of that volume, in other words where the cells are supposed to be placed during the exposures. The same approach was adopted for every exposure regime applied in this study (Table 3.5).

Table 3.5 – The results provided by the model compared to the actual measurements for every exposure regime.

FREQUENCY	144 MHz	144 MHz	434 MHz
INPUT POWER	5 W	50 W	50 W
MODELLED ELECTRIC FIELD	24.9 V/m	97.96 V/m	121.9 V/m
STANDARD ERROR	0.32	6.16	9.4
UN-HOMOGENEITY	7.13 %	7.98 %	7.31 %
HIGH PEAK SAR	0.49 W/kg	1.51 W/kg	2.6 W/kg
MEASURED ELECTRIC FIELD	29.98 V/m	102.13 V/m	129.2 V/m

It's important to underline that the E-field un-homogeneity across this section is less than 10%, because this means that all the cells inside each petri dish are exposed to the same conditions.

The theoretical parameters, calculated by the mathematical model of the RF exposure unit were validated by the measured values of E-field, recorded directly by the EF cube device. The E-field was actually measured in 36 points all across the bottom of the polystyrene support inside the TEM cell (Fig. 3.9). Two different kinds of exposure regimes has been tested: one of those used for the biological experiments (434 MHz 50 W) and one with the highest input power achievable (434 MHz 380 W), in order to check the reliability of the method adopted under more critical exposure conditions.

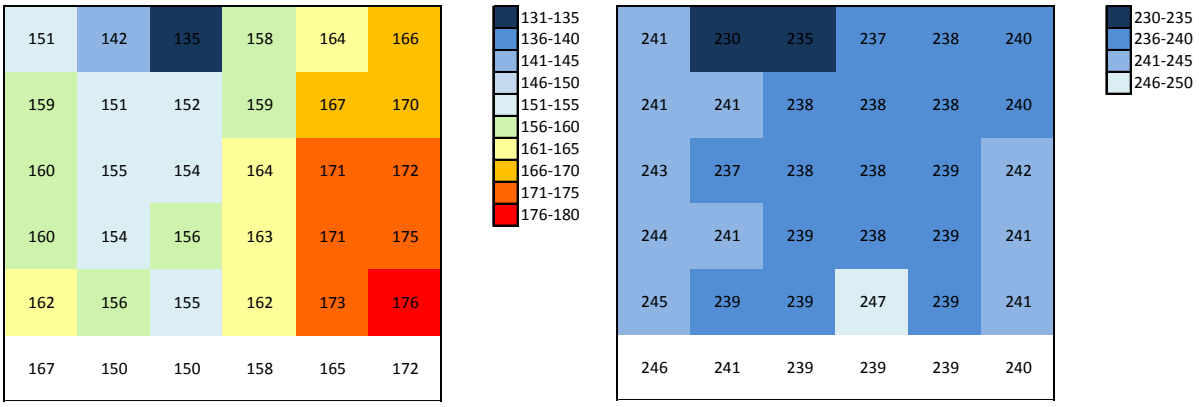

Fig 3.9 – The electric field values, as measured across the polystyrene support, for the 434 MHz 50 W (left) and 434 MHz 380 W (right) exposure regimes.

The spatial distribution obtained for the measured E-field is in good agreement with the numerical one provided by the model. For an exposure regime of 434 MHz 50 W the max E-field measured was 157.8 V/m, the min 123.1 V/m, (129.2 ± 9.4 V/m on average, SAR 2.6 W/kg) leading to an un-homogeneity of 7.31%, which is in agreement to the expected E-field of 121.9 V/m. For an exposure regime at 144 MHz 5 W the measurement of E-field was 29.98 ± 0.32 V/m on average (SAR 0.49 W/kg), that agrees with the expected E-field of 24.9 V/m. For an exposure regime of 144 MHz 50 W the measurement of E-field was 102.13 ± 6.16 V/m on average (SAR 1.51 W/kg), that agrees with the expected E-field of 97.96 V/m.

Thermal Parameters

The thermal properties of the cell culture medium are the same used for the 1.8 GHz apparatus (see table 3.3). No parameter has been set for the TEM cell, the polystyrene support, and the plastic ware. The initial temperature was set at 37˚C (310˚K), according to the constant temperature provided by the air circulating system applied to the TEM cell.

Thermal Analysis

The solver eventually provided the data of the temperature changes at the bottom of the culture medium layer (Table 3.6).

Table 3.6 – The temperature increase at the bottom of the medium layer, as calculated by the model.

FREQUENCY	144 MHz	144 MHz	434 MHz	434 MHz
INPUT POWER	5 W	50 W	50 W	380 W
ΔT	0.05 ˚C	0.08 ˚C	0.1 ˚C	11.8 ˚C

These results show that the temperature change due to the presence of electromagnetic fields is very small for most of the tested exposure regimes. In fact the temperature rise is ≤ 0.1°K for all the low-mid input power exposure and it can be considered absolutely negligible.

The only exposure regime where both the measured and the foreseen temperature increase is significant is the 434 MHz 380 W. Therefore the cells exposed to the RF exposure regimes used in this study should not suffer any thermal effect and any effect potentially measurable is probably due to the presence of an external electromagnetic field rather than to a hyperthermia effect.

3.2 - BIOLOGICAL ANALYSES

3.2.1 - HSP70 PROTEIN EXPRESSION IN HUMAN TROPHOBLASTS

The first biological target was the human trophoblast cell line. They are cells developed during the first three months of pregnancy, highly proliferative and particularly sensitive to stress factors: an alteration of these cells could seriously compromise the pregnancy. Therefore they are considered a valid biological model to assess the environmental stress factors on placenta.

One of the aims of this study, and of bioelectric research in general, is to find a parameter that quantifies the amount of interactions between electromagnetic waves and living organism. For this reason the effects that RF exposure produces on few cellular proteins were investigated.

The expression of the heat shock protein 70 (HSP70) was assessed in human trophoblasts. Heat shock proteins were chosen because of their huge involvement in cell cytoprotection and because of their good answer to stress factors.

Human trophoblasts were exposed at 1.8 GHz, 217 Hz amplitude modulation, 2 W/kg SAR. Exposure times were 1, 4, 16 and 24 hours and during exposure the apparatus was switched off for 10 minutes every 5 minutes, as described previously. Three hours after the end of the exposure the samples were collected and the HSP protein expression was performed by Western Blotting.

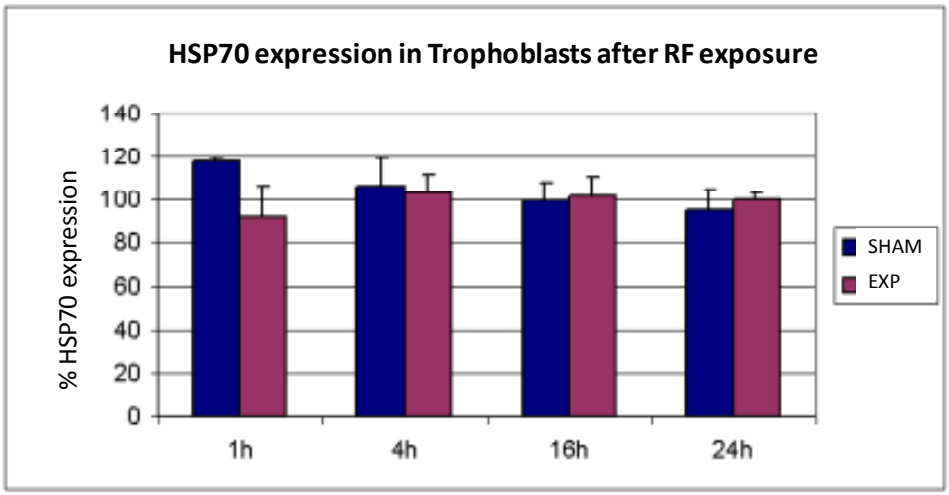

Fig 3.10 – The expression of HSP70 in trophoblasts after RF (1.8 GHz, 217 Hz AM) exposure.

Data presented (Fig. 3.10) came from triplicate exposures and each sample was analysed in triplicate. Exposure data were normalized against the sham data.

It's evident that this kind of RF exposure didn't affect the HSP expression, since the difference between sham and exposed samples was negligible ($p<0.05$). Also, the time of exposure didn't affect the HSP expression.

A positive control test was also performed. Cells exposed and sham-exposed were over-heated at 40 and 43˚C for 60 minutes and then collected straight after and 3 hours post exposure (Fig. 3.11). Samples have been analysed 3 hours after the RF EMF exposure according to preliminary experiments (data not shown) where cells have been collected at different times (0, 1, 2, 3, 4, 5, 6 hours) post-exposure and the most effective post-exposure time for HSP70 expression has been 3 hours.

A slight increase in the HSP expression can be seen for every sample, when compared to the controls kept in the incubator at 37˚C (referred to as 100%). Though no significant difference can be seen when the RF exposed and the sham exposed samples are compared.

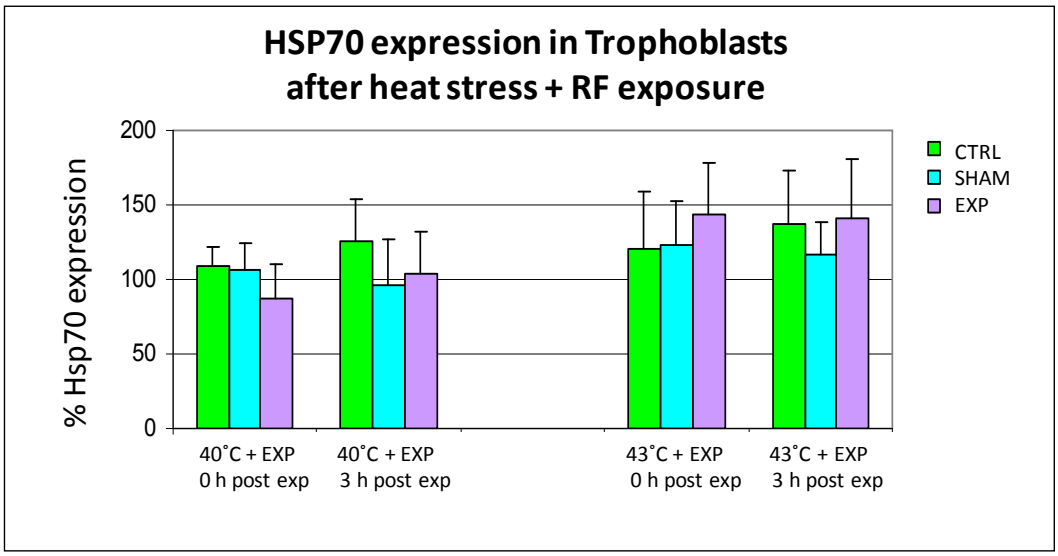

Fig 3.11 – The expression of HSP70 in trophoblasts after heat stress (40˚C - 43˚C) and RF (1.8 GHz, 217 Hz AM) exposure.

3.2.2 - ACETYLCHOLINESTERASE ACTIVITY AND KINETICS IN HUMAN TROPHOBLASTS

Acetylcholinesterase (AChE) belongs to Cholinesterases, the enzymes in the nervous tissue that remove coline from synaptic clefts. AChE hydrolizes acetylcholine into choline and acetic acid.

Acetylcholine and acetylcholinesterase are found also inside the placenta cells, where acetylcholinesterase behaves as a metabolic barrier against xenobiotics, such as pesticides, poison and drugs. It hydrolyzes these xenobiotics and protects the foetus.

Barteri et al. (2005) reported that after being exposed to the EMF emitted by a commercial cellular phone (SAR value 0.51 W/kg), the highly purified AChE showed an enormous change in its activity and kinetic parameters (Vmax and Km are both increased by high frequency after 20 minutes exposure) (Table 3.7).

Table 3.7 – The kinetic parameters of AChE after exposure to high frequency EMF (From: Barteri et al., 2005).

Table 1
Kinetic activity parameters of native and irradiated (20 min) EeAChE calculated by Lineaweaver–Burk plot (Fig. 4)

	V_M (μM L^{-1} sec^{-1})	K_M (μM^{-1} L)	k_{cat} 10^{-6} (sec^{-1})
Native	8.5±1.1	84.0±11.8	1.1±0.1
Irradiated	80.6±12.9	1372.1±226.4	4.2±0.6

Values represent the mean of three different experiments and their variability range.

This paper first demonstrates that GSM “dual band” cellular phone emissions affect the structural and biochemical characteristic of an important central nervous system enzyme. These results cannot be used to conclude that the cellular phone emission can lead to hazardous effects for human health, but they may be a significant model to verify these effects on other biological system (Barteri et al., 2005). For this reason, in this study the activity of this kind of enzyme inside a cell system, after 1.8 GHz exposures was evaluated.

Basal AChE Activity and Kinetics in Human Trophoblasts

The first step was to determine the characterization of the AChE in the human trophoblast cells. Two isoforms of cholinesterases are known in vertebrates, AChE, showing higher affinity for acetylcholine, and BChE, showing higher affinity for butyrylcholine. To determine which is present inside the trophoblasts, the enzymatic activity was measured in

the presence of two different substrates: acetylthiocholine iodide (ASCh) and butyrylthiocholine (BSCh). Three different concentrations for each substrate were assessed (0.05, 0.5 and 5 mM). The enzyme activity, expressed as nmol min^{-1} mg $protein^{-1}$, was calculated at 10 and 20 min of incubation (Fig. 3.12).

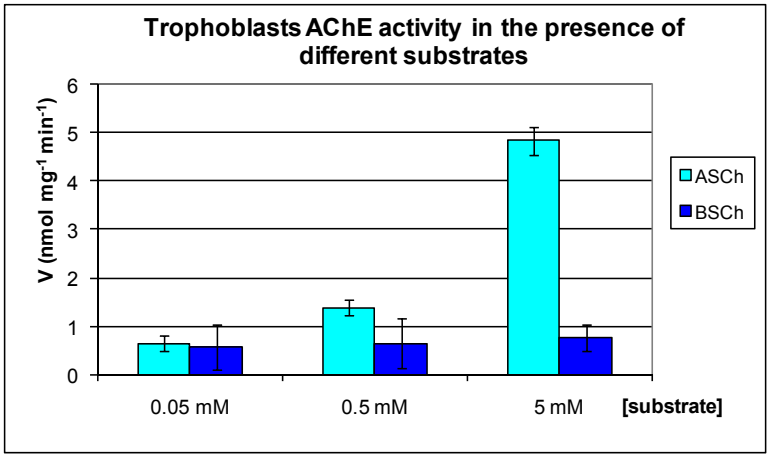

Fig 3.12 – The characterization of AChE in trophoblasts: activity in the presence of different substrates.

In the presence of BSCh, the enzyme activity didn't vary after increasing the substrate concentration, meaning that probably this is not the specific substrate for the enzyme under analysis. On the contrary, the ASCh induced a significant dose-dependent response in the AChE activity, therefore this latter can be considered a specific substrate and was chosen as the substrate for all the further analyses.

To establish the experimental protocol for the following assays, the time course of the ChE activity in 0.1 mg/ml protein preparations from human trophoblasts was examined in the presence of the two substrates, ASCh and BSCh, at 0.5 and 5 mM final concentration (Fig. 3.13). The experiments were carried out for 30 min at 30°C and optical densities measured at 30 sec intervals. A plateau was reached within 25 min for ASCh, while BSCh hydrolysis increased linearly up to the end of incubation. In routine experiments the AChE activity was assessed every minute and followed for 25 min, in the presence of 5 mM ASCh.

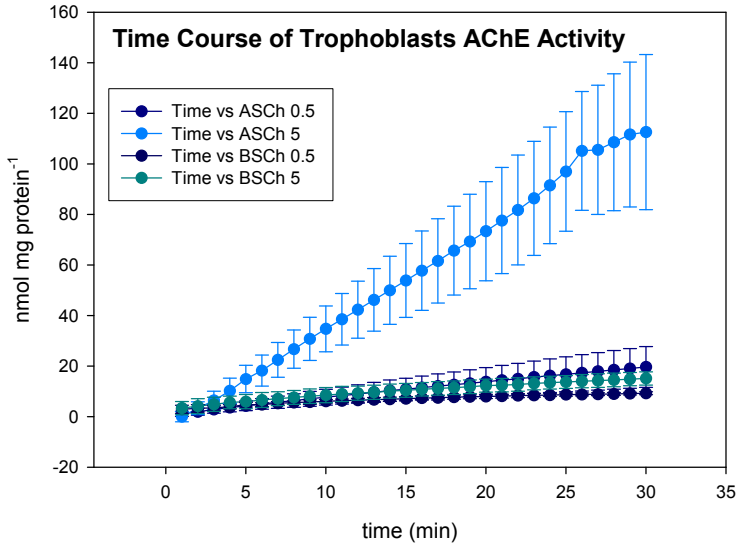

Fig 3.13 – The characterization of AChE in trophoblasts: time course in the presence of different substrates.

The basal enzymatic activity was then evaluated (Fig. 3.14). In each experiment a blank without substrate neither sample was measured to evaluate the reaction of thiols with DTNB at 405 nm. The enzymatic hydrolysis of acetylthiocholine was 4.83 ± 0.29 nmol min^{-1} mg^{-1} protein.

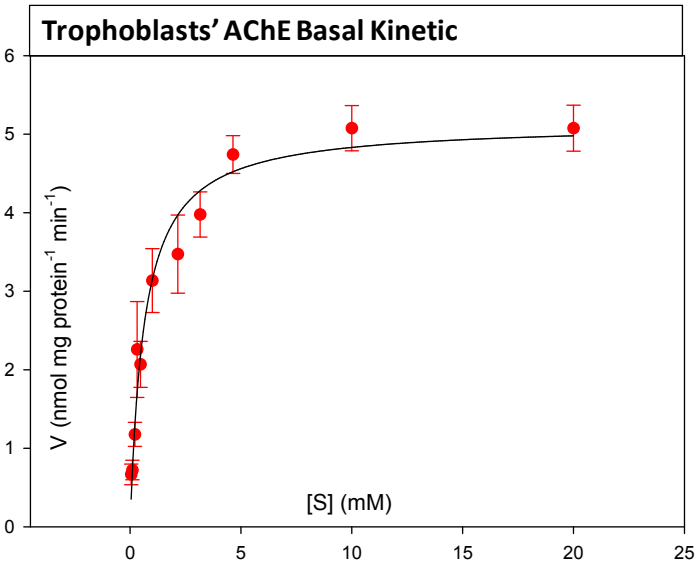

Fig 3.14 – The characterization of AChE in trophoblasts: kinetic in the presence of ASCh.

Kinetic experiments were carried out in the presence of ASCh. The effect of substrate concentration on trophoblasts AChE activity was assayed using twelve substrate

doses in the range 0.046 – 20 mM. AChE activity followed the Michaelis – Menten kinetic, and apparent Km values and Vmax values were calculated.

The Vmax and Km values were 5.14 ± 0.21 nmol min^{-1} mg^{-1} protein and 0.63 ± 0.10 mM, respectively. The regression analysis performed on these data provided a R^2 value of 0.984 ($p<0.001$), indicating that the experimental data fit the theoretical Michaelis-Menten plot.

AChE Activity and Kinetics in RF-Exposed Human Trophoblasts

Human trophoblast cells were exposed at 1.8 GHz, 217 Hz amplitude modulation, 2 W/kg SAR. Exposure times were 1, 4, 16 and 24 hours and during exposure the apparatus was switched off for 10 minutes every 5 minutes, as previously described. Since the relentless perishability of enzymes, the samples were collected straight after the end of the exposure, put on ice and then treated for the AChE activity and kinetic assay, following the method proposed by Ellman (1961).

Data presented are coming from triplicate exposures and triplicate protein analysis. Exposure data were normalized against the sham data (Fig. 3.15).

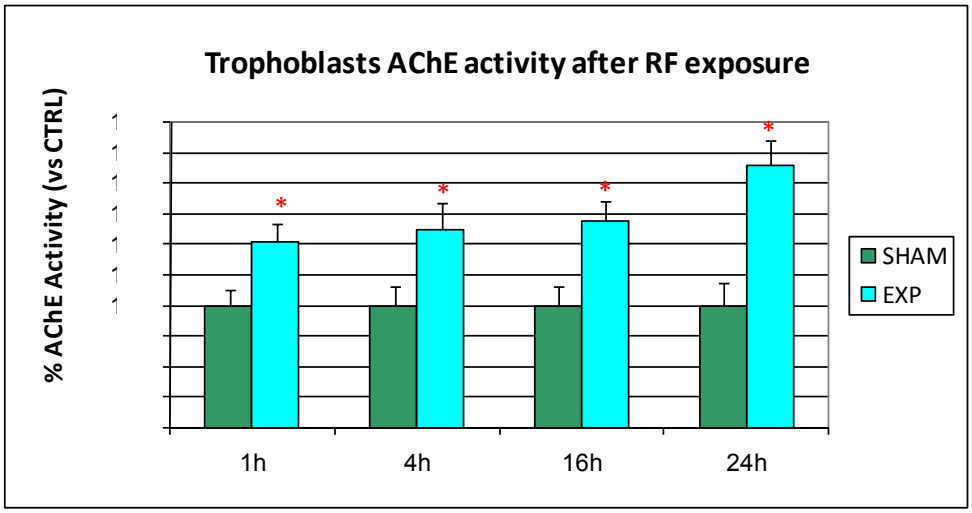

Fig 3.15 – The activity of AChE in trophoblasts after RF (1.8 GHz, 217 Hz AM) exposure.

Comparing the exposed to the sham-exposed samples it can be seen that the applied electromagnetic field induce a significant increase in the AChE enzymatic activity after every time of exposure. A duration-dependent relationship can also be seen: the longer the time of exposure, the higher the enzymatic activity ($p<0.05$).

Samples exposed to 1.8 GHz, GSM like EMFs were assessed also in terms of AChE kinetic in the presence of ASCh. The effect of substrate concentration on 0.1 mg/ml enzyme activity was assayed using twelve substrate doses in the range 0.046 – 20 mM. AChE activity followed the Michaelis – Menten kinetic, and apparent Km values and Vmax values were calculated (Table 3.8).

Table 3.8 – The kinetic parameters of AChE in trophoblasts after RF (1.8 GHz, 217 Hz AM) exposure.

Exposure		Vmax (nmol mg protein^{-1} min^{-1})	Km (mM)
Control		5.14 ± 0.21	0.63 ± 0.10
1h	Sham	5.66 ± 0.46	0.71 ± 0.23
	Exposed	7.27 ± 0.68	0.78 ± 0.29
4h	Sham	5.95 ± 0.48	0.72 ± 0.23
	Exposed	6.86 ± 0.68	0.56 ± 0.23
16h	Sham	5.58 ± 0.72	0.69 ± 0.24
	Exposed	6.97 ± 0.60	0.57 ± 0.19
24h	Sham	5.40 ± 0.77	0.68 ± 0.28
	Exposed	8.16 ± 0.52	0.69 ± 0.19

Vmax values showed a significant rise in the exposed samples compared to the sham exposed Vmax values, which remains similar to the control value. Furthermore, the Vmax values increase at increasing time of exposure, as seen above. Km values were not significantly modified after each kind of exposure.

3.2.3 - ACETYLCHOLINESTERASE ACTIVITY AND KINETICS IN PC-12s

Basal AChE Activity and Kinetics in PC-12s

Treatment with a specific inhibitor of acetylcholinesterase (BW284C51) and with a nonspecific cholinesterase inhibitor (Iso-OMPA) indicated that greater than 95% of the enzymatic activity in PC-12s was due to true acetylcholinesterase (Rieger et al., 1980). The chosen substrate for this new biological target was acetylthiocholine iodide (ASCh) accordingly. Several tests were performed to optimize the experimental procedure and identify the best substrate concentration, protein amount and time of incubation. The ideal AChE reaction rate for PC-12 cells can be gained by using 0.05 mg protein/ml, 0.5 mM ASCh and 0.33 mM DTNB and by following the reaction at 30°C for 5 min at 1 min reading intervals. The blank reaction was measured without substrate, to evaluate the reaction of

thiols with DTNB at 405 nm. All trials were performed in triplicates and data are expressed as nmol·min^{-1}·mg of protein^{-1} (Rieger et al, 1980; Schweitzer, 1993; Heo et al, 2002) following the method proposed by Ellman (1961).

The basal enzymatic activity was evaluated: the enzymatic hydrolysis of acetylthiocholine in control cultures was 8.91 ± 0.23 nmol min^{-1} mg^{-1} protein, according to the value previously gained by Greene and Rukenstein (1981) that was 8.2 nmol min^{-1} mg^{-1} protein.

In order to understand the mechanism that leads to an increase in the AChE activity after 1.8 GHz RF exposure, the enzymatic kinetic was studied. Kinetic experiments were carried out in the presence of ASCh. The effect of substrate concentration on trophoblasts AChE activity was assayed using sixteen substrate doses in the range 0.0001 – 10 mM. AChE activity followed the Michaelis – Menten kinetic, and apparent Km values and Vmax values were calculated

Both the cytoplasmic and the membrane-bound acetylcholinesterase kinetic were tested at this stage, in order to identify any possible difference in the two molecules (Fig. 3.16).

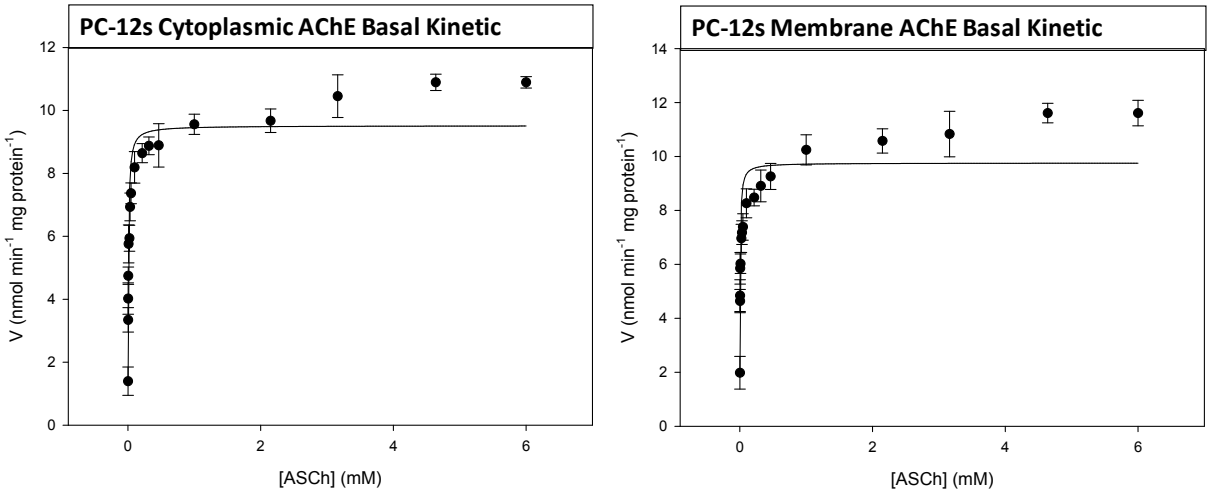

Fig 3.16 – The characterization of AChE in PC-12s: kinetic in the presence of ASCh assessed in the cystoplasmic (left) and membrane (right) fractions.

Cytoplasmic and membrane basal kinetic parameters showed very similar value: the Vmax and Km values of the cytoplasmic enzyme reaction were 10.74 nmol min^{-1} mg^{-1} protein and 0.001 mM, respectively, while the Vmax and Km values of the membrane enzyme reaction were 10.78 nmol min^{-1} mg^{-1} protein and 0.002 mM, respectively. The

regression analysis performed on these data provide a R^2 value of 0.998 ($p<0.001$), indicating that the experimental data fit the theoretical Michaelis-Menten plot. Because of this similarity the following exposed samples were tested only for the total enzyme fraction activity.

AChE Activity and Kinetics in RF-exposed PC-12s

Afterwards, cells were exposed to the conditions described above: carrier frequency of 1.8 GHz with intermittent exposure (5 min field on, 10 min field off) at the CW, GSM-217 Hz amplitude-modulation, and GSM-Talk (34% of speaking and 66% of hearing) conditions, with 2 W/kg of SAR.

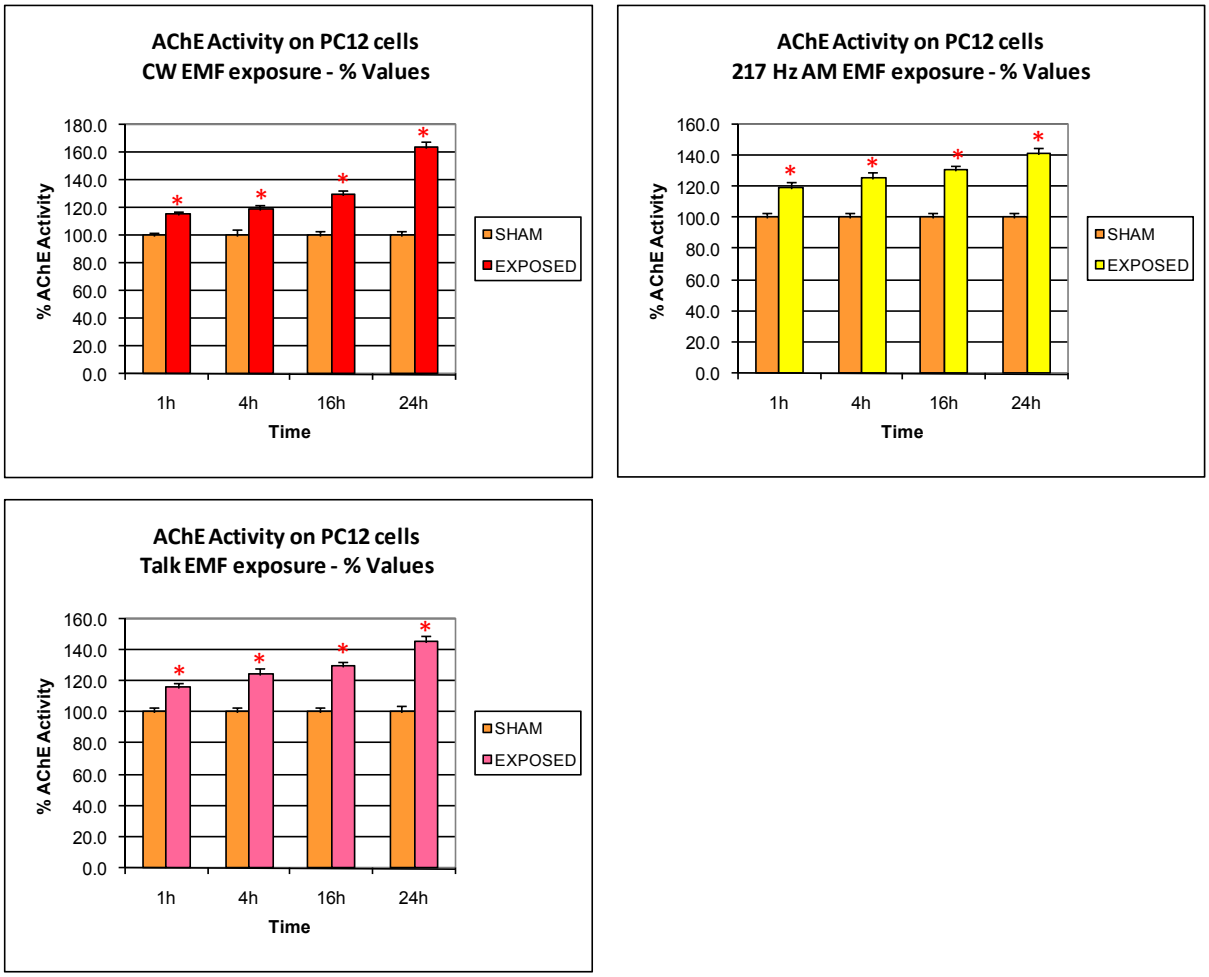

Fig 3.17 – The AChE activity (percentage referred to controls) in PC-12s after RF (1.8 GHz: CW, 217 Hz AM, Talk) exposures.

It's important to underline that between sham and external controls no significant differences were detected, meaning that the sham samples were validated as internal

control. It can be observed that exposed cells show a significant increase in AChE activity for every time of exposure, if compared to sham samples for every exposure conditions (Fig. 3.17).

A duration-dependent response can also be detected, since longer times of exposure determined higher increases in terms of enzyme activity. The highest effects can be seen after 24 hours of continuous wavelength exposure: a 63.73% increase in the enzymatic activity was recorded. Twenty-four hours was the most effective time of exposure, therefore it was decided to assay the kinetic parameters of AChE hydrolysis in PC-12 cells after 24 hours of different RF exposure regimes at 1.8 GHz. Samples exposed to the electromagnetic fields described above were assessed in terms of AChE kinetic parameters in the presence of ASCh (Fig. 3.18).

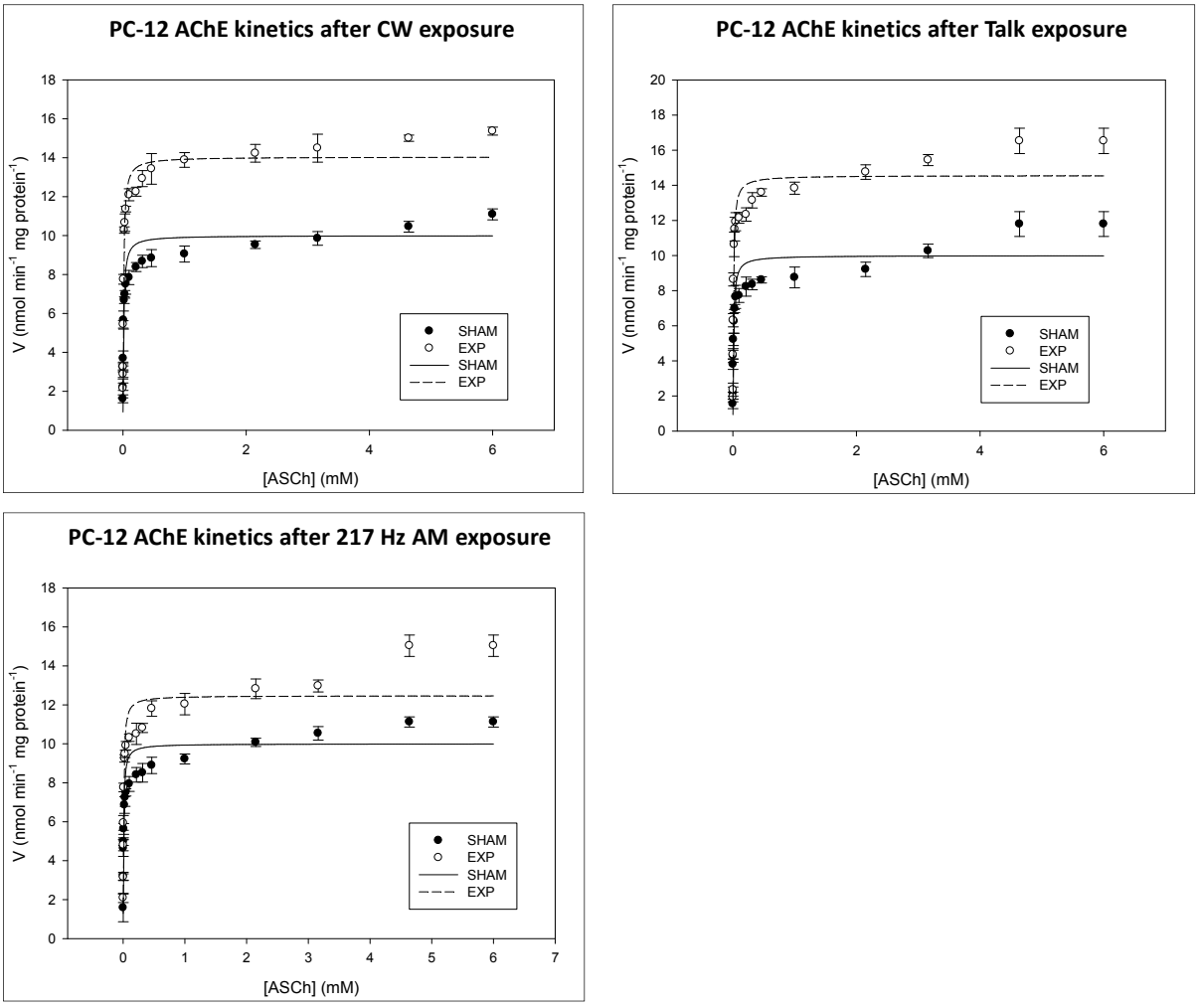

Fig 3.18 – The kinetic curves of AChE in PC-12s after 24 hours RF (1.8 GHz: CW, 217 Hz AM, Talk) exposure.

It can be observed that exposed cells show a significant increase in AChE kinetic curve, if compared to sham samples for every exposure conditions, confirming the results obtained when testing the enzyme activity.

Table 3.9 – The kinetic parameters of AChE in PC-12s after 24 hours RF (1.8 GHz: CW, 217 Hz AM, Talk) exposure.

Exposure		Vmax (nmol mg protein^{-1} min^{-1})	Km (mM)
Control		10.74 ± 0.52	0.010 ± 0.004
217 Hz	Sham	10.00 ± 0.35	0.007 ± 0.002
	Exposed	12.47 ± 0.42	0.007 ± 0.001
CW	Sham	10.00 ± 0.29	0.009 ± 0.002
	Exposed	14.04 ± 0.24	0.009 ± 0.001
Talk	Sham	10.00 ± 0.40	0.010 ± 0.002
	Exposed	14.56 ± 0.38	0.008 ± 0.001

In table 3.9 it can be seen that the reaction velocity increased in exposed cells, when compared to the non-exposed samples. The regression analysis performed on these data provide a R^2 value of 0.985 ($p<0.001$), indicating that the experimental data fit the theoretical Michaelis-Menten plot. Vmax values showed a significant rise in the exposed samples, compared to the sham exposed Vmax values, which remains similar to the control value: a 12.47% increase in the enzymatic activity was recorded after 217 Hz AM exposures, a 40.04% increase after CW exposure and a 40.56% increase after Talk exposures. Km values were not significantly modified after each kind of exposure.

3.2.4 - CELL PROLIFERATION RATE IN PC-3s AND PNT1As

Relative cell proliferation rate was determined in PC-3 and PNT1A cells in real time for 24 hours post exposure or sham exposure using an xCELLigence Cell Analyser (Roche, UK). All exposures were of 60 minutes duration and the cell index (CI) was recorded four times per hour for the duration of the experiment. According to data from preliminary real-time cell electronic sensing (RT-CES) experiments, the highest effects of RF exposure on cell viability can be found on samples exposed to every kind of exposure regimes for 60 minutes (data not shown).

RT-CES system showed that at both 144 MHz and 434 MHz there was a significant decrease in cell proliferation in the exposed tumour cells (Fig. 3.19).

Under the same physiological conditions, the more cells attach to the electrodes, the higher impedance value leading to a larger CI value. When the same number of cells attach to the electrodes, different cell status will lead to different values of CI. An increase in cell adhesion or cell spread leading to a larger cell substrate contact area lead to an increase in CI. On the other hand, cell death, detachment, or rounding up will lead to a decrease in CI. Therefore, CI is a measure of both the total contract area of cells on the electrodes and the strength of cell adhesion to the electrodes. The changes in the CI value reflected the changes in cell adhesion (Ge et al., 2009).

For each cell line data are expressed as relative cell proliferation rates, where data is expressed as a percentage of pre-exposed proliferation rates for each cell type at 4 hour intervals. This additional data processing step is included as it permits normalization of the data to internal controls and allows more relevant cross comparison between changes in rate of PC-3s and PNT1As growth.

After each exposure regime PNT1A cell proliferation continued increasing, while PC-3s showed a decrease in their growth rate, which is even bigger after double exposures. For double exposures also PNT1As showed a decrease in their cell growth rate, even though the relative cell proliferation rate remained higher than 1, denoting that they keep growing but slower. Four hours after single exposure a significant decrease in cell growth rate can be seen in PC-3s for every exposure regime, which is consistent with the results gained with the DNA content assay. 24 hours after the end of the 144 MHz exposures the cell growth rate in PC-3s was 0.59 for 5 W and 0.89 for 50 W of input power. Twenty-four hours after the end of the 434 MHz 50 W exposures the cell growth rate in PC-3s was 0.59.

When cells were exposed twice the most effective exposure regime for PC-3s was the 434 MHz 50 W, which lead to a cell growth rate of 0.10 compared to the controls. As for 144 MHz exposures, the most effective input power was 50 W, which influenced the cell growth rate to decrease to 0.23, while 5 W leaded to a cell growth rate of 0.41 compared to their respective controls.

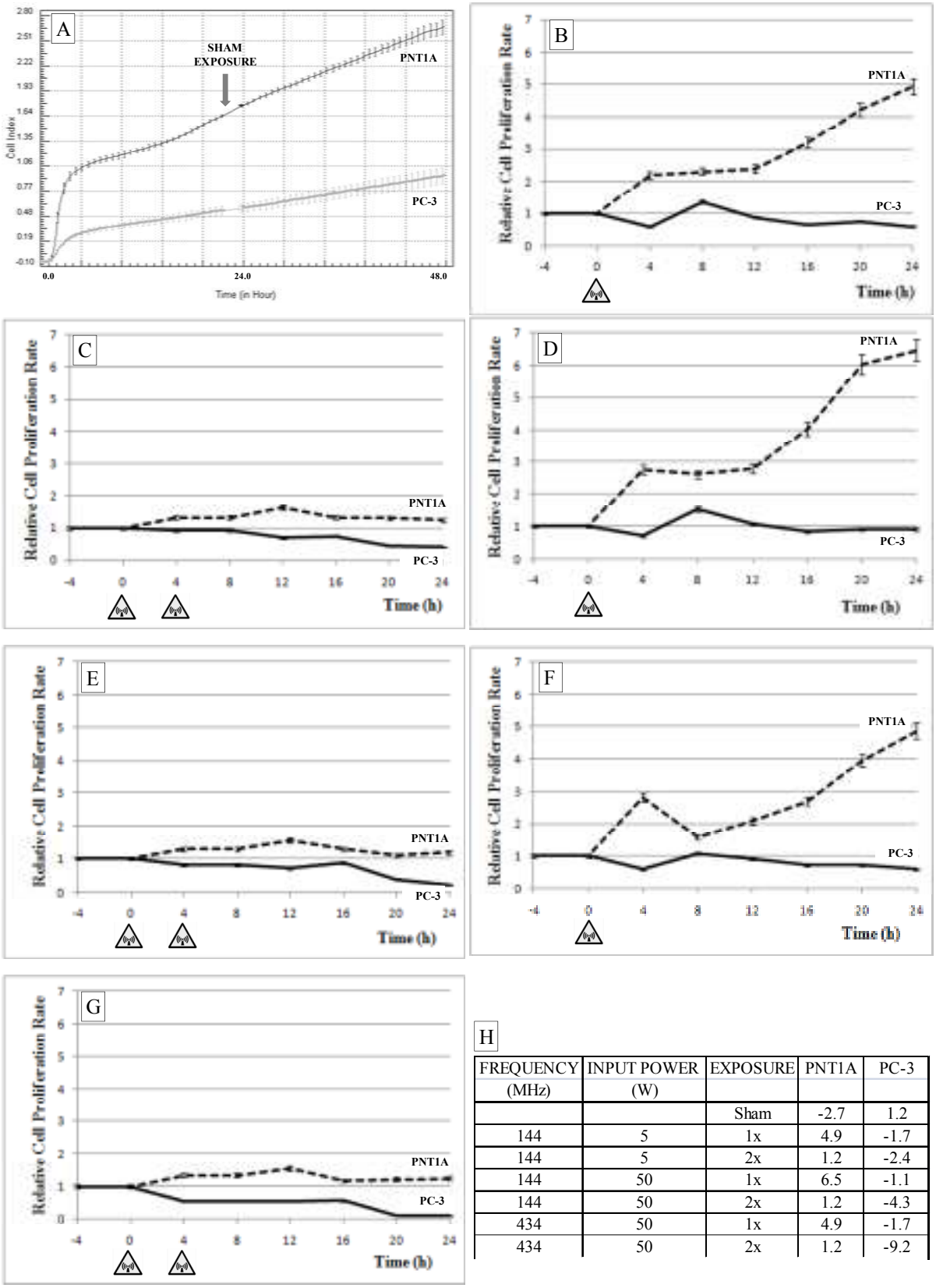

H

FREQUENCY (MHz)	INPUT POWER (W)	EXPOSURE	PNT1A	PC-3
		Sham	-2.7	1.2
144	5	1x	4.9	-1.7
144	5	2x	1.2	-2.4
144	50	1x	6.5	-1.1
144	50	2x	1.2	-4.3
434	50	1x	4.9	-1.7
434	50	2x	1.2	-9.2

Fig 3.19 – Relative cell proliferation rate in PC-3 and PNT1A cells in real time for 24 hours post exposure or sham exposure by xCELLigence cell analyser. (B-G) illustrate changes in proliferation rate at 4 hour intervals pre and post exposure normalised against sham proliferation rates. Cells were exposed once to 144 MHz 5 W (B), 144 MHz 50 W (D) or 434 MHz 50 W (F) and twice to 144 MHz 5 W (C), 144 MHz 50 W (E) or 434 MHz 50 W (G). (H) is a summary of changes in proliferation rate 24 hours post exposure compared to control.

3.2.5 - CELL SURVIVAL ASSAY IN TROPHOBLASTS, PC-3s AND PNT1As

Trophoblast, PNT1A and PC-3 cells were counted using a Z2 Cell and Particle Counter (Beckman Coulter, USA) 24 hours and 7 days post single and double exposure to 144 MHz 5 W, 144 MHz or 434 MHz 50 W or sham exposure. Cell numbers are expressed as a fraction of sham-exposed cell populations. Data are expressed as the mean +/- standard deviation of 3 or more separate experiments (Fig. 3.20).

Cell Count Assay is expressed as a fraction of control. Total cell number was counted in cell populations +/- RF exposure after 1 and 7 days. There was a significant change in the PC-3s cell number of RF-exposed groups, compared to the sham-exposed, either 1 or 7 days after the exposure.

The cell number was significantly decreased in exposed PC-3s 7 days after the exposure (up to 50% less), while it was not significantly different in exposed trophoblasts for all kind of exposure regimes tested. PNT1As are significantly affected by 144 MHz 50 W exposure regime: 7 days after single or double exposures a decrease in their cell number can be seen.

Different exposure regimes affect PC-3s differently: the lower 144 MHz frequency is less effective than 434 MHz at 5 W. But when a 50 W power input is applied, the decrease in PC-3s cell number is highly comparable between samples exposed to 144 MHz and samples exposed to 434 MHz. Furthermore, the cell number in PC-3s exposed twice is significantly lower than in PC-3s exposed once.

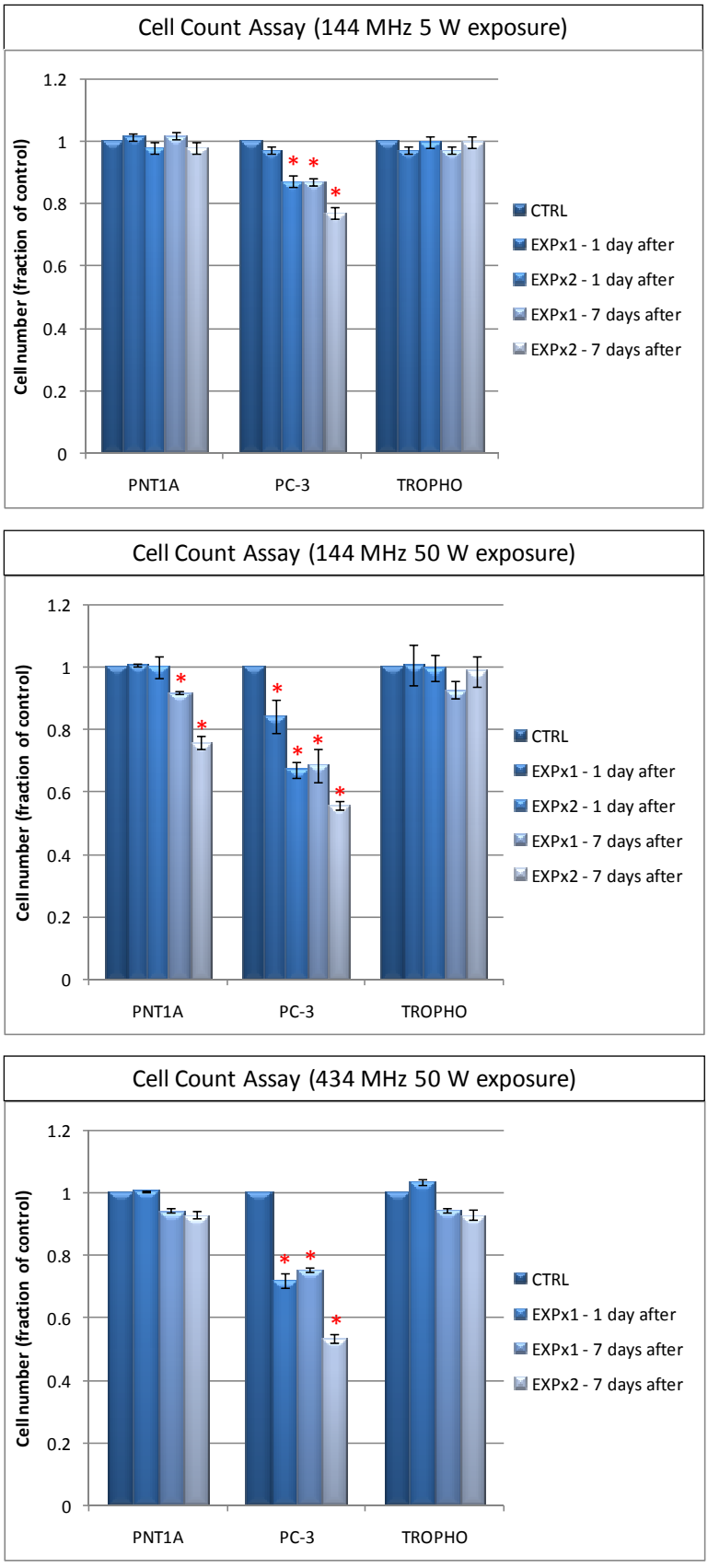

Fig 3.20 – Cell count assay in PNT1As, PC-3s and trophoblasts 1 and 7 days post exposure. Cells were exposed once or twice to 144 MHz 5 W, 144 MHz 50 W and 434 MHz 50 W.

3.2.6 - RELATIVE QUANTIFICATION OF CELLULAR DNA IN TROPHOBLASTS, PC-3s AND PNT1As

Total DNA was determined in trophoblast, PC-3 and PNT1A cells 24 hours post single and double exposure to 144 MHz 5 W, 144 MHz 50 W and 434 MHz 50 W. All exposures were of 60 minute duration and protein was determined using the PicoGreen dsDNA kit. Data obtained from PicoGreen assay 24 h after the exposures were normalized against the results gained with the cell count assay, in order to the have the actual DNA amount in each cell. Then results were expressed as a fraction of control. All experiments were performed in triplicate and results are expressed as the mean +/- standard deviation of the mean (Fig. 3.21).

There were no significant changes observed in cellular DNA content in either PC-3 or PNT1A cells post 144 MHz 5 W or post 144 MHz 50 W, except for a small, but significant increase post 2x exposure to 144 MHz 50 W in PC-3s. Notably a modest but significant reduction in DNA was observed in both PNT1As (15%) and PC-3s (16%) cells post single exposure to 434 MHz 50 W but not post double exposure. No effect was detected in trophoblasts after every kind of exposure regime applied.

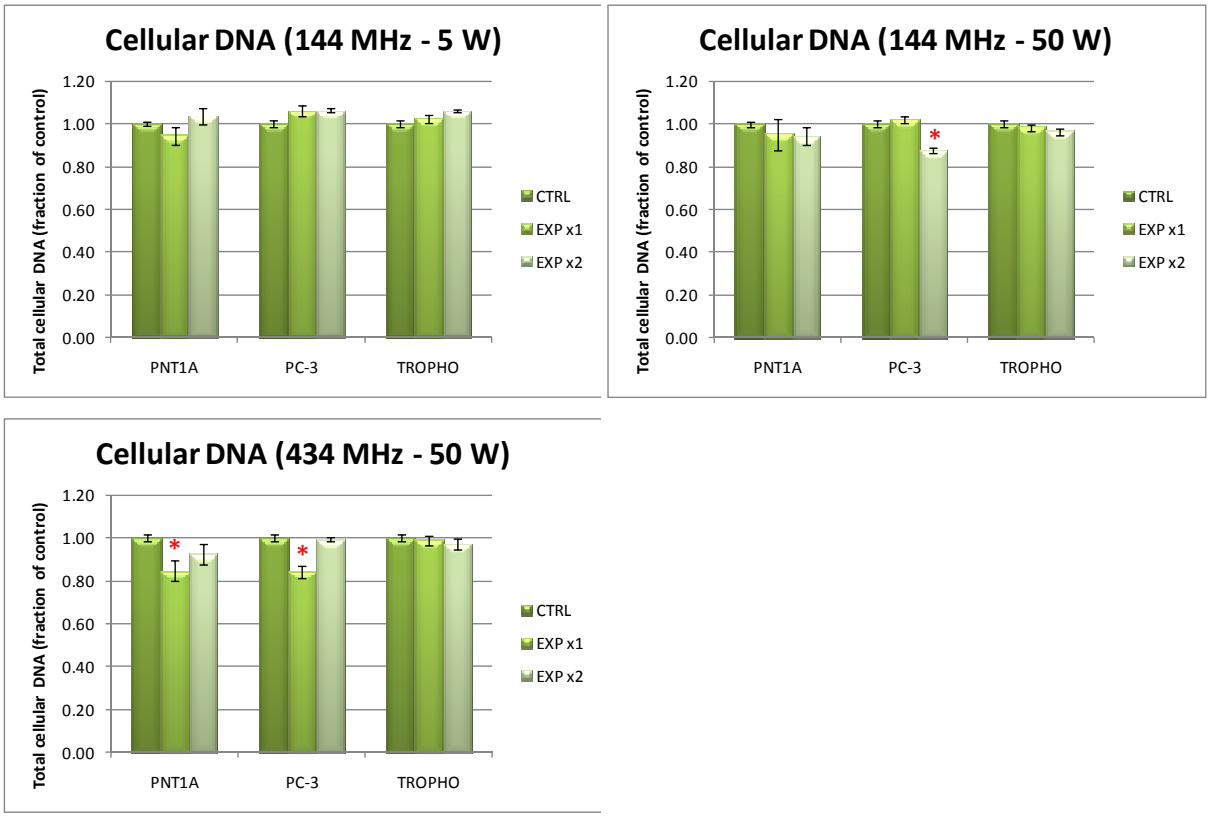

Fig 3.21 – Normalized total DNA in PNT1As, PC-3s and trophoblasts 24 hours post single and double exposure to 144 MHz 5 W, 144 MHz and 434 MHz 50 W.

3.2.7 - QUANTIFICATION OF TOTAL PROTEIN IN TROPHOBLASTS, PC-3s AND PNT1As

Total protein was determined in trophoblast, PC-3 and PNT1A cells 24 hours post single and double exposure to 144 MHz 5 W, 144 MHz 50 W and 434 MHz 50 W. All exposures were of 60 minute duration and protein was determined using the Bradford Assay (1976). Bradford data 24 h after the exposure have been normalized against the results gained with the cell count assay, in order to the have the actual protein amount in each cell. Then results were expressed as the mean +/- standard deviation of the mean (fig. 3.22).

No change in PNT1As cellular protein post exposure was observable except for a small, but significant increase post 2x exposure to 144 MHz 50 W (1.1 fold that of control). No significant increase can be measured in trophoblasts protein content. However, significant increase in PC-3s cellular protein was observed post all exposures employed in the study (ranging from 1.5 to 2.0 fold that of control). Increases in PC-3s cellular protein did not vary with frequency or input power but did increase with repeat exposure post both 144 MHz 5 W and post 434 MHz 50 W.

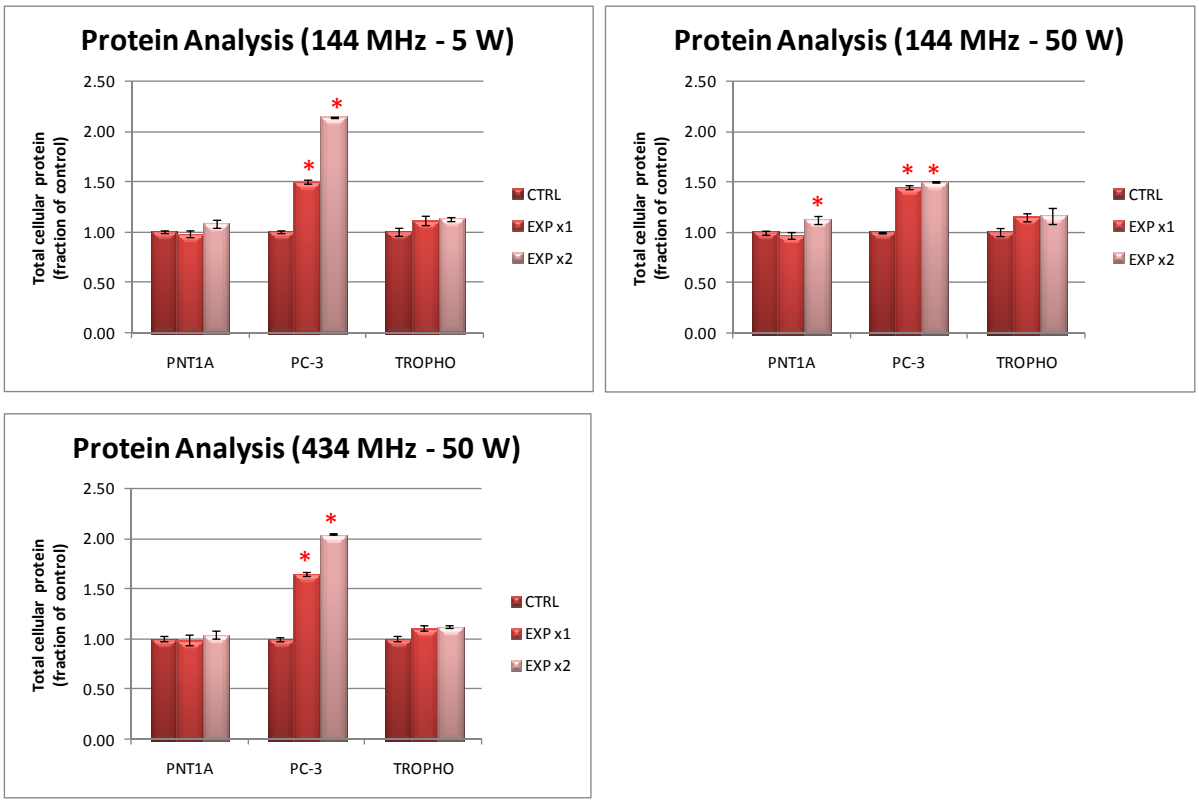

Fig 3.22 – Normalized protein content in PNT1As, PC-3s and trophoblasts 24 hours post single and double exposure to 144 MHz 5 W, 144 MHz and 434 MHz 50 W.

3.2.8 - NUCLEAR DNA DAMAGE MARKER ANALYSIS IN TROPHOBLASTS, PC-3s AND PNT1As

Specificity of RT-PCR products was documented with high resolution gel electrophoresis and resulted in a single product with the desired length PARP1 = 248 bp, XLF = 218 bp, 18s = …

In addition, a LightCycler melting curve analysis was performed which resulted in single product specific melting temperatures as follows: (PARP1 = 87˚C, XLF = 88˚C, 18s = 83˚C). No primer-dimers were generated during the applied 35 real-time PCR amplification cycles.

Real-time PCR efficiencies were calculated from the given slopes in LightCycler software. The corresponding real-time PCR efficiency (E) of one cycle in the exponential phase was calculated according to the equation $E = 10^{[-1/slope]}$. Investigated transcripts showed high real-time PCR efficiency rates: for PARP1 = 2.0, XLF = 2.3, 18s = 2.0 in the investigated range from 0.1 to 10 ng cDNA input (n = 3) with high linearity (correlation coefficient $R^2 > 0.98$).

To confirm accuracy and reproducibility of real-time PCR the intra-assay precision was determined in three repeats within one LightCycler Run.

The relative quantification of a target gene (PARP1 and XLF) in comparison to a reference gene (18s) was performed, according to Pfaffl, 2001. The relative expression ratio (R) of a target gene is calculated based on E and CP deviation of an unknown sample versus a control, and expressed in comparison to a reference gene.

The expression of PARP1 and XLF mRNA was examined by real-time PCR in trophoblasts, PNT1As and PC-3 cells exposed to the high-frequency EMF. Cells were exposed to 144 MHz 5 W, 144 MHz, 50 W and 434 MHz 50 W for one hour (Fig. 3.23 and 3.25), and to 1.8 GHz 2 W CW mode (1 hour exposure in continuous and 1 hour exposure 5 minutes on, 10 minutes off) (Fig. 3.24 and 3.26). Using specific primers, nuclear DNA damage was analyzed, by assessing the gene expression of two proteins involved in DNA double strand break repair: XLF and PARP1. Cernunnos-XLF is a core factor which plays a key role in Non Homologous End Joining Repair (NHEJ) since it's involved in most NHEJ reactions activating or enhancing the basic NHEJ ligation reactions. PARP1 signals DNA rupture and participates in base-excision repair, promoting the activity of DNA transcription factors.

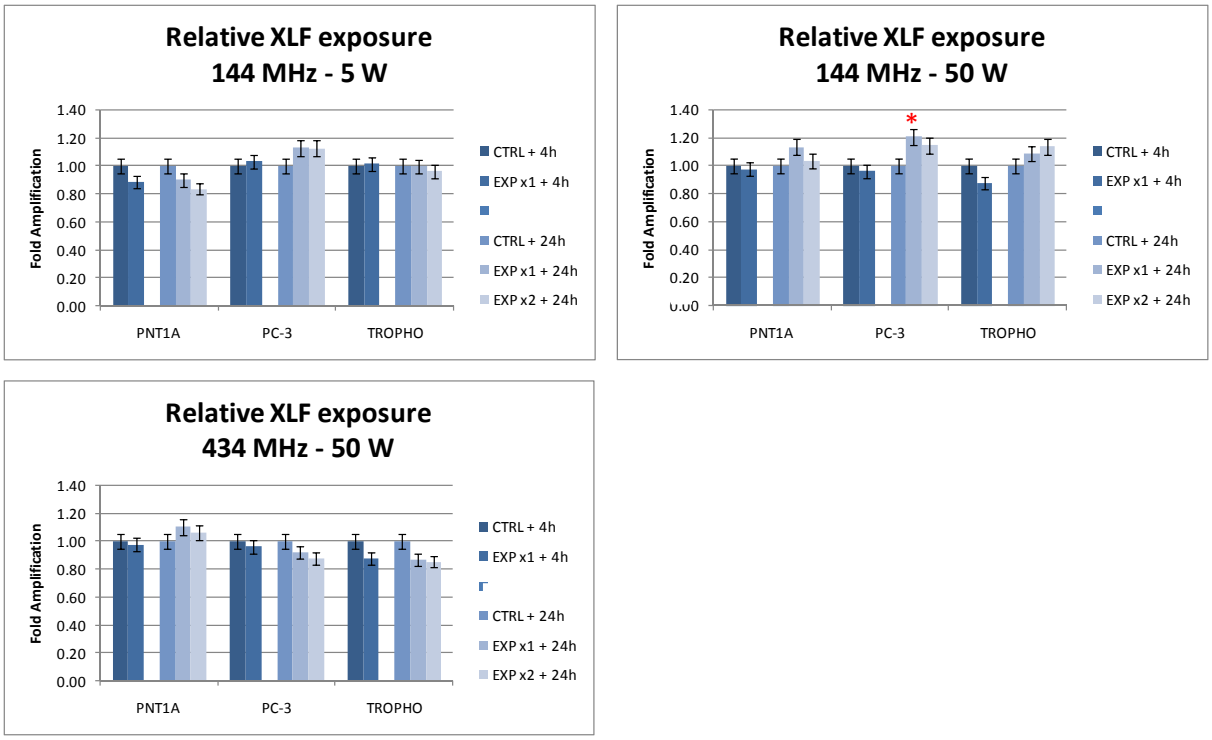

Fig 3.23 – Gene expression of XLF by real-time PCR in PNT1As, PC-3s and trophoblasts after single or double exposure to 144 MHz 5 W, 144 MHz, 50 W and 434 MHz 50 W.

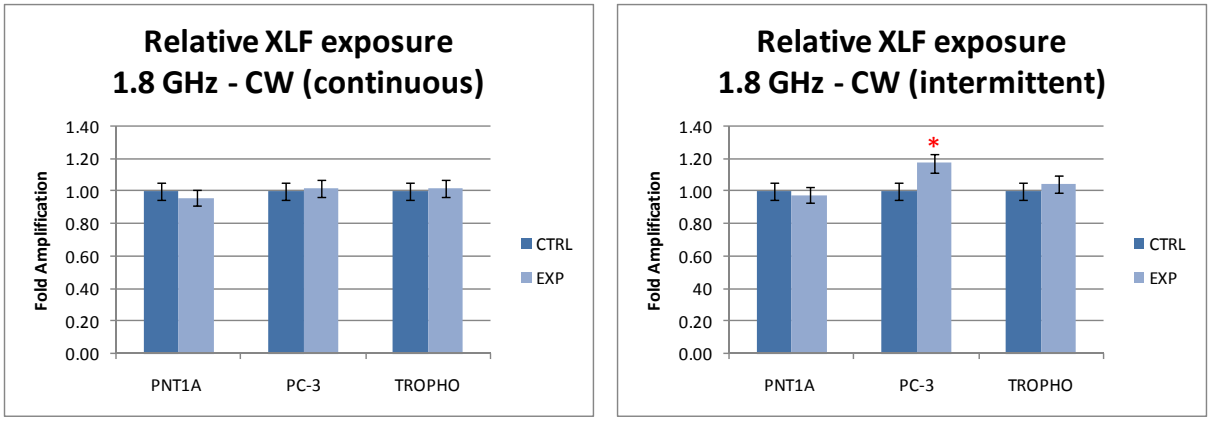

Fig 3.24 – Gene expression of XLF by real-time PCR in PNT1As, PC-3s and trophoblasts after exposure to 1.8 GHz 2 W CW mode: 1 hour exposure in continuous (left) and 1 hour exposure 5 minutes on, 10 minutes off (right).

As illustrated no significant differences were observed between controls (sham-exposed cells) and exposed samples for every kind of exposure regime applied in the non-tumour cell lines (PNT1As and trophoblasts). A slightly significant increase in the expression of XLF can be detected in PC-3 cells 24 hours after being once exposed to 144 MHz 50 W (Fig. 3.24) and intermittent 1.8 GHz exposure regimes (Fig. 3.25).

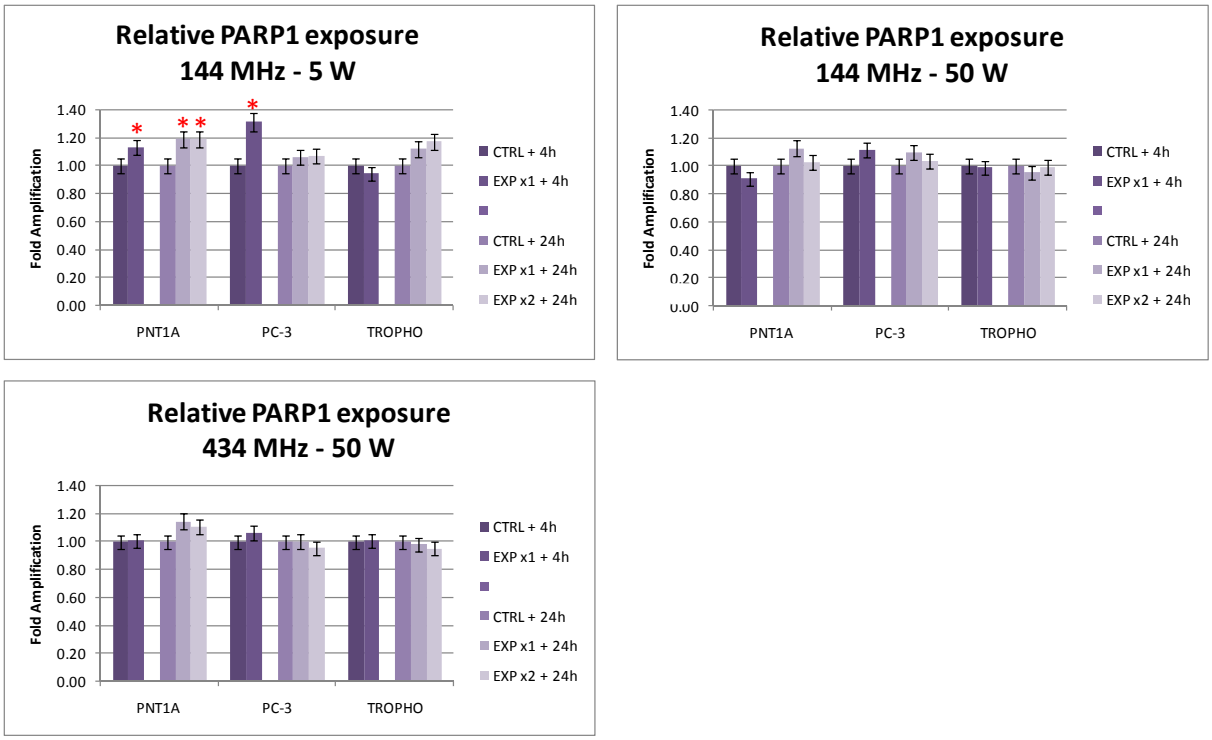

Fig 3.25 – Gene expression of PARP1 by real-time PCR in PNT1As, PC-3s and trophoblasts after single or double exposure to 144 MHz 5 W, 144 MHz, 50 W and 434 MHz 50 W.

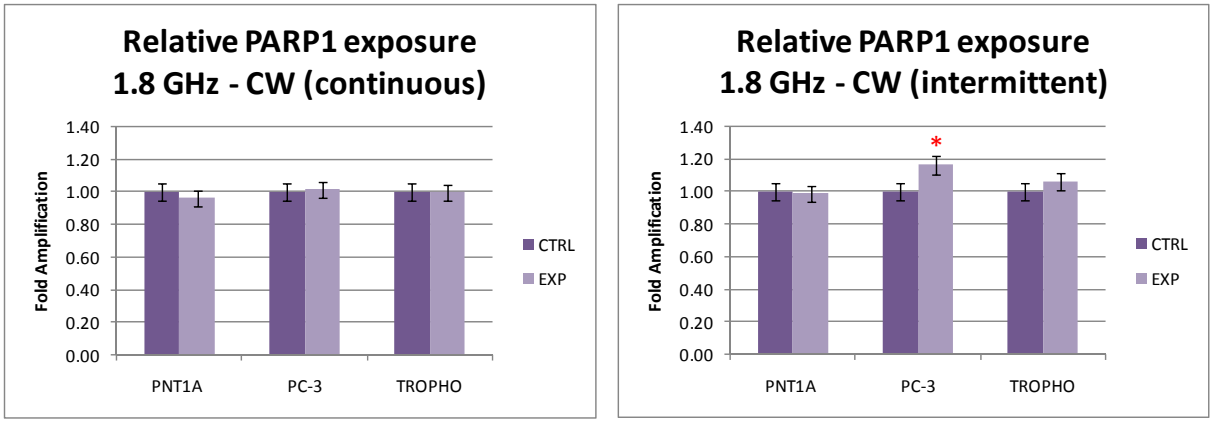

Fig 3.26 – Gene expression of PARP1 by real-time PCR in PNT1As, PC-3s and trophoblasts after exposure to 1.8 GHz 2 W CW mode: 1 hour exposure in continuous (left) and 1 hour exposure 5 minutes on, 10 minutes off (right).

The most effective exposure regime was the 144 MHz 5 W (Fig. 3.26), which leaded to a significant expression of the PARP1 gene in the exposed PNT1A cells, both 4 and 24 hours post-exposure, and to an increase in the exposed PC-3 cells 4 hours post-exposure. A slightly significant increase can also be seen in PC-3 cells 24 hours after being exposed to intermittent 1.8 GHz CW (5 min on, 10 min off) EMF (Fig. 3.27).

No significant differences were observed between controls (sham-exposed cells) and exposed samples for all the other exposure regimes applied both in the non-tumour cell lines (PNT1As and trophoblasts) and in the tumour cell lines (PC-3s).

Chapter 4

DISCUSSION

4.1 - AIM OF THE STUDY

Much research has originally focused on low frequency electromagnetic fields, while on high frequency electromagnetic fields studies are more recent. One of the main reasons is that the instruments required for the physical simulation are very complex to set up. Furthermore the studies carried out so far involved several different biological targets and different exposure conditions and results are not easily comparable.

No decisive answer can therefore be given to the questions about short-term or long-term effects of high frequency electromagnetic fields on biological targets. To begin to address this, the present study is mainly based on some of the effects that high frequency electromagnetic fields exert on biological systems.

The aim of this study was to investigate the effects of some EMFs humans might experience in their daily lives. Two different areas were investigated: possible detrimental effects of the daily use of GSM mobile phones and possible beneficial effects of high frequency electromagnetic fields on human health to be employed in medical applications as a therapy in cancer cure.

Further research is certainly warranted given for instance the growing public concern over GSM mobile phones and antennas. And similarly, the limits of the current conventional cancer treatments could be overcome by a more complete understanding of the mechanisms that high electromagnetic fields trigger in living systems.

The same approach was adopted to investigate the two stages of this research: an initial phase of modelling the apparatus employed and a second phase of evaluating the EMF effects on living cultured cells by means of assessing specific biological endpoints. Different exposure parameters were assessed, to identify any SAR level-dependence or time-dependence patterns.

4.2 - SIMULATION: MATHEMATICAL MODEL OF THE EXPOSURE SYSTEMS

The possible disturbance generated by high frequency EMFs on cell physiology remains controversial, even though epidemiological studies report no detrimental effects on human health (Rothman, 2000; Schuz et al., 2006). In addition, the question remains as to whether high frequency EMFs have no significant effects or cells are able to compensate or

counteract the potential consequences. Also, the same cells can be affected differently by different signals while the same signal may affect different cells differently.

The main idea behind a software modelling is to have a good knowledge of the instrument used for exposing the biological targets, in order to know how the electromagnetic parameters affect the biological matter during the exposure. Mathematical modelling (computer simulation) using finite-element modelling (FEM) shall be used to investigate different antenna designs and sample/antenna geometries and the effect on the RF dose received by the sample and the absorption of RF by the living cells. In this study the predictions from the mathematical models were also tested against experimental data.

The parameters of the human body tissue on which the model is based had to be identified. These parameters which affect the energy absorbed by the patient's body included:

- relative dielectric constant (permittivity) (ε_r)
- dielectric loss factor (δ)
- impedance (Z_0)
- mass density of tissue (ρ)
- electrical conductivity (σ)
- thermal conductivity (k)
- specific heat (˚C).

The parameters are frequency-dependent and tissue-dependent, so different values should be used for different tissue, such as fat, fibro-connective tissue, muscle, bone, but also for normal and tumour tissue. For these reasons well-defined exposure conditions for biological experiments are an obvious and indispensable prerequisite for interpretation and repeatability of results. The difficulties involved in obtaining such conditions have been severely underestimated by most groups conducting radio frequency (RF) experiments, consequently, design and characterization of exposure setups have become top priority within most research programs addressing the health effects of RF exposures (WHO (Repacholi, 1998); WTR (Carlo, 1998)). Indeed, the design and realization of exposure setups is a considerable engineering and scientific challenge requiring profound knowledge of numerical simulation methods and especially their application, near-field measurement techniques, open and closed transmission systems, anatomy, dosimetry, material science and more.

The models realised in this study helped to establish the exposure conditions and how they can accordingly affect the biological targets. After establishing the details of the setup, the electrodynamic performance of the setup have been assessed through a detailed numerical representation, including the metallic and plastic materials, as well as biological sample. The results of the numerical dosimetry included a detailed description of induced E-fields, SAR distribution and temperature changes.

Based on the preliminary results, some changes in the details of the model have been necessary, involving a return to the adaptation and optimization stage: the features of the antenna and the mesh were refined and optimized several times, before reaching the optimal description of the actual features of the exposure system. Several such cycles have been repeated until the final design of the setup was fixed.

The models realized in this study suited very well with the features of the exposure systems applied (Kuster and Schönborn, 2000), and they can therefore be considered valid.

The simulation results (the spatial distribution of the electric field, the SAR and the temperature change in the medium layer) were calculated by the use of the finite difference time domain (FDTD) analysis. They were verified extensively using E-field and temperature probes. The results showed the following:

- The required uniformity of E-field inside each exposed petri dish, as well as the required uniformity among the 6 dishes, is fully achieved by the model of the 1.8 GHz exposure system. A similar result was gained with the model of the TEM cell, where the uniformity of E-field across the exposure area is absolutely consistent with the apparatus features.
- The absolute uncertainty on the SAR due to the non-uniformity of the E-field distributions is much less than 10% for both the exposure systems, even though a non-uniformity of the E-field up to 29% is still considered acceptable to have a variation of the SAR delivered to the cells lower than 20%. The exposure is strongly dependent upon the medium volume for cell monolayer and is characterized by high vertical SAR gradients. Since the field impedance for monolayer exposure is five times lower than for suspension, the evaluation of the parameters only at the bottom of the medium layer could be considered a reliable approximation. Also, because of the cells are not in the meniscus area, an evaluation of SAR in the

medium excluding the meniscus is appropriate and leads to much lower non-uniformity of SAR than for cell suspensions (10% versus 117%).

- The temperature of the monolayer cells is in both cases uniformly distributed without localized temperature ‘‘hot spots’’ (Schuderer et al., 2004) and, for the 1.8 GHz instrument, the temperature difference between sham and exposed cells is much lower than 0.1˚C. This result is very important because it verifies that the temperature conditions between the sham and the exposed cells are the same and it confirms that any effects measured in the biological samples can be ascribed to the EMF and not to a form of hyperthermia.
- Finally, the increase in temperature due to the high frequency EMF is well below 0.1˚C per unit SAR in each apparatus.

The E-field, SAR and ΔT values calculated by the model were in perfect agreement with the expected or measured values for all the exposure regimes under analysis, therefore these models can be employed whenever different exposure conditions are required in order to foresee any changes in the electromagnetic parameters distribution.

This approach is fundamental to understand how the different factors are responsible for the conflicting results obtained so far in terms of biological response to EMF. It has been seen that the cellular and molecular modifications induced by exposure to high frequency EMFs depend on the duration of exposure, tissue penetration, and heat generation, which are in turn related to the intensity and frequency of the EMF. In addition, cellular responses could also depend on type of field (static or oscillatory), waveform (sinusoidal, square, etc.), modulation scheme, and biological status and type of cells exposed. To have a complete knowledge of how cells react to an external applied EMF a fixed and well known exposure system is required.

Moreover, the current understanding remains that RF and MW health effects are the result of hyperthermia as the only characterized biological mechanism for explaining health effects (Adair and Black, 2003; Tuschl et al., 2006), contrary to the fact that a number of recent studies suggested significant RF-induced effects on a number of cellular activities in experimental systems under isothermal conditions (Pacini et al., 2002; Lee et al., 2005; Nikolova et al., 2005; Del Vecchio et al., 2009).

However, if radiofrequency and microwave effects were only due to increased temperatures, then it should be possible to detect changes in cellular activities depending

only on temperature changes in the experimental system. Consequently, there should be no difference between the cellular activities of field exposed and non-exposed cells. On the contrary, Velizarov et al., 1999 reported that exposure of transformed human epithelial amnion cells to a modulated RF field at 960 MHz at different power levels and exposure times, resulted in significant changes in cell proliferation while no significant changes depending only on temperature changes were seen.

If the applied HF EMFs don't cause any increase of the temperature inside the medium layer, any biological effect seen in the cells can therefore be attributed to the field itself and not to any hyperthermic effect. This result is even more valuable for the 144 and 434 MHz exposure system, since its potential application in cancer treatments. RF fields are currently employed by physiotherapists to accelerate recovery from strains and are also in use by the oncology community for breast tumour ablation, through hyperthermia (Wu et al., 2006; Van Wieringen et al., 2009) and as an adjunct therapy to radiotherapy, by heat-sensitizing tumours prior to radiotherapy (Franckena et al., 2009). However the current exploitation of RF for therapeutic gain may be described as rudimentary at best and will not change without improving our current understanding of the precise understanding of the bio-effects of RF exposure at a cellular and sub-cellular level. Most clinicians view RF as merely a vehicle by which direct and focused heating may be achieved.

Current cancer treatments involving RF employ EMF heating of cancers through 1 of 2 methods: (1) thermal ablation where direct cell destruction is achieved through coagulation of malignant tissue and (2) hyperthermia treatment where the temperature of the tumour tissue is raised to 40-44°C. A new approach to cancer treatments is a therapy that uses radiofrequency radiation as a pre-sensitizing agent, combined to low-dose, external-beam radiotherapy (X-rays or y-rays). In particular, the metabolism of cancer cells seems to be affected at the specific frequency of 434 MHz, which is supposed to have a non-thermal effect on the physiology of cancer cells (Holt, 1977).

The realization of a mathematical model that confirms the absence of any thermal effect during exposure is of basic importance to undertake this new approach to cancer cure, based on the application of the radiofrequency EMFs themselves and not on their hyperthermic effects.

4.3 - BIOLOGICAL ANALYSES AFTER 1.8 GHz GSM EXPOSURE

After the models have been realized, some biological endpoints were investigated, in order to find a biological parameter that might help to understand the mechanism of interaction between the HF EMF and the living matter. There is indeed a lot of controversy on the effects of exposure to high-frequency electromagnetic fields (ranging from 30 kHz to 300 GHz), since both detrimental and non-detrimental effects on human health were reported and recently reviewed. In this context, the identification of cellular targets for high frequency EMFs remains a major challenge.

To assess the possible detrimental effects of the daily use of GSM mobile phones two main biological endpoints were investigated, both regarding the interaction between EMF and the cellular proteins.

Some results indicate that external electromagnetic fields enhance cellular proliferation and protein synthesis. That's because the membrane of cells seems to be very sensitive to external EMF: it has been proposed that magnetic fields might interfere with cell membrane functions, such as ion flux and that the radiation might interact with the signalling pathways involved in cellular functions (Dimberg, 1995).

An increase in protein amount was seen after HF EMF exposure by Kwee et al. (2001) and it has been explained by the hypothesis of alterations in the conformation of cellular proteins and synthesis of stress-response proteins caused by the applied fields. For this reasons the expression of a stress-related protein (heat shock protein 70, HSP70) was firstly investigated, and then the activity of one of the main cellular enzyme (Acetylcholinesterase, AChE) was assessed after 1.8 GHz exposures. Two biological targets were chosen: trophoblast and PC-12 cell lines.

Trophoblasts are highly proliferative placental cells, which play an important role to guarantee adequate exchanges between mother and foetus. They represent a good model for the in vitro study of molecular mechanisms at the basis of placentation. Their high responsiveness to external stimuli also makes them an attractive model for investigating putative effects of HF EMF exposure on reproductive tissues.

PC-12 cells have been shown to synthesize three identifiable molecular forms of AChE (Schweitzer, 1993) and therefore they appear to be a useful model system for the study of numerous problems in neurobiology and neurochemistry, such as in the study of various aspects of acetylcholine metabolism (Greene and Rein, 1977a; 1977b). This cell line

could be modulable between a state in which it can replicate and a state in which it is non-dividing as well as neuronally differentiated, thanks to its capacity to respond to nerve growth factors (NGF), proteins which profoundly influence the growth and development of sympathetic and sensory neurons. Since PC12 has cholinacetyltransferase (ChAT) and acetylcholinesterase (AChE), further investigations can be conducted to understand the mechanism involved in AChE increased activity after RF exposure.

4.3.1 - HSP70 PROTEIN EXPRESSION

Several studies have indicated that high-frequency EMFs may modify the stress status of the cell and thus affect cellular homeostatic mechanisms (Tokalov and Gutzeit, 2004). The heat-shock proteins are regarded as important cellular stress markers and have been proposed as suitable candidates to infer the biological effects of high-frequency EMFs (Cotgreave, 2005; 2006 WHO research agenda for RF fields).

HSP over-expression was suggested as an early sign of cell response to stress and as a possible biomarker of EMF exposure, and the World Health Organization set the confirmation of such effects as a high-priority research need (2006 WHO research agenda for RF fields). High-frequency EMFs are reported to cause changes in the expression and/or phosphorylation status of HSPs in human cells (Kwee et al., 2001; Leszczynski et al., 2002). However, other studies have not confirmed these findings (Cotgreave, 2005), and further investigations of the heat shock response to high-frequency EMFs were encouraged to clarify these conflicting results.

The hypothesis that an over-expression of HSPs could be a marker for cell exposure to EMFs was supported by a relatively large body of literature showing changes in expression or phosphorylation state after exposure to high frequency EMFs (Leszczynski et al., 2002; De Pomerai et al., 2000; Miyakoshi et al., 2006), although De Pomerai et al. (2000) suggested in a subsequent paper that their observations could have arisen as a result of confounding thermal effects (Dawe et al., 2006). The possibility that high frequency EMF radiation might interact with biological structures and cause protein damage by mechanisms that do not directly involve heat was taken into account (De Pomerai et al., 2000). One key factor in this effect might be the resonant frequencies of the weak bonds that maintain proteins in their biologically active three-dimensional configuration, whose disruption leads to protein denaturation and hence to HSP gene activation.

On the other hand, despite the scarce experimental evidence, substantial public concern exists regarding the putative adverse effects of EMFs on the reproductive outcomes, mainly due to the ubiquity of EMFs and the consequent extent of the population potentially exposed. It was reported that high intensity microwave exposure increased embryo lethality in the early stages of mouse gestation (Nawrot et al., 1985) and induced micronucleus formation in the erythrocytes of offspring in rats (Ferreira et al., 2006). A large increase in HSP70 protein levels was reported in vitro in human amnion cells (Kwee et al., 2001). However, Nakamura et al. (2003) did not observe microwave effects on rat utero placental circulation or placental endocrine and immune functions; moreover, there is no convincing epidemiological evidence indicating that occupational or daily-life exposures to microwaves harm the reproductive process (Robert, 1999).

Because trophoblast cells play a crucial role in maintaining placental physiology, the study of the putative effects of high-frequency EMFs on trophoblast functions could provide new insights into the molecular basis of the interaction between EMFs and human reproductive tissues. The objective of this study was to investigate the possible effects induced in human trophoblast-derived cells by a 1.8 GHz signal, amplitude modulated with repetition frequency of 217 Hz and an applied SAR of 2 W/kg; this signal represents the safety limit for mobile phone emissions according to the ICNIRP (1998).

Under control conditions (37˚C), both the constitutive (HSC70) and the inducible (HSP70) protein forms were detected in the cells under analysis. HSC70 acts as a molecular chaperone and is thought to assist in the maintenance of cellular homeostasis and viability (Frydman, 2001). In contrast, the inducible HSP70 form represents an early-activated molecular mechanism for cytoprotection after exposure of cells to a wide range of physicochemical insults (Scharf et al., 1998). Only the expression of the inducible form was enhanced by thermal stress, with a maximum response seen after 1 h of exposure at 43˚C and 3 h of post-stress recovery at 37˚C. Expression of HSC70 and HSP70 was not modified by exposures to the EMF applied. Also, expression of HSC70 and HSP70 was not modified after different exposure periods (1 h, 4 h, 16 h and 24 h).

This finding is consistent with a relatively large body of literature showing that high frequency EMFs did not affect HSP70 protein expression in human cells (McNamee et al., 2002; Capri et al., 2004; Dawe et al., 2006; Lantow et al., 2006; Sanchez et al., 2007). Sanchez et al. (2008) also showed no change in HSP70 expression in rat skin cells after single

or repeated exposure to GSM 900 or GSM 1800. Moreover, it has been reported that the exposure to high frequency EMFs using different signals didn't modify the expression of the HSC70 and HSP70 proteins in human trophoblasts (Valbonesi et al., 2008; Franzellitti et al., 2008).

However, other studies found a differential expression of HSP70 in cells exposed to high frequency EMFs. For example, increased protein levels were observed in human amnion cells exposed to the GSM 217 Hz signal (Kwee et al., 2001). Significant HSP70 over-expression was also found in human reconstructed epidermis (3D model) after exposure to 900 MHz GSM EMFs (Sanchez et al., 2006). The different exposure systems and the different cell models used, along with possible uncontrolled experimental variables, may account for these different results.

4.3.2 - ACETYLCHOLINESTERASE ACTIVITY AND KINETICS

The second biological effect tested was the enzymatic activity of AChE. It was assessed firstly in trophoblasts and then in PC-12 cells. This second cell line is considered a more specific target for the analysis of this endpoint and it was chosen in order to improve the knowledge of how EMFs exert their action on the kinetic of this enzyme.

The results gained for the trophoblasts and the PC-12s were nonetheless similar: the activity of the enzyme acetylcholinesterase increases after the exposure to 1.8 GHz EM field, following a time-response pattern.

This increase can be due to the feature of acetylcholinesterase, which, since it's involved in neurotransmission, has some features peculiar to an electric dipole. Thanks to these features, an external electric field can stimulate its electrical dipole behaviour and induce its activation.

It seems that external EM fields can induce a cellular proliferation and an increase in protein synthesis, as well (Dimberg, 1995; Kwee et al., 2001).

Alternatively, this variation might be due to an alteration in the catalytic site of the acetylcholinesterase molecule. For instance, it has been suggested that alterations in enzyme activity may be due to microwave induced changes in the shape of the catalytic site of the protein (Galvin et al., 1981; Lixia et al., 2006).

Analysing the kinetic parameters, in both cell lines the maximum velocity of reaction (Vmax) increases after every kind of exposure regime applied. A similar result was seen

previously on the purified AChE molecule by Barteri et al. (2005), who explained that by is the presence on the AChE molecule of a large negative potential near the active site dominion (gorge), due to the presence of negatively charged residues located at the entrance, midway down and near the gorge base. This charged group distribution leads to an electrostatic field, that changes quickly and hugely when a cellular phone sends or receives a signal for a standard call. The strong AChE first moment, created by the charge distribution of the protein, is sensitive to fluctuation of the RF emission from the cellular phone (Barteri et al., 2005). Similarly, Fraser and Frey (1968) suggested that the neurotransmitter, acetylcholine, behaves as an electric dipole capable of producing, by its orientation at the endplate, an electric field strong enough to conduct positive ions beyond the post-synaptic barrier. This may initiate stimulation or produce depolarization. The application of an external electromagnetic field might be capable of stimulating this bipolar behaviour of the neurotransmitter and may explain the observed activations of the diverse enzymatic compounds (De Pedro et al., 2005).

At the same time the Michaelis constant (km) remains unaltered: it doesn't vary between exposed and non-exposed, and neither among different treatments. That means that apparently the electromagnetic fields increase the AChE enzyme activity but don't affect its affinity for the substrate. Therefore AChE active site is supposed not to be structurally affected by an external electromagnetic field. The most probable explanation is that the field induces an increased synthesis of this protein, leading to an increased number of enzyme molecules.

The only 1.8 GHz electromagnetic field tested on human trophoblasts was the GSM 217 Hz AM signal and the results showed that longer exposures caused higher increases in the AChE activity. Using the PC-12 cells all the exposure regimes were investigated, in order to understand if different wave mode can affect the enzyme activity differently. Previous results showed that modulation schemes, and in particular the time distribution and magnitude of high SAR pulses, may play a role in evoking the biological response. For instance the transcription of the HSP70C gene product in human trophoblasts was significantly modified by amplitude modulated GSM signals and was unaffected by the un-modulated 1.8 GHz frequency, suggesting that the carrier frequency itself did not influence that kind of response (Franzellitti et al., 2008).

In the present study, instead, the highest effect can be seen after 24 hours of exposure in CW mode. It can be probably due to the interaction of this field with the particular enzyme under analysis.

Sanchez et al. (2006) found decreased levels of HSC70 protein expression in human fibroblasts exposed to 900 MHz GSM fields depending on the time of exposure and culture conditions and hypothesized the activation of adaptive cell behaviour in response to RF radiation. Several theories were also proposed to explain the influence of frequency modulation on radiofrequency-induced biological effects (Berg, 1999; Challis, 2005), but no consistent experimental evidence regarding the possible mechanisms is currently available. Different studies based on the application of different exposure systems and EMF fields show different response in terms of activation or inhibition of AChE.

A decrease in the AChE enzymatic activity was found in different cell lines by Morelli et al. (2005) after exposure at 50 Hz pulsed field and by Vukova et al. (2005) after a 2.45 GHz EMF. Similarly, Kunjilwar and Behari (1993) showed a significant decrease in activity of AChE in developing rat brain exposed to amplitude modulated RF radiation at a 147 MHz carrier wave. Stegemann et al. (1993) studied the effect of a static magnetic field (SMF) of 1.4 T of strength in mice bone marrow cells and found an inhibitory effect on AChE.

Other authors found controversial effects of external EMF on AChE activity: Vukova et al. (2005) showed a statistically significant decrease in AChE activity on the day of exposure at continuous 2.45 GHz irradiation, followed by a slight increase in enzyme activity 24 hours after.

Other author didn’t find any significant effect on the activity of this enzyme: Millar et al. (1984) evaluated the effect of exposure of acetylcholinesterase, prepared from the electroplax of the ray fish, to 2450 MHz microwave radiation and showed no significant change in AChE activity. Similarly, Baranski and Edelwejn (1975) exposed rabbits to pulsed microwaves and they detected no effects on AChE activity after long-term exposure.

On the other hand, an increase of AChE activity due to an external EMF was reported by other authors. Abramov and Merkulova (1980) stated that a single 6 hours' application of a pulsed electromagnetic field (80 kA/m) results in an increased cholinesterase activity in all cardiac structures. Galvin et al. (1981) showed that in vitro exposure of rabbit blood to 2.45 GHz EMF resulted in an increase in AChE activity. Lai et al. (1987, 1989, 1994) investigated the effects of microwave exposure on cholinergic systems in rat brain showing that, when

different microwave power densities were used, it was possible to establish a dose–response relationship for each brain region. They found that, in the rat brain, microwaves activate endogenous opioid neurotransmitters, with morphine-like properties, which are involved in many important physiological and behavioural functions revealing long-term effects such as pain perception and motivation. Daily exposures for 20 min caused an increase in cholinergic activity and a decrease in the concentration of receptors in the frontal cortex and hippocampus. Dimberg (1995) investigated the long-term effects of prenatal exposure to a magnetic field and the consequences on the growth and development of mouse brain and found that MF treatment led to a decrease in DNA and protein contents and an increase in the activity of AChE in the cortex. Enhanced AChE activity in chicken brain tissue occurred after the exposure to 50, 147 and 450 MHz radio frequency electromagnetic irradiation (Dutta et al., 1992). After infrared radiation the newborn rat's brain cells exposed by Zubkova et al. (2007) showed an increase in AChE activity 1, 3 fold higher than the controls**.**

Such changes of enzyme activity may reflect complex membrane or enzyme transformations that reflect a direct or indirect light effect on the enzyme or the cell membrane (fluidity, potential) (Kujawa et al., 2003). The field action is mediated by the membrane organization and structure which is crucial in determining the conditions of the enzyme inactivation.

However, the effect of the field on the membrane is not sufficient alone to explain the change in enzymatic activity. Acetylcholinesterase is known to be anchored to the membrane through a glycosylphosphatidylinositol. The lipid moiety linked to the enzyme is embedded into the lipid bilayer and allows the protein to move along the membrane surface to search for the substrate molecules. Changing the conditions of the lipid matrix where the enzyme is inserted through its anchor may have profound influence on the protein flexibility, a requisite for its functional activity. The external field could modify the membrane organization and structure by acting directly on the strong anisotropy of diamagnetic susceptibility of membrane phospholipids (Morelli et al., 2005).

Many studies confirm the effects of external EMF on the cell's ion flux, particularly focusing on the effects on the release of Ca^{2+} ions. Although the excitability of cholinergic neurons is controlled mainly by AChE activity, and although the secretory release of ACh is Ca^{2+} dependent, it's still not known if there is a casual biochemical connection between

field-induced changes in calcium-membrane association and changes in AChE activity or whether some more fundamental membrane change plays an active role in both events. Dutta et al. (1992) indicates that exposure to modulated radio frequency at different SARs differentially affects AChE activity of neuroblastoma NG108-15 cells in culture. This change in enzyme activity can affect the excitability of cells in response to ACh stimulation.

The animal experimental studies indicated that exposure to EMF of the microwave frequency activates the endogenous opioid system in the brain, while the studies of the brain neurotransmitter activity have not produced univocal results, some of them showed decline, others increase in acetylcholinesterase activity. In vitro studies reveal that EMF even below maximum permissible levels may induce changes in the blood-brain permeability barrier and disorders in active transport of Na^+, K^+ ions and release of Ca^{2+} ions by cellular membranes (Bortkiewicz, 2001).

The results gained so far may appear quite controversial, but even though the studies carried out involved different biological targets and different EMFs applied, they all lead to the conclusion that the cellular proteins are undoubtedly affected by external electromagnetic fields.

4.4 - BIOLOGICAL ANALYSES AFTER 144-434 MHz RADIOWAVE THERAPY EXPOSURE

The biochemical action of radiowaves at a cellular level has been investigated to identify its cancer therapeutic potential and to understand the biophysical effect of RF exposure on the human body in relation to antennae design and dosimetry. The requirements for this research were: absorbed E-field (SAR assessment), heating side effects (via modelling), biochemical effects on tumour cells *in-vitro* and effects of delivery of different radiofrequency EMFs.

The main aim was to evaluate the bio-effects of several frequencies in the MHz range, observing the differences in terms of cellular responses in tumour and non-tumour derived cells. The response of human non-tumour prostate cells (PNT1As) and human tumour prostate cells (PC-3s) was evaluated and compared after they were exposed *in vitro* to 144 MHz and 434 MHz EMF in a purpose built WaveCell Transverse Electromagnetic (TEM) Cell (WaveControl, Spain).

The proposed study has the potential to radically alter common perceptions of cancer therapy. There is a huge volume of anecdotal evidence from private patients in Australia and Ireland who received a basic form of this radiowave therapy approach. They reported no side-effects with most also reporting a substantial improvement in their condition.

Once it has been elucidated that no hyperthermic but electromagnetic effect of RF exposure is the key effector of preferential RF damage of tumour cells, electromagnetic bio-effects on exposed cells were investigated, in order to evaluate any difference between tumour and non-tumour cells in terms of cellular responses.

The study employed cell proliferation and cell count to evaluate the biological effect of RF with the inclusion of cellular protein and DNA as additional indicators of cellular stress. The comparison among the results gained aims to establish if different RF exposure regimes exert different effects on tumour (PC-3) or non-tumour (PNT1A) prostate cells. Any possible detrimental effect on PC-3s which is not exerted on PNT1As could be applied for more in-depth studies, aimed to find any potential application of RF in the MHz range (144 and 434 MHz at different input power level) in future cancer therapy design.

Another cell line was employed in this study: the human trophoblasts. This is considered an ideal target to evaluate the effects of stress factors, therefore it was used as a further control, to confirm that the EMFs applied have no detrimental effects on normal tissues.

These preliminary results from initial in vitro prostate cell exposure studies confirm tumour cells to be more sensitive to RF exposure. Based on the results of related studies it appears likely that non-thermal RF field exposure induces alterations in the proliferation of tumour cells and in their expression of proteins. Different RF exposure regimes lead to different effect on cells, though a linear relationship between dose and effect cannot be detected. Data from these preliminary studies show a selective sensitivity to RF of tumour cells rather than non-tumour, indicating that RF indeed has biological effects or, in other words, that living cells can be treated by RF.

The precise sub-cellular effects of exposure to high frequency, high energy radiowaves have yet to be elucidated limiting our ability to exploit its therapeutic potential to the full. This study and more specifically follow on studies will address this gap in the current understanding of how radiowaves might greatly advance cancer therapy. Further

investigations should be addressed, in a methodical manner, how to maximize the targeting of only tumour cells, without damaging non-tumour cells.

This study must be improved to determine if radiowaves can be employed as a cure for cancer on its own, or in combination with other therapy based on some new chemotherapy drugs or hypoxic environment in the cells. The rationale for future therapeutic approach to different tumour types will be based on a specific wavelength selection, determined according to the penetration of radiowaves into tissue, which is inversely related to the wavelength.

4.4.1 - CELL PROLIFERATION RATE AND SURVIVAL

Cell populations were assessed for cell death, and cellular proliferation were monitored in real time post exposure using an xCELLigence real-time cell analyser (Roche, UK). Previous results obtained using this instrument have been shown to be comparable and indeed superior to more traditional cytotoxicity assays such as those employing 3-(4,5-Dimethylthiazol-2-yl)-2,5-diphenyltetrazolium bromide (MTT), neutral red uptake (NRU), lactate dehydrogenase, and acid phosphatase tests (Xing et al., 2006; Zhu et al., 2006; Boyd et al., 2008).

Under the experimental conditions used in this study, it was observed that RF fields of 434 MHz and 144 MHz cause significant changes in cell proliferation rates and most notably was the observation that the capacity of PNT1A cells to grow and proliferate after exposure was largely unaffected, while the capacity of PC-3s to grow is disrupted by exposure to RF. Trophoblast cell proliferation rate and survival were not affected by the applied RF EMFs.

For double exposures non-tumour PNT1As showed a slight decrease in their cell growth rate, but since their relative cell proliferation rate was still higher than 1, it can be assumed that they kept growing, even though slower than under normal condition.

Moreover, comparing the cell proliferation rate in tumour and non-tumour cell lines, it can be seen that PC-3 cells are apparently more RF sensitive than PNT1A cells. This observation is of great significance for further therapeutic applications and it is discussed in more detail below.

What is clear initially is that the RF exposure regimes employed in this study were not lethal to the exposed cells, however a reduced cell numbers were observed in RF-exposed populations confirming the real-time cell proliferation data reported.

Alteration in proliferation is one of the most sensitive parameter that can be used to elucidate the cellular stress response. There are relatively few reports about the effects of high frequency electromagnetic fields on proliferation and the results are conflicting. A number of contradictory studies have been reported on the non-thermal bio-effects of RF fields on cell proliferation, including the observation of a decrease in proliferation in a human astrocytoma cell line (French et al. 1997) and the observation of no significant modification in growth curve and cell doubling times in primary glial cells and glioma cell lines (Stagg et al. 1997). Also Higashikubo et al. (2001) observed no changes in cell cycle parameters in glioblastoma cells exposed to RF of short and long duration. Cleary et al (1996) showed a significant growth modulation in a T-lymphocyte cell line exposed to an RF field (2.45 GHz, SAR>25 W/kg) after addition of interleukin, where as Vijayalaxmi et al (2001) did not observe any modification of the mitotic index of human lymphocytes when exposed to either a continuous wave RF field at 2.45 GHz (12.5 W/kg SAR) or a modulated RF field at 847.74 MHz (SAR≈5 W/kg). Furthermore, Capri et al (2004a; 2004b) reported no change in either proliferation, apoptosis or the mitochondrial membrane potential of human lymphocytes exposed to 900 MHz CW and GSM modulated RF though a decrease in DNA synthesis was observed after exposure that was not ascribable to hyperthermia. Moreover, Kwee and Raskmark (1998) found a decrease in growth of human epithelial amniotic cells following exposure to 960 MHz at SARs of 0.021, 0.21 and 2.1 W/kg and a general linear correlation between exposure time and growth changes was observed for the highest and lowest power intensity.

These findings suggest that different responses to RF fields are likely related to the varied cell types and different exposure regimes (such as electric field, frequency, input power, etc).

The changes observed in this study in cell proliferation rate and total cell numbers are unlikely to have been a direct result of RF-induced heat generation (as a maximal heating of 0.1˚C was observable over 60 minutes) and are therefore attributable to electromagnetic effects. It has been reported recently that the critical temperature required to induce bio-effects via hyperthermia is 43˚C (Overgaard et al., 2009). The changes in cell

proliferation due to exposure to RF fields cannot be a result of heat generation, if any, from these fields. It can be assumed that within this range and under isothermal conditions, temperature changes are not the cause of the biological effects due to field exposure.

It is likely that the cells response to the RF stress by slowing down their division activities, resulting in a decreased cell proliferation rate in tumour cells. The delayed cell division may provide opportunities for repairing on one hand and apoptosis on the other (Lee et al., 2005). This different response in tumour and non-tumour derived cells can be considered of primary importance and warrant further investigation to explore the potential of RF as a stand-alone approach to cancer therapy.

4.4.2 - RELATIVE QUANTIFICATION OF CELLULAR DNA

DNA quantification per cell is a fast, convenient and efficient measure of the nuclear DNA dynamics of the cell. Reduced DNA content has been previously associated with apoptosis (Guijarro et al., 1998) as well as a reduced Mitotic Index (Grove et al., 1969).

There were no significant changes observed in cellular DNA content post RF exposure except in PC-3 and PNT1A cells post single exposure to 144 MHz 50 W. What was notable also was that cells exposed to a repeat exposure of 144 MHz 50 W did not show any change in DNA content when compared to controls.

In this study cell proliferation decreases 4 hours after RF exposure and a slight effect on DNA content can be seen 4 hours after the end of the exposure, but it disappears 24 hours after. Some authors interpret this phenomenon as a stress effect, which can disappear after the cellular system had adapted to RF radiation. Tuschl et al. (2006) investigated immune parameters after exposure of human cells to GSM modulated radiofrequency radiation (2.45 GHz) and saw that proliferation in human immune cells was stimulated immediately after exposure, but decreased 24 hours after radiation.

4.4.3 - QUANTIFICATION OF TOTAL PROTEIN

Protein quantification, by the Bradford Assay (Bradford, 1976), is considered easy to perform, practical and more sensitive than other methods (Okutucu et al., 2007) and is another fast and convenient measure of cellular stress that has been found previously associated with reduced cell proliferation rate (Reif et al., 2003), reduced cellular metabolism (Morris and Mathews, 1989) and ionising radiation exposure (Kim et al., 1999).

When protein content data are normalised against cell count data, no pronounced changes are evident, while even low doses of 144 MHz and 434 MHz effect selective increases in cellular protein levels in tumour cells only, suggesting that the cell size could have been affected as well. Even low doses of 144 MHz (5 W) effects a selective increase in cellular protein of PC-3 cells only, a trend largely repeated in cells exposed to 144 MHz 50 W and 434 MHz 50 W. A number of hypotheses have been proposed to describe how RF fields may interact with cells and/or animals to induce adverse biological effects. One such hypothesis suggests that RF fields may cause alterations in the conformation of cellular proteins and the eventual synthesis of stress-response proteins (Galvin et al., 1981; Lixia et al., 2006). Several studies have supported this hypothesis through detection of increased protein expression following exposure of cells to low intensity RF fields (Dimberg Y, 1995; Kwee et al., 2001).

It has been postulated that HF EMF might cause protein denaturation; indeed, there are reports suggesting that non-thermal exposure affects protein structural rearrangements with authors being of the opinion that the target of MW effects is cell proteins (Dutta et al., 1992; Vukova et al., 2005). Indeed such a postulation could explain the observation, in the present study, of the increase in protein in some RF exposed PC-3 cells to almost twice the protein in un-exposed PC-3 cells, with these cells possibly having to increase the rate of protein translation to counteract an increase in protein denaturation rate. No significant effects were detected in trophoblasts, in terms of total proteins.

Based on the results of related studies it appears likely that non-thermal RF field exposure induced alterations in the proliferation of tumour cells and in their expression of proteins. Different RF exposure regimes lead to different effect on cells, though a linear relationship between dose and effect cannot be detected.

The results gained from this analysis confirm that one of the main targets of high frequency electromagnetic fields are the cellular proteins and that the fields applied in radiowave therapy (frequency range 144-434 MHz) exert a greater effect on tumour cells than on non-tumour. This selective sensitivity to RF of tumour cells rather than non-tumour, even at low power, suggests that a cancer therapeutic approach could be developed and further research in this area is certainly warranted.

The endpoints used to assess the effect of radiowave therapy EMFs on cellular processes (cell proliferation and survival, and cellular DNA and protein content) are to be

considered a preliminary step towards a better knowledge of how radiowave treatments can influence differently tumour and non-tumour cells. They provide only for an initial interpretation of cellular events to determine whether RF EMFs can affect tumour cells more than non-tumour cells. Nonetheless it is recognized that for more in depth analysis other endpoints have to be investigated.

4.4.4 - NUCLEAR DNA DAMAGE MARKER ANALYSIS

Conventional and Real Time PCR was employed to evaluate the potential for radiowave exposure to induce nuclear DNA damage in tumour cells. This endpoint was analyzed by assessing the gene expression of two proteins involved in DNA double strand break repair: XLF and PARP1. Cernunnos-XLF is a core factor which plays a key role in non homologous end joining repair (NHEJ) since it's involved in most NHEJ reactions activating or enhancing the basic NHEJ ligation reactions. PARP1 (poly ADP ribose polymerase) is an unfailing housekeeper, that signals DNA rupture and participates in base-excision repair, promoting the activity of DNA transcription factors.

The gene expression of these proteins was evaluated in the three cell lines (Trophoblasts, PC-3s and PNT1As) after the exposure to 144 MHz, 434 MHz and 1.8 GHz EMF. The aim of this part of the study was to assess any possible effect of the applied EMF in terms of DNA damage, comparing the response in tumour and non-tumour cell lines, in order to confirm that the DNA in the non-tumour cell lines is not damaged by the RF-treatments.

Amongst many biological targets, the DNA molecule has received the greatest attention with respect to potential HF-EMF damage, because of its relevance for cell function, proliferation, viability, mutation and cancer. Again, no convincing evidence supports that exposure to HF-EMF at levels that did not cause significant temperature increases, can damage the DNA molecule or induce carcinogenesis (Brusick et al., 1998; Heynick et al, 2003; Vijayalaxmi and Obe, 2004;). However, some laboratory investigations on non-thermal effects of HF-EMF provided positive findings (Sarkar et al., 1994; Lai and Singh, 1995; Lai and Singh, 1997; Maes et al., 1997; Tice et al., 2002). Some studies report the induction of DNA damage in cells after high-frequency EMF exposure (Diem et al., 2005 and Nikolova et al., 2005), but these results have not been confirmed (Scarfì et al., 2006 and

Speit et al., 2007). Controversial results are also accumulating as to the potential genotoxic effects of high-frequency EMFs.

In general, the prevailing opinion (Vijayalaxmi and Obe, 2004) does not support the hypothesis that high-frequency EMFs induce genotoxic effects. Similarly, Valbonesi et al. (2008) reports no alteration in the levels of primary DNA damages, evaluated by the alkaline comet assay, in the human trophoblast cells following a 1 h exposure to 217 Hz amplitude-modulated GSM signals (1.8 GHz carrier frequency, SAR=2 W/Kg), largely used in mobile telephony.

As for the expression of XLF gene, no significant effect was seen in PNT1As and trophoblasts, proving that no double strand break occurred in non-tumour cells after the exposure regimes applied. The only exposure regime that slightly affects the non-tumour prostate cells is 144 MHz, 50 W, probably because of the features of the signal applied and how far radiowaves can penetrate through the biological sample until they are completely absorbed or reduced in intensity. Several studies reported differential responses of cells exposed to different fields applied (Lai and Singh, 1995; D'Ambrosio et al., 2002).

In terms of single strand damage (PARP1 gene expression), no cell line seems to be affected by the 144 or 434 MHz fields applied with an input power of 50 W. With the 144 MHz 5 W exposure regime, both PNT1As and PC-3s are affected by the EMF applied, showing an increase in the gene expression after exposure. The PARP1 gene expression in PC-3s has an increase only 4 hours after the exposure and recovers 24 hours after. PNT1As, instead, are heavily affected both 4 and 24 hours post-exposure and after both single and double exposure, showing that this kind of exposure regime apparently affects non-tumour cells more than tumour cells. The exposure regimes that seems to exert no effects in terms of single and double DNA strand break damage is the one at 434 MHz 50 W.

According to these findings, so far the 434 MHz 50 W exposure regime seems to be at the same time the most effective on tumour prostate cells and the least effective on non-tumour prostate cells. This result can be considered a starting point for further investigations, aimed at confirming those findings and at establishing whether and how the application of this RF EMF can be used as a stand-alone therapy for cancer cure.

The effects on DNA damage were examined after continuous and intermittent exposure (5 min field on and 10 min field off) to 1.8 GHz CW signal, showing an increase of XLF and PARP1 gene expression in PC-3 cells after intermittent exposure. Once again, the

literature about the intermittency effectiveness is controversial and the reason for such contradictory findings remains unclear: a report stating that intermittent exposure was effective in eliciting the genotoxic effect was published by Diem et al. (2005), but other authors critically commented the biological significance of those results (Vijayalaxmi et al., 2005). An independent replication of the same experiment was performed by Speit et al., 2007, under the same exposure conditions (1.8 GHz, SAR 2 W/kg), testing a field without modulation and intermittent exposures (5 min on and 10 min off) for different exposure times (1, 4 and 24 hours). In conclusion, they weren't able to confirm the genotoxic effects reported by Diem et al, 2005, even though they can't exclude a genotoxic effect of RF EMF in general.

4.5 - FURTHER DISCUSSION

The experimental design of this study aimed to better understand the mechanisms involved in the interaction between high frequency electromagnetic fields and biological systems at a cellular level. Understanding the consequences for a cell after RF exposure is the first step in determining the effects on the organs, on the whole organism and on public health.

Several in vitro studies have established that low frequency EMF exposure induce biological changes ranging from increased enzymatic rates to increased gene transcription (Hong, 1995; Lai and Singh, 2004; Merola et al., 2006). In contrast, the effects of high frequency EMF are less well studied and what has been investigated to date regarding cell proliferation and apoptosis is frequently contradictory (French et al., 1997; Stagg et al., 1997; Kwee and Raskmark, 1999; Higashikubo et al., 2001; Port et al., 2003; Marinelli et al., 2004).

While several studies indicated that high-frequency EMFs affect cell cycle regulation (Velizarov et al., 1999; Tokalov and Gutzeit, 2004; Buttiglione et al., 2007;), protein amount (Dimberg, 1995; Kwee et al., 2001), gene and protein expression (Kwee et al., 2001; Leszczynski et al, 2002; Lee et al., 2005; Lixia et al., 2006; Sanchez et al., 2006), and genome stability (Sarkar et al., 1994; Lai and Singh, 1995; Lai and Singh, 1997; Maes et al., 1997; D'Ambrosio et al., 2002; Tice et al., 2002), other investigations did not detect any significant effects on cellular systems (Stagg et al., 1997; Higashikubo et al., 2001; Capri et al., 2004;

Vijayalaxmi and Obe, 2004; Cotgreave, 2005; Dawe et al., 2006; Lantow et al., 2006; Qutob et al., 2006; Scarfì et al., 2006; Sanchez et al., 2007).

The number of reports on radiofrequency and microwaves induced effects on various cellular processes is increasing rapidly and a greater understanding of the potential bio-effects of RF is warranted given the huge increase in our daily exposure to RF through mobile telephones, wireless broadband, power cables, radio and television. However, satisfactory descriptions of the biophysical and biological mechanism by which these fields exert their effects have yet to be offered (Repacholi, 1998; Leszczynski et al., 2002; Merola et al., 2006).

It appears that different factors are responsible for the conflicting results obtained so far. Indeed, the cellular and molecular modifications induced by exposure to high-frequency EMFs depend on the duration of exposure, tissue penetration, and heat generation, which are in turn related to the intensity and frequency of the EMF. In addition, cellular responses could also depend on type of field (static or oscillatory), waveform (sinusoidal, square, etc.), modulation scheme, and biological status and type of cells exposed.

There is indeed a lot of controversy, since both detrimental and non-detrimental effects on human health were reported and recently reviewed (Obe and Vijayalaxmi, 2004, Meltz, 2003, Otto and von Mühlendahl, 2007, Verschaeve et al., 1998, Verschaeve, 2009 and Khurana et al., 2009). The majority of these studies, however, concluded that there are no persuasive scientific data suggesting a health risk due to HF EMF exposure (WHO, Electromagnetic fields and public health, 2006).

In conclusion, these results demonstrate that exposure to HF (1.8 GHz) GSM EMFs can induce alterations in some principal activities of the cell, such as the regulation of protein synthesis. In the light of the results gained with this study, no decisive conclusion can be drawn about the hazards of GSM mobile phone use to human health. More detailed studies are evidently required. Nonetheless some cellular effects can be seen after exposure to GSM-like EMFs: the activation of the acetylcholinesterase enzyme is a clear sign that some sort of interactions between the electromagnetic fields and the biological matter do exist, even at 2 W/kg of SAR as safety limit for telecommunication, established by ICNIRP (International Commission on Non-Ionizing Radiation Protection).

Similarly, the exposure to 144 MHz and 434 MHz HF EMFs can induce alterations in some principal activities of the tumour cells, such as rate of proliferation and regulation of protein synthesis. Different RF exposure regimes lead to different amplitude of effects on cells, though a linear relationship between dose and effect was not observable. Perhaps the most critical observation of the present study was the greater sensitivity of tumour cells to RF exposure compared to non-tumour cells.

Such observations warrant further investigation to explore the potential of RF as a stand-alone approach to cancer therapy and have been expanded to include the investigation of several other cell-type models. When the energy of these radiowaves is applied in a controlled way and cancerous and normal tissue are exposed, the cancer cells behave much differently than the normal cells, such that, with the proper development of the technique, tumours in the body could be targeted and destroyed by radiowaves that harmlessly pass through normal tissue on their way to the tumour site.It is now widely accepted that to significantly advance the current success rates of cancer treatment, new avenues of therapeutic approach must be identified as the maximal benefit of current therapeutic approaches will soon be realized. One such alternate therapeutic approach is the one analysed in this study.

The radiowave therapies are based on several biochemical and biophysical hypotheses:

- Exposure of cancer cells to RF waves decreases the rate at which the cancer cells divide.
- Exposure of cancer cells to RF waves has some non-hyperthermic biochemical and biophysical effect on the cells when compared to non-tumour cells other than the hypothesised increase in mitotic rate. Possible effects include changes in cell membrane potential, mitosis of mitochondria, changes in DNA sensitivity and cell polarity.
- RF waves "sensitize" cancer cells so that they are more likely to be killed by subsequent radiotherapy. The cause of this sensitization is unknown other than the suggestion made by Holt (1977) that it involves electrical resonance and fluorescence effects.
- RF waves increase the rate at which normal stem cells of the immune system divide.

Few therapeutic approaches to date have been reported to demonstrate divergent properties in tumour and normal tissue as may be observed from radiowave exposure. Dr Hagness and her group at the University of Wisconsin-Madison have shown breast tumour tissue and normal tissue to have very different properties when exposed to radiowaves in the 100 MHz to 20 GHz range, with cancerous tissue showing an approximate 10 fold higher dielectric constant and 50-100 fold greater effective conductivity than normal tissue (Lazebnik et al., 2006). The observation of such contrasting properties provides great impetus to develop and exploit the full therapeutic potential of radiowave exposure and more specifically to focus on advancing different cancer therapy.

As mentioned previously, the human population conduct their daily lives in an ever increasing sea of electromagnetic waves and a better understanding of how they may influence human health is now well overdue. The present study employed *in vitro* analyses to further elucidate EMF effects at a cellular level. This included simulating EMF typical of environmental exposure through mobile phone use and also of wavelengths in the range typically employed at present in the medical community for a variety of reasons.

Some cellular effects can be seen after exposure to GSM EMFs indicating an interaction between the electromagnetic field and the biological matter, even at the safety SAR limit of 2 W/kg.

Several pioneering oncologists around the world employ EMF in the MHz range as an adjunct therapy, however much of the data in this study suggests that, given further development, radiowaves in the 140-434 MHz range have potential as a stand-alone approach to cancer therapy.

4.6 - ACKNOWLEDGEMENT

Funds for the purchase of the HF (1.8 GHz) GSM EMF exposure system were provided by the Fondazione Flaminia (Ravenna) and funding for the research was granted by the Italian Ministry of University and Scientific Research (PRIN 2005, PRIN 2007).

Research conducted at IT Sligo was funded by Radiowave Therapy Research Institute (RTRI), Western Australia.

Chapter 5

REFERENCE

2006 WHO Research Agenda for Radio Frequency Fields. WHO, Geneva, 2006. [available online at www.who.int]

Abramov LN, Merkulova LM, 1980. Histochemical study of the cholinesterase activity in the structures of the rat heart normally and during exposure to a pulsed electromagnetic field [Article in Russian]. Arkh Anat Gistol Embriol, 79(11); 66-71.

Adair ER, Black DR. 2003. Thermoregulatory responses to RF energy absorption. Bioelectromagnetics Supplement, 6; 17 – 38.

Ahnesorg P, Smith P, Jackson SP, 2006. XLF interacts with the XRCC4-DNA ligase IV complex to promote DNA nonhomologous end-joining. Cell. 124(2); 301-13.

Baranski S, Edelwejn Z, 1975. Experimental morphologic and electroencephalographic studies of microwave effects on the nervous system. Ann NY Acad Scy, 247; 109–16.

Barteri M, Pala A, Rotella S, 2005. Structural and kinetic effects of mobile phone microwaves on acetylcholinesterase activity. Biophysical Chemistry, 113; 245-253

Bauditz J, Quinkler M, Beyersdorff D, Wermke W, 2008. Improved detection of hepatic metastases of adrenocortical cancer by contrast-enhanced ultrasound. Oncol Rep, 19(5); 1135-1139.

Berg H, 1999. Problems of weak electromagnetic field effects in cell biology. Bioelectrochem Bioenerg, 48; 355–360.

Bonnet S, Archer SL, Allalunis-Turner J, Haromy A, Beaulieu C, Thompson R, Lee CT, Lopaschuk GD, Puttagunta L, Bonnet S, Harry G, Hashimoto K, Porter CJ, Andrade MA, Thebaud B, Michelakis ED, 2007. A mitochondria-K^+ channel axis is suppressed in cancer and its normalization promotes apoptosis and inhibits cancer growth, Cancer Cell, 11; 37–51

Bortkiewicz A, 2001. A study on the biological effects of exposure mobile-phone frequency EMF [article in Polish]. Med Pr, 52(2); 101-106.

Boyd JM, Huang L, Xie L, Moe B, Gabos S, Li XF, 2008. A cell-microelectronic sensing technique for profiling cytotoxicity of chemicals. Analytica Chimica Acta, 615; 80-87.

Bradford MM, 1976. A rapid and sensitive method for the quantitation of microgram quantities of protein utilizing the principle of protein-dye binding. Anal Biochem, 72; 248-254.

D. Brusick, R. Albertini, D. McRee, D. Peterson, G. Williams, P. Hanawalt and J. Preston, Genotoxicity of radiofrequency radiation. Environ Mol Mutagen, 32; 1–16.

Buck D, Malivert L, de Chasseval R, Barraud A, Fondanèche MC, Sanal O, Plebani A, Stéphan JL, Hufnagel M, le Deist F, Fischer A, Durandy A, de Villartay JP, Revy P, 2006. Cernunnos, a novel nonhomologous end-joining factor, is mutated in human immunodeficiency with microcephaly. Cell, 124(2); 287-99

Buttiglione M, Roca L, Montemuro E, Vitiello F, Capozzi V, Cibelli G, 2007. Radiofrequency radiation (900 MHz) induces Egr-1 gene expression and affects cell-cycle control in human neuroblastoma cells. J Cell Physiol, 213; 759–767.

Callebaut I, Malivert L, Fischer A, Mornon JP, Revy P, de Villartay JP, 2006. Cernunnos interacts with the XRCC4 x DNA-ligase IV complex and is homologous to the yeast nonhomologous end-joining factor Nej1. J Biol Chem, 281(20); 13857-13860.

Capri M, Scarcella E, Fumelli C, Bianchi E, Salvioli S, Mesirca P, Agostini C, Antolini A, Schiavoni A, Castellani G, Bersani F, Franceschi C, 2004a. In vitro exposure of human lymphocytes to 900 MHz CW and GSM modulated radiofrequency; studies of proliferation, apoptosis and mitochondrial membrane potential. Radiat Res, 162(2); 211-218.

Capri M, Scarcella E, Bianchi E, Fumelli C, Mesirca P, Agostini C, Remondini D, Schuderer J, Kuster N, Bersani F, 2004b. 1800 MHz radiofrequency (mobile phones, different Global System for Mobile communication modulations) does not affect apoptosis and heat shock protein 70 level in peripheral mononuclear cells from young and old donors. Int J Radiat Biol, 80; 389–397.

Cardinal J, Klune JR, Chory E, Jeyabalan G, Kanzius JS, Nalesnik M, Geller DA, 2008. Noninvasive radiofrequency ablation of cancer targeted by gold nanoparticles. Surgery, 144(2); 125-132.

Carlo GL, editor. 1998. Wireless phones and health: scientific progress. Boston: Kluwer Academic Publishers. 413 p.

Caselli F, Gastaldi L, Gambi N, Fabbri E, 2006. In vitro characterization of cholinesterases in the earthworm *Eisenia andrei*. Comp Biochem Physiol C Toxicol Pharmacol, 143(4); 416-421.

Challis LJ, 2005. Mechanisms of interaction between RF fields and biological tissue. Bioelectromagnetics, 26; S98–S106.

Chakraborty C, Gleeson LM, McKinnon T, Lala PK, 2002. Regulation of human trophoblast migration and invasiveness. Can J Physiol Pharmacol, 80; 116–124.

Chauhan V, Mariampillai A, Gajda GB, Thansandote A, McNamee JP, 2006. Analysis of proto-oncogene and heat-shock protein gene expression in human derived cell-lines exposed *in vitro* to an intermittent 1.9 GHz pulse-modulated radiofrequency field. Int J Radiat Biol, 82(5); 347-354.

Chiarugi A, 2002. Poly(ADP-ribose) polymerase; killer or conspirator? The 'suicide hypothesis' revisited. Trends Pharmacol Sci, 23(3); 122-9. Review.

Chorostowska-Wynimko J, Szpechcinski A, 2007. The impact of genetic markers on the diagnosis of lung cancer: a current perspective. J Thorac Oncol, 2; 1044-1051.

Cleary SF, Du Z, Cao G, Liu LM, McCrady C, 1996. Effect of isothermal radiofrequency radiation on cytolytic T lymphocytes. FASEB J, 10; 913-919.

Cotgreave IA, 2005. Biological stress responses to radio frequency electromagnetic radiation; are mobile phones really so (heat) shocking? Arch Biochem Biophys, 435; 227–240.

Dale HH, 1914. The action of certain ethers of choline, and their relation to muscarine. J. Pharmacol Exp Ther, 6; 147-190.

D'Ambrosi N, Murra B, Vacca F, Volonté C, 2004. Pathways of survival induced by NGF and extracellular ATP after growth factor deprivation. Prog Brain Res, 146; 93-100.

D'Ambrosio G, Massa R, Scarfì MR, Zeni O, 2002. Cytogenetic damage in human lymphocytes following GMSK phase modulated microwave exposure. Bioelectromagnetics, 23; 7–13.

Dawe AS, Smith B, Thomas DWP, Greedy S, Vasic N, Gregory A, Loader B, de Pomerai DI, 2006. A small temperature rise may contribute towards the apparent induction by microwaves of heat-shock gene expression in the nematode Caenorhabitis elegans. Bioelectromagnetics, 27; 88–97.

Del Vecchio G, Giuliani A, Fernandez M, Mesirca P, Bersani F, Pinto R, Ardoino L, Lovisolo GA, Giardino L, Calzà L, 2009. Effect of radiofrequency electromagnetic field exposure on in vitro models of neurodegenerative disease. Bioelectromagnetics, 30(7); 564-72.

De Maio A, 1999. Heat shock proteins: facts, thoughts, and dreams. Shock, 11; 1–12.

De Pedro JA, Pérez-Caballer AJ, Dominguez J, Collía F, Blanco J, Salvado M, 2005. Pulsed electromagnetic fields induce peripheral nerve regeneration and endplate enzymatic changes. Bioelectromagnetics, 26(1); 20-7.

De Pomerai D, Daniells C, David H, Allan J, Duce I, Mutwakil M, Thomas D, Sewell P, Tattersall J, Candido P, 2000. Non-thermal heat-shock response to microwaves. Nature, 405; 417–418.

Diamantino TC, Almeida E, Soares AM, Guilhermino L, 2003. Characterization of cholinesterases from *Daphnia magna Straus* and their inhibition by zinc. Bull Environ Contam Toxicol, 71; 219-225.

Diem E, Schwarz C, Adlkofer F, Jahn O, Rudiger H, 2005. Nonthermal DNA breakage by mobile-phone radiation (1800 MHz) in human fibroblasts and in transformed GSFH-R17 rat granulosa cells in vitro. Mutat Res, 583; 178–183.

Dijkman GA, Debruyne FM, 1996. Epidemiology of prostate cancer. Eur Urol, 30(3); 281-295. Review.

Dimberg Y, 1995. Neurochemical effects of a 20 kHz magnetic field on the central nervous system in prenatally exposed mice. Bioelectromagnetics, 16(4); 263-267.

Drouet J, Frit P, Delteil C, de Villartay JP, Salles B, Calsou P, 2006. Interplay between Ku, Artemis, and the DNA-dependent protein kinase catalytic subunit at DNA ends. J Biol Chem, 281(38); 27784-27793.

Dutta SK, Das K, Ghosh B, Blackman CF, 1992. Dose dependence of acetylcholinesterase activity in neuroblastoma cells exposed to modulated radio-frequency electromagnetic radiation. Bioelectromagnetics, 13(4); 317-322.

Ellman GL, Courtney KD, Andres V, Feather-Stone RM, 1961. A new and rapid colorimetric determination of acetylcholinesterase activity. Biochem Pharmacol, 7; 88-95.

Feder ME, Hofmann GE, 1999. Heat-shock proteins, molecular chaperones, and the stress response. Annu Rev Physiol, 61; 243–282.

Fenn AJ, Wolf GL, Fogle RM, 1999. An adaptive microwave phased array for targeted heating of deep tumours in intact breast: animal study results. Int J Hyperthermia, 15(1); 45-61.

Ferreira AR, Knakievicz T, Pasquali MA, Gelain DP, Dal-Pizzol F, Fernandez CE, de Salles AA, Ferreira HB, Moreira JC, 2006. Ultra high frequency-electromagnetic field irradiation during pregnancy leads to an increase in erythrocytes micronuclei incidence in rat offspring. Life Sci, 80; 43-50.

Finnie JW, Chidlow G, Blumbergs PC, Manavis J, Cai Z, 2009. Heat shock protein induction in fetal mouse brain as a measure of stress after whole of gestation exposure to mobile telephony radiofrequency fields. Pathology, 41(3); 276-279.

Franckena M, Fatehi D, de Bruijne M, Canters RA, van Norden Y, Mens JW, van Rhoon GC, van der Zee J, 2009. Hyperthermia dose-effect relationship in 420 patients with cervical cancer treated with combined radiotherapy and hyperthermia. Eur J Cancer, 45(11); 1969-78.

Fraser A, Frey AH, 1968. Electromagnetic emission at microwave length from active nerves. Biophysics J, 7; 88-95.

Franzellitti S, Valbonesi P, Contin A, Biondi C, Fabbri E, 2008. HSP70 expression in human trophoblast cells exposed to different 1.8 Ghz mobile phone signals. Radiat Res, 170(4); 488-497.

French PW, Donnellan M, McKenzie DR. 1997. Electromagnetic radiation at 835 MHz changes the morphology and inhibits proliferation of a human astrocytoma cell line. Bioelectrochem Bioenerget, 43;13–18.

Frydman J, 2001. Folding of newly translated proteins in vivo; the role of molecular chaperones. Annu Rev Biochem, 70; 603–647.

Gaipl U, Schildkopf P. Ott O, Mantel F, Sieber R, Weiss E, Janko C, Fietkau R, Frey B, 2009. Hyperthermia treatment results in immunogenic tumour cell death forms consequences for multimodal cancer treatments. 25th Annual Meeting of the European Society for Hyperthermic Oncology.

Galvin MJ, Parks DL, McRee DI, 1981. Infl uence of 2.45 GHz microwave radiation on enzyme activity. Radiat Environ Biophys, 19; 149–56.

Gambi N, Pasteris A, Fabbri E, 2007. Acetylcholinesterase activity in the earthworm *Eisenia andrei* at different conditions of carbaryl exposure. Comp Biochem Physiol C Toxicol Pharmacol, 145(4); 678-685.

Gao Y, Chen L, Gu W, Xi Y, Lin L, Li Y, 2008. Targeted nanoassembly loaded with docetaxel improves intracellular drug delivery and efficacy in murine breast cancer model. Mol Pharm, 5(6); 1044-1054.

Garaj-Vrhovac V, Fucic A, Horvat D, 1992. The correlation between the frequency of micronuclei and specific chromosome aberrations in human lymphocytes exposed to microwave radiation *in vitro*. Mutat Res, 281; 181–186.

Ge Y, Deng T, Zheng X, 2009. Dynamic monitoring of changes in endothelial cell-substrate adhesiveness during leukocyte adhesion by microelectrical impedance assay. Acta Biochim Biophys Sin, 41(3); 256–262.

Graham CH, Hawley TS, Hawley RG, MacDougall JR, Kerbel RS, Khoo N, Lala PK, 1993. Establishment and characterization of first trimester human trophoblast cells with extended lifespan. Exp Cell Res, 206; 204–211.

Greene LA, 1978. Nerve growth factor prevents the death and stimulates the neuronal differentiation of clonal PC12 pheochromocytoma cells in serum-free medium. J Cell Biol, 78(3); 747-755.

Greene LA, Rein G, 1977a. Release, storage and uptake of catecholamines by a clonal cell line of nerve growth factor (NGF) responsive pheo-chromocytoma cells. Brain Res, 129(2); 247-63.

Greene LA, Rein G, 1977b. Synthesis, storage and release of acetylcholine by a noradrenergic pheochromocytoma cell line. Nature, 268(5618); 349-351.

Greene LA, Tischler AS, 1976. Establishment of a noradrenergic clonal line of rat adrenal pheochromocytoma cells which respond to nerve growth factor. Cell Biology, 73(7); 2424-2428.

Greene LA, Tischler AS, 1982. PC12 pheochromocytoma cultures in neurobiological research. Advan Cell Neurobiol, 3; 373-414.

Gromoll C, Lamprecht U, Hehr T, Buchgeister M, Bamberg M, 2000. An on-line phase measurement system for quality assurance of the BSD 2000. Part I: technical description of the measurement system. Int J Hyperthermia, 16(4); 355-363.

Grove D, Nair KG, Zak R, 1969. Biochemical correlates of cardiac hypertrophy. III. Changes in DNA content; the relative contributions of polyploidy and mitotic activity. Circ Res, 25(4); 463-471.

Guijarro C, Blanco-Colio LM, Ortego M, Alonso C, Ortiz A, Plaza JJ, Díaz C, Hernández G, Egido J, 1998. 3-Hydroxy-3-methylglutaryl coenzyme a reductase and isoprenylation inhibitors induce apoptosis of vascular smooth muscle cells in culture. Circ Res, 83(5); 490-500.

Hahn T, Desoye G, Lang I, Skofitsch G, 1993. Location and activities of acetylcholinesterase and butyrylcholinesterase in the rat and human placenta. Anat Embryol (Berl), 188(5); 435-440.

Hendee WR, Boteler JC, 1994. The question of health effects from exposure to electromagnetic fields. Health Phys, 66(2); 127-136.

Heo HJ, Hong SC, Cho HY, Hong B, Kim HK, Kim EK, Shin DH, 2002. Inhibitory effect of zeatin, isolated from Fiatoua villosa, on acetylcholinesterase activity from PC12 cells. Mol Cells, 13(1); 113-117.

Heynick LN, Johnston SA, Mason PA, 2003. Radiofrequency electromagnetic fields: Cancer, mutagenesis, and genotoxicity. Bioelectromagnetics, 24 (6); 74–100.

Higashikubo R, Ragouzis M, Moros EG, Straube WL, Roti Roti JL, 2001. Radiofrequency electromagnetic fields do not alter the cell cycle progression of C3H 10T and U87MG cells. Radiat Res, 156(6); 786–795.

Hofmann GA, Dev SB, Dimmer S, Nanda GS, 1999. Electroporation therapy: a new approach for the treatment of head and neck cancer. IEEE Trans Biomed Eng, 46(6); 752-759.

Holt JAG, 1977. Increase in X-Ray Sensitivity of Cancer After Exposure to 434 MHz Electromagnetic Radiation. Microwave Symposium Digest, MTT-S International, 77(1); 259-262.

Holt JAG, 1988. Microwaves are not hyperthermia. The Radiographer, 35; 151-162.

Holt JAG, 1997. A theoretical biochemical basis of cancer: confirmation by electromagnetic radiation. J Orthomolecular Medicine, 12; 149-163.

Holt JAG, Nelson A, 1985. Combined microwave therapy. The Medical J Australia, 142; 707.

Hong FT, 1995. Magnetic field effects on biomolecules, cells, and living organisms. Biosystems; 36(3); 187-229. Review.

Hynynen K, Pomeroy O, Smith DN, Huber PE, McDannold NJ, Kettenbach J, Baum J, Singer S, Jolesz FA, 2001. MR imaging-guided focused ultrasound surgery of fibroadenomas in the breast: a feasibility study. Radiology, 219(1); 176-185.

International Commission on Non-Ionizing Radiation Protection, 1998. Guidelines for limiting exposure to time-varying electric, magnetic, and electromagnetic fields (up to 300 GHz). Health Phys, 74; 494–522.

Joines WT, Jirtle RL, Rafal MD, Schaefer DJ, 1980. Microwave power absorption differences between normal and malignant tissue. Nat J Radiation Oncology Biol Phys, 6; 681-687.

Khurana VG, Teo C, Kundi M, Hardell L, Carlberg M, 2009. Cell phones and brain tumors; a review including the long-term epidemiologic data, Surg Neurol, 72; 205–214.

Kim GD, Choi YH, Dimtchev A, Jeong SJ, Dritschilo A, Jung M, 1999. Sensing of ionizing radiation-induced DNA damage by ATM through interaction with histone deacetylase. J Biol Chem, 29; 31127-31130.

Kirson ED, Gurvich Z, Schneiderman R, Dekel E, Itzhaki A, Wasserman Y, Schatzberger R, Palti Y, 2004. Disruption of cancer cell replication by altering electric fields. Cancer Research, 64; 3288-3295.

Kousba AA, Poet TS, Timchalk C, 2003. Characterization of the in vitro kinetic interaction of chlorpyrifos-oxon with rat salivary cholinesterase: a potential biomonitoring matrix. Toxicology, 188 ; 219-232.

Krokosz A, Szweda-Lewandowska Z, 2005. Changes in the activity of acetylcholinesterase and Na,K-ATPase in human erythrocytes irradiated with X-rays. Cell Mol Biol Lett, 10(3); 471-478.

Kujawa J, Zavodnik L, Zavodnik I, Bryszewska M, 2003. Low-intensity near-infrared laser radiation-induced changes of acetylcholinesterase activity of human erythrocytes. J Clin Laser Med Surg, 21; 351-355.

Kunjilwar KK, Behari J, 1993. Effect of amplitude-modulated radio frequency radiation on cholinergic system of developing rats. Brain Res, 601(1-2); 321-324.

Kuster N and Schönborn F, 2000. Recommended minimal requirements and development guidelines for exposure setups of bio-experiments addressing the health risk concern of wireless communications. Bioelectromagnetics, 21; 508-514.

Kwee S, Raskmark P, Velizarov P, 2001. Changes in cellular proteins due to environmental non-ionising radiation. Electro Magnetobiol, 20; 141–152.

Lai H, Horita A, Chou CK, Guy AW, 1987. Low-level microwave irradiations affect central cholinergic activity in the rat. J Neurochem, 48(1); 40-45.

Lai H, Carino MA, Horita A, Guy AW, 1989. Low-level microwave irradiation and central cholinergic activity; a dose-response study. Bioelectromagnetics, 10(2); 203-208.

Lai H, Horita A, Guy AW, 1994.Microwave irradiation affects radial-arm maze performance in the rat. Bioelectromagnetics, 15(2); 95-104.

Lai H, Singh NP, 1995. Acute low-intensity microwave exposure increases DNA single-strand breaks in rat brain cells, Bioelectromagnetics, 16; 207–210.

Lai H, Singh NP, 1997. Melatonin and a spin-trap compound block radiofrequency electromagnetic radiation-induced DNA strand breaks in rat brain cells. Bioelectromagnetics, 18; 446–454.

Lang SH, Stower M, Maitland NJ 2000. In vitro modelling of epithelial and stromal interactions in non-malignant and malignant prostates. Br J Cancer, 82(4); 990-997.

Lantow M, Schuderer J, Hartwing C, Simko M, 2006. Free radical release and HSP70 expression in two human immune-relevant cell lines after exposure to 1800 MHz radiofrequency radiation. Radiat Res, 165; 88–94.

Lazebnik M, Converse MC, Booske JH, Hagness SC, 2006. Ultrawideband temperature-dependent dielectric properties of animal liver tissue in the microwave frequency range. Phys Med Biol, 51(7); 1941-1955.

Lazebnik M, Popovic D, McCartney L, Watkins CB, Lindstrom MJ, Harter J, Sewall S, Ogilvie T, Magliocco A, Breslin TM, Temple W, Mew D, Booske JH, Okoniewski M, Hagness SC, 2007. A large-scale study of the ultrawideband microwave dielectric properties of normal, benign, and malignant breast tissues obtained from cancer surgeries. Phys Med Biol, 52; 6093-6115.

Lee S, Johnson D, Dunbar K, Dong H, Ge X, Kim YC, Wing C, Jayathilaka N, Emmanuel N, Zhou CQ, Gerber HL, Tseng CC, Wang SM, 2005. 2.45 GHz radiofrequency fields alter gene expression in cultured human cells. FEBS letters, 579; 4829-4836.

Leszczynski D, Xu Z, 2010. Mobile phone radiation health risk controversy: the reliability and sufficiency of science behind the safety standards. Health Research Policy and Systems, 8.

Leszczynski D, Joenvaara S, Reivinen J, Kuokka R, 2002. Non-thermal activation of the hsp27/p38MAPK stress pathway by mobile phone radiation in human endothelial cells; molecular mechanism for cancer- and blood-brain barrier-related effects. Differentiation, 70; 120–129.

Li Z, Maccarini PF, Arabe OA, Stakhursky V, Joines WT, Stauffer PR, Vogel M, Crawford D, 2008. Towards the Validation of a Commercial Hyperthermia Treatment Planning System. Microwave J, 51(12); 28-42.

Lixia S, Yao K, Kaijun W, Deqiang L, Huajun H, Xiangwei G, Baohong W, Wei Z, Jianling L, Wei W, 2006. Effects of 1.8 GHz radiofrequency field on DNA damage and expression of heat shock protein 70 in human lens epithelial cells. Mutat Res, 602; 135–142.

Lowry, O.H., Rosebrough, N.J., Farr, A.L., Randall, R.J., 1951. Protein measurement with Folin

phenol reagent. J Biol Chem, 193; 265-275.

Maes A, Collier M, Van Gorp U, Vandoninck S, Verschaeve L, 1997. Cytogenetic effects of 935.2-MHz (GSM) microwaves alone and in combination with mitomycin C. Mutat Res, 393; 151–156.

Maisch D, Rapley B, 1998. Powerline Frequency Electromagnetic Fields and Human Health - Is it the time to end further research? An Overview of Three Recent Studies. J Aust Coll Nutr & Env Med, 17 (1); 5-16.

Malinen M, Huttunen T, Hynynen K, Kaipio JP, 2004. Simulation study for thermal dose optimization in ultrasound surgery of the breast. Med Phys, 31(5); 1296-1307.

Marinelli F, La Sala D, Cicciotti G, Cattini L, Trimarchi C, Putti S, Zamparelli A, Giuliani L, Tomassetti G, Cinti C, 2004. Exposure to 900 MHz electromagnetic field induces an unbalance between pro-apoptotic and pro-survival signals in T-lymphoblastoid leukemia CCRF-CEM cells. J Cell Physiol, 198(2); 324–332.

McNamee JP, Bellier PV, Gajda GB, Miller SM, Lemay EP, Lavallè B, Marro L, Thansandote A, 2002 DNA damage and micronucleus induction in human leukocytes after acute in vitro exposure to a 1.9 GHz continuous-wave radiofrequency field. Radiat Res, 158; 523–533.

Meltz ML, 2003. Radiofrequency exposure and mammalian cell toxicity, genotoxicity, and transformation. Bioelectromagnetics, 6; S196–S213.

Merola P, Marino C, Lovisolo GA, Pinto R, Laconi C, Negroni A, 2006. Proliferation and apoptosis in a neuroblastoma cell line exposed to 900 MHz modulated radiofrequency field. Bioelectromagnetics, 27; 164-171.

Michaelson SM, 1980. Microwave biological effects; an overview. Proceedings of the IEEE, 68(1); 40-49.

Millar DB, Christopher JP, Hunter J, Jeandle SS, 1984. The effect of exposure of acetylcholinesterase to 2450 MHz microwave radiation. Bioelectromagnetics, 5(2); 165–172.

Miyakoshi J, Takemasa K, Takashima Y, Ding GR, Hirose H, Koyama S, 2006. Effects of exposure to a 1950 MHz radio frequency field on expression of Hsp70 and Hsp27 in human glioma cells. Bioelectromagnetics, 26; 251–257.

Morelli A, Ravera S, Panfoli I, Pepe IM, 2005. Effects of extremely low frequency electromagnetic fields on membrane-associated enzymes. Arch Biochem Biophys, 15, 441(2); 191-198.

Morris GF, Mathews MB, 1989. Regulation of proliferating cell nuclear antigen during the cell cycle. J Biol Chem, 264(23); 13856-13864.

Nakamura H, Matsuzaki I, Hatta K, Nobukuni Y, Kambayashi Y, Ogino K, 2003. Non-thermal effects of mobile-phone frequency microwaves on uteroplacental functions in pregnant rats. Reprod Toxicol, 17; 321–326.

Nawrot PS, McRee DI, Galvin MJ, 1985. Teratogenic, biochemical, and histological studies with mice prenatally exposed to 2.45 GHz microwave radiation. Radiat Res, 102; 35–45.

Nikolova T, Czyz J, Rolletschek A, Blyszczuk P, Fuchs J, Jovtchev G, Schuderer J, Kuster N, Wobus AM, 2005. Electromagnetic fields affect transcript levels of apoptosis-related genes in embryonic stem cell-derived neural progenitor cells. FASEB J, 19; 1686–1688.

Okutucu B, Dinçer A, Habib O, Zihnioglu F, 2007. Comparison of five methods for determination of total plasma protein concentration. J Biochem Biophys Methods, 70(5); 709-711.

Otto M, von Mühlendahl KE, 2007. Electromagnetic fields (EMF); do they play a role in children's environmental health (CEH)? Int J Hyg Environ Health, 210; 635–644.

Overgaard J, Gonzalez Gonzalez D, Hulshof MC, Arcangeli G, Dahl O, Mella O, Bentzen SM, 2009. Hyperthermia as an adjuvant to radiation therapy of recurrent or metastatic malignant melanoma. A multicentre randomized trial by the European Society for Hyperthermic Oncology. 1996. Int J Hyperthermia, 25(5); 323-334.

Pacini S, Ruggiero M, Sardi I, Aterini S, Gulisano F, Gulisano M, 2002. Exposure to global system for mobile communication (GSM) cellular phone radiofrequency alters gene expression, proliferation, and morphology of human skin fibroblasts. Oncology Research, 13; 19-24.

Pałecz D, Leyko W, 1983. Effect of gamma radiation on enzymatic activity and sulphydryl groups of human erythrocyte membrane. Int J Radiat Biol, 44; 293-299.

Pawlowski KM, Krol M, Majewska A, Badowska-Kozakiewicz A, Mol JA, Malicka E, Motyl T, 2009. Comparison of cellular and tissue transcriptional profiles in canine mammary tumor. J Physiol Pharmacol, 60(1); 85-94.

Pfaffl MW, 2001. A new mathematical model for relative quantification in real-time RT-PCR. Nucleic Acids Res, 29(9); e45.

Phillips JL, Singh NP, Lai H, 2009. Electromagnetic fields and DNA damage, Pathophysiology, 16; 79–88.

Port M, Abend M, Romer B, Van Beuningen D. 2003. Influence of high-frequency electromagnetic fields on different modes of cell death and gene expression. Int J Radiat Biol, 79(9); 701–708.

Qutob SS, Chauhan V, Bellier PV, Yauk CL, Douglas GR, Berndt L, Williams A, Gajda GB, Lemay E, McNamee JP, 2006. Microarray gene expression profiling of a human glioblastoma cell line exposed in vitro to a 1.9 GHz pulse-modulated radiofrequency field. Radiat Res, 165; 636–644.

Rancourt A, Satoh MS, 2009. Delocalization of nucleolar poly(ADP-ribose) polymerase-1 to the nucleoplasm and its novel link to cellular sensitivity to DNA damage. DNA Repair (Amst). [Epub ahead of print]

Reif S, Lang A, Lindquist JN, Yata Y, Gabele E, Scanga A, Brenner DA, Rippe RA, 2003. The role of focal adhesion kinase-phosphatidylinositol 3-kinase-akt signaling in hepatic stellate cell proliferation and type I collagen expression. J Biol Chem, 278(10); 8083-8090.

Repacholi MH, 1998. Low-level exposure to radiofrequency electromagnetic fields: health effects and research needs. Bioelectromagnetics, 19; 1:19.

Rieger F, Shelanski ML, Greene LA, 1980. The effects of nerve growth factor on acetylcholinesterase and its multiple forms in cultures of rat PC12 pheochromocytoma cells; increased total specific activity and appearance of the 16 S molecular form. Dev Biol, 76; 238-243.

Ristow M, 2006. Oxidative metabolism in cancer growth. Curr Opin Clin Nutr Metab Care, 9(4); 339-45. Review.

Ritossa F, 1962. A new puffing pattern induced by temperature shock and DNP in Drosophila. Experientia, 18; 571–573.

Robert E, 1999. Intrauterine effects of electromagnetic fields (low frequency, mid-frequency RF, and microwave); review of epidemiologic studies. Teratology, 59; 292–298.

Röösli M, 2008. Radiofrequency electromagnetic field exposure and non-specific symptoms of ill health: a systematic review. Environ Res, 107(2); 277-287. Review.

Rothman KJ, 2000. Epidemiological evidence on health risks of cellular telephones. Lancet, 356; 1837–1840.

Sanchez S, Milochau A, Ruffiè G, Poulletier De Gannes F, Lagroye I, Haro E, Surleve-Bazeille JE, Billaudel B, Veyret B, 2006. Human skin cell stress response to GSM-900 mobile phone signals. FEBS J, 273; 5491–5507.

Sanchez S, Haro E, Ruffiè G, Veyret B, Lagroye I, 2007. In vitro study of the stress response of human skin cells to GSM-1800 mobile phone signals compared to UVB radiation and heat shock. Radiat Res, 167; 572–580.

Sanchez S, Masuda H, Ruffié G, De Gannes FP, Billaudel B, Haro E, Lévêque P, Lagroye I, Veyret B, 2008. Effect of GSM-900 and -1800 signals on the skin of hairless rats. III: Expression of heat shock proteins. Int J Radiat Biol, 84(1); 61-68.

Sanchez-Hernandez JC, Moreno-Sanchez B, 2002. Lizard cholinesterases as biomarkers of pesticide exposure: enzymological characterization. Environ Toxicol Chem, 21; 2319-2325.

Sarkar S, Ali S, Behari J, 1994. Effect of low power microwave on the mouse genome: A direct DNA analysis. Mutat Res, 320; 141-147.

Sastry, BV, 1997. Human Placental Cholinergic System. Commentary. Biochem Pharmacol, 53(11); 1577-1586.

Scarfi MR, Fresegna AM, Villani P, Pinto R, Marino C, Sarti M, Altavista P, Sannino A, Lovisolo G, 2006. Exposure to radiofrequency radiation (900 MHz, GSM signal) does not affect micronucleus frequency and cell proliferation in human peripheral blood lymphocytes; An interlaboratory study. Radiat Res, 165; 655–663.

Scharf KD, Hohfeld I and Nover L, 1998. Heat stress response and heat stress transcription factors. J Biosci, 23; 313–329.

Schönborn F, Pokovic K, Wobus AM, Kuster N, 2000. Design, optimization, realization, and analysis of an in vitro system for the exposure of embryonic stem cells at 1.71 GHz. Bioelectromagnetics, 21; 372–384.

Schuderer J, Samaras T, Oesch W, Spät D, Kuster N, 2004. High Peak SAR Exposure Unit With Tight Exposure and Environmental Control for In Vitro Experiments at 1800 MHz. Ieee Transactions On Microwave Theory and Techniques, 52(8); 2057-66.

Schuz J, Bohler E, Schlehofer B, Berg G, Schlaefer K, Hettinger I, Kunna-Grass K, Wahrendorf J, Blettner M, 2006. Radiofrequency electromagnetic fields emitted from base stations of DECT cordless phones and the risk of glioma and meningioma (Interphone Study Group, Germany). Radiat Res, 166; 116–119.

Schweitzer ES, 1993. Regulated and constitutive secretion of distinct molecular forms of acetylcholinesterase from PC12 cells. J Cell Sci, 106; 731-740.

Simone C, Derewlany LO, Oskamp M, Johnson D, Knie B, Koren G, 1994. Acetylcholinesterase and butyrylcholinesterase activity in the human term placenta; implications for fetal cocaine exposure. J Lab Clin Med, 123(3); 400-406.

Speit G, Schütz P, Hoffman H, 2007. Genotoxic effects of exposure to radiofrequency electromagnetic fields (RF-EMF) in cultured mammalian cells are not independently reproducible. Mutat Res, 626; 42–47.

Stagg RB, Thomas WJ, Jones RA, Adey WR. 1997. DNA synthesis and cell proliferation in C6 glioma and primary glial cells exposed to a 836.55 MHz modulated radiofrequency field. Bioelectromagnetics, 18(3); 230–236.

Stegemann S, Altman KI, Mühlensiepen H, Feinendegen LE, 1993. Influence of a stationary magnetic field on acetylcholinesterase in murine bone marrow cells. Radiat Environ Biophys, 32(1); 65-72.

Sternfeld M, Rachmilewitz J, Loewenstein-Lichtenstein Y, Andres C, Timberg R, Ben-Ari S, Glick C, Soreq H, Zakut H, 1997. Normal and atypical butyrylcholinesterases in placental development, function, and malfunction. Cell Mol Neurobiol, 17(3); 315-332.

Storm FK, 1981. Hyperthermia. Henry Ford Hospital medical journal, 29(1); 5-9.

Szpechcinski A, Struniawska R, Zaleska J, Chabowski M, Orlowski T, Roszkowski K, Chorostowska-Wynimko J, 2008. Evaluation of fluorescence-based methods for total vs. amplifiable DNA quantification in plasma of lung cancer patients. J Physiol Pharmacol, 59 Suppl 6; 675-681.

Tice RR, Hook GG, Donner M, McRee DI, Guy AW, 2002. Genotoxicity of radiofrequency signals. I. Investigation of DNA damage and micronuclei induction in human blood cells. Bioelectromagnetics, 23; 113–126.

Tokalov SV, Gutzeit HO, 2004. Weak electromagnetic fields (50 Hz) elicit a stress response in human cells. Environ Res, 94; 145–151.

Trotter JM, Edis AJ, Blackwell JB, Lamb MH, Bayliss EJ, Shepherd JM, Cassidy B, 1996. Australas Radiol, 40(3); 298-305.

Tuschl H, Waltraud N, Molla-Djafari H, 2006. In vitro effects of GSM modulated radiofrequency fields on human immune cells. Bioelectromagnetics, 27; 188-196.

Valbonesi P, Franzellitti S, Piano A, Contin A, Biondi C, Fabbri E, 2008. Evaluation of HSP70 expression and DNA damage in cells of a human trophoblast cell line exposed to 1.8 GHz amplitude-modulated radiofrequency fields. Radiat Res, 169(3); 270-279.

Valcana T, Timiras PS, 1974. Effects of X-radiation on the development of the cholinergic system of the rat brain. I. Study of alterations in choline acetyltransferase and acetylcholinesterase synthesis. Environ Physiol Biochem, 4; 47-57.

Van Nguyena J, Marks R, 2002. Pulsed Electromagnetic Fields for Treating Osteo-arthritis. Physiotherapy, 88 (8); 458-470.

Van der Zee J, González González D, Van Rhoon GC, Van Dijk JD, Van Putten WL, Hart AA, 2000. Comparison of radiotherapy alone with radiotherapy plus hyperthermia in locally advanced pelvic tumours: a prospective, randomised, multicentre trial. Lancet, 355(9210); 1119-1125.

Van Wieringen N, Wiersma J, Zum Vörde Sive Vörding P, Oldenborg S, Gelvich EA, Mazokhin VN, van Dijk JD, Crezee J. Characteristics and performance evaluation of the capacitive Contact Flexible Microstrip Applicator operating at 70 MHz for external hyperthermia. Int J Hyperthermia, 25(7); 542-53.

Velizarov S, Raskamrk P, Kwee S, 1999. The effects of radiofrequency fields on cell proliferation are non-thermal. Bioelectrochem Bioenerg, 48; 177–180.

Verschaeve L, 2009. Genetic damage in subjects exposed to radiofrequency radiation. Mutat Res, 681; 259–270.

Verschaeve L, Maes A, 1998. Genetic, carcinogenic and teratogenic effects of radiofrequency fields. Mutat Res, 410; 141–165.

Vijayalaxmi, Obe G, 2004. Controversial cytogenetic observations in mammalian somatic cells exposed to radiofrequency radiation. Rad Res, 162; 481-496. Review.

Vijayalaxmi, McNamee JP, Scarfi MR, 2005. Comments on: “DNA strand breaks” by Diem et al. [Mutat Res. 583 (2005) 178–183] and Ivancsits et al. [Mutat Res 583 (2005) 184–188]. Mutat Res, 603; 104–106.

Vukova T, Atanassov A, Ivanov R, Radicheva N, 2005. Intensity-dependent effects of microwave electromagnetic fields on acetylcholinesterase activity and protein conformation in frog skeletal muscles. Med Sci Monit, 11(2); BR50-56.

Warburg O, 1956. On respiratory impairment in cancer cells. Science, 124(3215); 269-270.

WHO, Electromagnetic fields and public health, Base station and wireless technologies. www.who.int/mediacentre/factsheets/fs304/en/index.html, 2006.

Wu L, McGough RJ, Arabe OA, Samulski TV, 2006. An RF phased array applicator designed for hyperthermia breast cancer treatments. Phys Med Biol, 51(1); 1–20.

Wu PY, Frit P, Malivert L, Revy P, Biard D, Salles B, Calsou P, 2007. Interplay between Cernunnos-XLF and nonhomologous end-joining proteins at DNA ends in the cell. J Biol Chem, 282(44); 31937-31943.

Wust P, Nadobny J, Felix R, Deuflhard P, Louis A, John W, 1991. Strategies for optimized application of annular-phased-array systems in clinical hyperthermia. Int J Hyperthermia, 7(1); 157-173.

Xing JZ, Zhu L, Gabos S, Xie L, 2006. Microelectronic cell sensor assay for detection of cytotoxicity and prediction of acute toxicity. Toxicol In Vitro, 20(6); 995-1004.

Yi MQ, Liu HX, Shi XY, Liang P, Gao XW, 2006. Inhibitory effects of four carbamate insecticides on acetylcholinesterase of male and female Carassius auratus in vitro. Comp Biochem Physiol C, 143; 113:116.

Zhu J, Wang X, Xu X, Abassi YA, 2006. Dynamic and label-free monitoring of natural killer cell cytotoxic activity using electronic cell sensor arrays. J Immunol Methods, 309 (1-2); 25-33.

Zubkova EV, Vasil'eva IG, Oleksenko NP, Samosiuk NI, Chopik NG, Galanta ES, Tsiubko OI, 2007. Influence of magnitolaser radiation on the acetylcholinergic neurons in culture [Article in Russian]. Lik Sprava, (5-6); 108-10.

I would like to thank:

My supervisors: Elena Fabbri, Andrea Contin and James Murphy. A huge thank for your trust, guidance, patience and this great opportunity you gave me.

The following people, for their advices, suggestions, supports and precious help during these years:
Pietro Mesirca and Ferdinando Bersani at the Department of Physics (CIG), Bologna University;
Alessandro Giuliani and Laura Calzà at the Department of Veterinary Morphophysiology and Animal Production, Bologna University;
Paolo Galloni at the Toxicology and Biomedical Sciences Unit, Enea Casaccia Research Center, Rome;
Padraig McEvoy, Giuseppe Ruvio, Sergio Curto and Max Ammann at the Antenna and High Frequency Research Centre, Dublin Institute of Technology;
Jordy Accensi at WaveControl, Barcelona;
Isabelle Lagroye at the Laboratoire de Bioélectromagnétisme EPHE, Pessac;
Jeremy Birds at the Institute of Technology, Sligo.

My colleagues in Ravenna and Sligo: Sabrina Guerrini, Paola Valbonesi, Silvia Franzellitti, Nicola Ciancaglini, Sara Buratti, Kajsa Yngvesson, Luciene Zanchetta and Clodagh Kivlehan. Thanks also to Edda and Grazia. The best of luck to you in the future!

All my friends all around the world, but in particular thanks to: Melania, Sabrina & Klaus, Fra, Gavino, Paola and Camilla for always being there whenever I needed you. And also to Kajsa, Luciene, Clodagh, James, Alan, Angel, Ann Sophie, Julien, Sheila, Michelle and whoever I forgot for the good times together (coffees, chats, pints, serious and stupid conversations, nights out, etc.).
Thanks a million for all the support you gave me, but also for the fun we had over the years!

And, last but sure not least, my fantastic family: mamma e papà (se sono arrivata fin qui lo devo solo ed esclusivamente a voi...grazie di tutto!), Riccardo (sei il migliore, sempre e comunque), Riccardo e Giacomo (la luce dei miei occhi), and Patrick (because I've been so lucky…!).
Nothing would have been the same without you… Thanks for every single thing! I love you so much!

Naimj